POLYADENYLATION AND PROCESSING OF THE

POLYCISTRONIC *RPSJ* MESSENGER RNA TRANSCRIPT

IN *ESCHERICHIA COLI* K-12

by

KRISTEN BROWN MILDENHALL

(Under the Direction of Sidney R. Kushner)

ABSTRACT

The processing or decay of RNA in *Escherichia coli* involves an array of endonucleases and exonucleases. In addition, the decay of RNA transcripts also involves the post-transcriptional addition of 3’ poly(A) tails to mRNAs, rRNAs, and pre-tRNAs by poly(A) polymerase I (PAP I) and polynucleotide phosphorylase (PNPase). The addition of poly(A) tails helps target the RNAs for more rapid degradation. In this work, the processing and/or breakdown along with polyadenylation of the large polycistronic *rpsJ* mRNA transcript has been examined.

Our data suggest that RNase E is the major enzyme involved in the initial processing of the *rpsJ* transcript and is responsible for the removal of the 3' Rho-independent transcription terminator. The results also suggest that the 5' untranslated region of the *rpsJ* transcript remains intact in wild-type cells. Additionally, the processing pattern of the *rpsJ* transcript indicates that other endonucleases generate secondary cleavages. Interestingly, the cell maintains constant ratios of the individual ORF transcripts of the polycistronic *rpsJ* operon, despite changes in the processing of the

full-length transcript in RNase E mutants. These results suggest a greater flexibility in controlling ribosomal protein transcript levels than previously observed.

Furthermore, through our experiments involving the polyadenylation of the *rpsJ* operon transcript, we show that polyadenylation of mRNAs by PAP I is directly linked to an intact RNase E-based degradosome. The polyadenylation profiles of individual mRNAs encoded within the *rpsJ* operon (*rpsJ* and *rpsQ*) and a control transcript (*lpp*) changed dramatically both in the location of the tails and in their nucleotide composition when the scaffold region of the RNase E protein was deleted. Specifically, in the absence of degradosome assembly, the majority of the tails for these specific mRNA transcripts were heteropolymeric and were added by PNPase. Our data suggest the existence of a much larger polyadenylation complex and a more direct link between mRNA degradation and polyadenylation than previously envisioned.

INDEX WORDS: Polyadenylation, mRNA processing, RNase E, PAP I, PNPase, degradosome, *rpsJ*, *Escherichia coli*

POLYADENYLATION AND PROCESSING OF THE POLYCISTRONIC *RPSJ* MESSENGER RNA TRANSCRIPT IN *ESCHERICHIA COLI* K-12

by

KRISTEN BROWN MILDENHALL

B.S., Brigham Young University, 2007.

A Dissertation Submitted to the Graduate Faculty of The University of Georgia in Partial Fulfillment of the Requirements for the Degree

DOCTOR OF PHILOSOPHY

ATHENS, GEORGIA

2013

POLYADENYLATION AND PROCESSING OF THE POLYCISTRONIC *RPSJ* MESSENGER RNA TRANSCRIPT IN *ESCHERICHIA COLI* K-12

by

KRISTEN BROWN MILDENHALL

Major Professor: Sidney R. Kushner

Committee: Lawrence Shimkets
Anna Karls
Robert Maier

Electronic Version Approved:

Maureen Grasso
Dean of the Graduate School
The University of Georgia
December 2013

DEDICATION

To the two most important people in my life—my husband, Taylor, and my son, Clark. And for my father-in-law, Tom—I feel privileged to vicariously carry on the family scientific PhD legacy; I only wish you had lived to see it to its fulfillment.

ACKNOWLEDGEMENTS

I would like to express my gratitude to my major advisor, Dr. Sidney R. Kushner, for his guidance, support and encouragement. I would also like to thank the other members of my advisory committee for their direction and suggestions. I also wish to thank the past and present members of the Kushner lab for their guidance, answers to questions, commiseration, encouragement, camaraderie, and support through the past few years.

Many thanks to my dear family and friends, who have supported and encouraged me throughout this process. Without you all, I would have never accomplished what I have been able to do.

TABLE OF CONTENTS

Page

LIST OF TABLES

Page

LIST OF FIGURES

Page

CHAPTER 1

INTRODUCTION AND LITERATURE REVIEW

INTRODUCTION

Survival of a bacterial cell requires the adjustment of metabolic and physiological processes to changing environmental conditions. RNA turnover/decay is key to this rapid adaptation. RNA turnover is controlled by a combination of endonucleases and exonucleases, which leads to messenger RNA (mRNA) half-lives that vary anywhere from approximately 10 seconds to 20 minutes (1). The processing and breakdown of mRNAs directly affects steady-state transcript levels, leading to alterations in protein levels and the ability of the cell to rapidly adapt to changes in its growth environment.

Understanding the processes by which RNA processing, degradation, and polyadenylation occur in *Escherichia coli* is one key to the understanding the basics of cellular metabolism and regulation. Here we examine in detail the extensive work that has been done previously with regard to ribonucleases involved in the complex processes that control mRNA decay.

RIBONUCLEASES

The processing of RNA transcripts into mature forms along with the degradation of mRNAs, tRNAs, rRNAs, and sRNAs in *E. coli* is performed by a set of ribonucleases (RNases) consisting of endonucleases, which cleave at internal locations, and

exonucleases, which act in either a 5'→3' or 3'→5' manner to remove nucleotides from the extremities of RNA transcripts (Fig. 1.1, 1.2). [See (2) for an extensive comparison of the overlap in the functional activities of ribonucleases involved in mRNA decay and RNA processing.] To date, all the exonucleases in *E. coli* proceed in the 3'→5' direction. It has been shown that both endo- and exonucleolytic action is required for the cell's proper function and viability (3). These processing or degradative pathways are often complex, with multiple enzymes acting on a single substrate at varying rates and efficiencies causing a complex intertwined network of initial, secondary and tertiary cleavages.

Endoribonucleases involved in *E. coli* RNA metabolism

A. RNase E

The endonuclease, ribonuclease E (RNase E), encoded by the *rne* gene, prefers A/U rich single-stranded RNA regions as cleavage sites (4,5), especially those near stem-loops (6). RNase E is involved in many initial cleavage events and is regarded as the main endonuclease involved in RNA turnover (Fig 1.1). Tiling arrays have shown that more than half the RNA transcripts are targeted for RNase E cleavages (7). As such, RNase E has been shown experimentally to be involved in both rRNA and mRNA processing and the rapid degradation of mRNAs and sRNAs, including the processing of 5S rRNA precursors (8,9), 16S rRNA (10), tRNAs (11), and tmRNA (12).

Structurally, RNase E forms a 260kDa homotetramer organized as a dimer-of-dimers with each dimer resembling the blade and handles of an open pair of scissors (13-15). RNase E has a highly structured and essential catalytic region from amino acid

residues 1-529 (16), followed by a largely unstructured C-terminal scaffold domain from residues 530-1061 (17). Scaffold enzyme associations occur between residues 701-1061 (16-18) (Fig.1.3). The scaffold region provides binding sites that lead to the formation of a multimeric complex called the degradosome, which will be discussed in greater detail later in this chapter. The catalytic region is composed of five main domains, which include an S1 domain, a 5' sensor pocket, a non-catalytic RNase H domain, a DNase I domain, and a dimer-dimer interaction region (13-15)

RNase E is a 5'-end-dependent endonuclease that has a preference for 5' monophosphate substrates (19). This affinity is due to the physical constraints of the 5' sensing pocket of RNase E (13,14), whereby RNase E interacts with the 5' phosphate of the RNA transcript, causing the S1 domain to clamp down and properly orient the RNA for RNase E cleavage (Fig 1.1a).

The removal of the 5' triphosphate from primary RNA transcripts, which then allows RNase E to rapidly process or degrade the resulting 5' monophosphorylated RNA transcript (20), is performed by RppH, an RNA pyrophosphohydrolase. However, RNase E has also been shown to work on some substrates in a 5'-independent manner referred to as "internal entry" (Fig 1.1b), but which occurs at a slower rate than 5'-dependent processing by RNase E (21,22). Additionally, microarray analysis of *rppH* mutants suggests that the majority of transcripts processed by RNase E are likely processed in the slower 5'-independent manner (23).

B. RNase G

RNase G, encoded by the *rng* gene, is a paralogue of the RNase E catalytic domain (10,24,25). It has no comparable C-terminal scaffold domain like RNase E and forms a homodimer rather than a dimer of dimers like RNase E (26). Additionally, unlike RNase E, RNase G is not essential for cell viability (10,25), and is found at lower levels in the cell (27). If overproduced at very high levels, RNase G has been shown to partially overcome the temperature sensitivity of *rne* mutants (27-29). Recently a single amino acid mutation in RNase G has been shown to allow RNase G to substitute for *rne* even at normal levels (30). In addition to substituting for or being a backup enzyme to RNase E, especially in 5S rRNA maturation, RNase G plays a role in its own right in the maturation of 16S rRNA (10,25), 6S RNA (31), some tRNAs (32,33), and mRNAs (28).

C. RNase III

After RNase E, RNase III is considered to be the second most important endonuclease involved in initial cleavage events. RNase III, encoded by the *rnc* gene, is an endonuclease with substrate specificity for double-stranded RNA, particularly double-stranded loops in intercistronic regions, which it cleaves at the base of the stem (34,35). Its phosphodiesterase cleavages generate a 2-nucleotide overhang on the 3’ end and a 5’-monophosphate and a 3’-hydroxyl terminus (36). It is the primary enzyme responsible for the separation of the pre-16S rRNA and pre-23S rRNA species from a 30S rRNA primary transcript (Fig. 1.2) (34,37). It also separates some mRNA transcripts between protein coding regions, such as *rpsO pnp* (35). Tiling arrays of *rnc* mutants have

indicated its role in processing or degradation of approximately 12% of all genes in the *E. coli* genome (7).

D. RNase P

RNase P, encoded by the *rnpA* and *rnpB* genes, is a ribonucleoprotein, made up of a protein subunit (M9) and a catalytic RNA subunit. It is an essential endonuclease and is responsible for the 5' maturation of tRNAs (Fig. 1.2). In addition, RNase P processes a number of polycistronic tRNAs and/or mRNA transcripts (32,33,38).

E. RNase Z/BN

In some eukaryotes and prokaryotes, RNase Z is essential for the maturation of tRNA precursors lacking encoded 3' terminal CCA sequences. However, since all *E. coli* tRNAs have chromosomally encoded CCA sequences (39), the function of RNase Z in *E. coli* was initially unclear. RNase Z has since been shown to be an endonuclease that plays a role in mRNA decay, including cleavage of the *rpsT* transcript at distinct sites separate from its known RNase E cleavages (39). Other work has shown that RNase Z cleaves endonucleolytically, producing a 3' RNA byproduct that can be as small as 4 nucleotides (40).

RNase Z was initially discovered as a 3'→5' exonuclease and was called RNase BN (41). Its role as a potential exonuclease involved in RNA maturation will be discussed in greater detail later in this chapter. The enzyme is most commonly referred to RNase Z when acting as an endonuclease and RNase BN when acting as an exonuclease.

F. Other Endoribonucleases

Ribonuclease H (RNase H) is an endonuclease found in both in prokaryotes and eukaryotes and cleaves RNA/DNA hybrids, including the RNA primers involved in DNA replication (42). RNase LS is an endonuclease that was thought to serve as an antagonist of infection by bacteriophage T4 (43), but has recently been suggested to encode the toxin of a novel toxin/antitoxin system (44). RNase I, and its altered form RNase M (45), is a nonspecific endonuclease that is found primarily in the periplasmic space and whose role in mRNA decay, if any, is still largely unknown.

Exoribonucleases involved in *E. coli* RNA metabolism

The major exoribonucleases in *E. coli* are discussed below. It is interesting to note that only PNPase, RNase II, RNase R and oligoribonuclease (Orn) are involved in mRNA decay (Fig. 1.1d). The other exonucleases are primarily involved in the 3' maturation of precursor tRNAs (46).

A. PNPase

Polynucleotide phosphorylase (PNPase), encoded by the *pnp* gene, is a homotrimeric protein (47,48) that functions as a 3'→5' exonuclease. PNPase has also been shown to be both a member of the degradosome complex (18,49) and to work biosynthetically as a poly(A) polymerase (50), both of which topics will be discussed in greater detail later in this chapter.

PNPase has been shown to be essential only if RNase II or RNase R are missing (3,51). PNPase is a phosphorylytic exonuclease that is inhibited by secondary structure,

stalling 6-8 nucleotides downstream of secondary structures. It is also ineffective on short oligonucleotides (52,53). PNPase's enzymatic catalysis occurs in the central channel of the protein (54,55), into which the RNA molecules travel for cleavage. However, PNPase degrades secondary structures in conjunction with RhlB, an RNA helicase also found as part of the RNase-E based degradosome (56,57).

Recently PNPase has been shown to have a role in sRNA metabolism. PNPase can protect sRNAs from decay in exponentially growing cells (58), but in stationary phase PNPase actively degrades sRNAs, especially those not bound to Hfq (59).

B. RNase II

RNase II is a hydrolytic exonuclease that degrades single-stranded RNA, but is inhibited by secondary structures (53,60). However, RNase II degrades RNA transcripts that contain poly(A) tails (53,60). In fact, overproduction of RNase II can suppress the toxicity of overproduction of the poly(A) polymerase PAP I (60). RNase II also plays a minor role in 3' maturation of tRNAs (61).

RNase II requires a single-stranded region of 10 nucleotides or more to bind effectively, as only single-stranded RNA can fit into the catalytic site due to steric hindrance (53,62). Interestingly, RNase II can also bind DNA but it does not degrade it; thus DNA can act as an inhibitor (63).

C. Other Exoribonucleases

Other exoribonucleases, including RNase R, oligoribonuclease, RNase T, RNase D, RNase PH, RNase BN, have been shown to play a role in RNA processing or decay.

Many of the functions of RNase T, RNase D, RNase PH, RNase II and RNase BN exonucleases are overlapping. A cell is viable with a wild-type copy of any one of these genes, even when the other four enzymes are missing (64), with RNase T, RNase PH, RNase D, RNase II, then RNase BN, respectively, being the most to least effective at supporting growth (64).

RNase R is a hydrolytic exonuclease with an ability to degrade structured single-stranded RNA, but requires single-stranded regions longer than 7 nucleotides to bind, leaving 2-5 nucleotide fragment byproducts (65). RNase R degrades defective tRNAs or rRNAs, mRNAs, especially those with poly(A) tails, and also in conjunction with YbeY to work on 70S rRNA degradation (66-71). Additionally, levels of RNase R have been shown to dramatically increase under cold shock conditions (72-75).

Oligoribonuclease (Orn) is an essential exonuclease (76) responsible for degradation into mononucleotides of the short 2-5 mer single-stranded RNA oligonucleotides that remain from the activity of other nucleases (77-79).

RNase T is a single-stranded specific hydrolytic exonuclease involved in the 3’ maturation of rRNAs and tRNAs (Fig. 1.2) (80,81). RNase T has also been shown to have DNA exonuclease activity (81).

RNase D is another hydrolytic exonuclease shown to act on denatured or damaged tRNAs, tRNA precursors, or other small structured RNAs (82-85).

RNase PH is a phosphorylytic exonuclease that works predominately on 3’ maturation of tRNA precursors (64,86-88) and is a paralogue of PNPase. It has also been shown to be involved in the modification of the 3’ end of sRNAs (89-91). It is

essential only in the absence of PNPase and RNase T (61,64,92), suggesting its function overlaps with the function of those two more prominent exonucleases.

RNase Z/BN is an endonuclease that has been shown to have *in vitro* exonuclease activity (40), and has also been suggested to function exonucleolytically *in vivo* as well (93). It has been hypothesized that the substrate range of the *E. coli* RNase Z/BN, as opposed to RNase Z family enzymes in other organisms, such as *Bacillus subtilis*, which have only endonucleolytic activity, is due to its narrower and more rigid channel downstream of its catalytic site (93). As an exonuclease, it is proposed to be active on both single-stranded and double-stranded RNA, but with double-stranded or duplexed RNA preferred (40). The exonuclease activity of RNase BN is inhibited by a run of C residues or the presence of either a phosphoryl group or CCA sequence on the 3' RNA terminus (40).

THE RNASE E-BASED DEGRADOSOME

The RNase E-based degradosome is a key complex involved in mRNA degradation. [See (94,95) for extensive reviews on the subject.] It has been shown to be involved in the majority of mRNA degradation in the cell (7), including the degradation of its own transcript (96-98). RNase E was first shown to be involved the degradation of small non-coding RNAs in 2003 by Massé *et al.* (99). Since then, it has been shown to be involved in the degradation of numerous sRNAs. [See (100) for a review of the past ten years of research on RNase E-dependent degradation of sRNAs.]

Enzymes involved in the RNase E-based Degradosome

The degradosome is composed of the RNase E endonuclease, along with PNPase, the RhlB RNA helicase, and enolase (49,56,101,102) which associate with the C-terminal scaffold domain of RNase E. Additionally, other proteins have been suggested to have the ability to interact under other physiological conditions, such as cold shock (103). It is also important to note that all the components of the degradosome are not present in equimolar amounts in the cell. Data has shown that PNPase and enolase are present in large excess relative to RNase E (5-10 fold during exponential growth), while RhlB is present in almost equimolar amounts (104).

A. RNase E

As discussed earlier in this chapter, RNase E is involved in rRNA and mRNA processing (4) and the rapid degradation of mRNAs and sRNAs. The protein has a highly structured catalytic region from amino acid residues 1-529, followed by a largely unstructured scaffold C-terminal domain from residues 530-1061 (17), with scaffold enzyme associations occurring between residues 701-1061 (16-18). It has been shown that mutants which contain a wild-type catalytic region of RNase E, even if missing the scaffold region, function normally with regards to mRNA decay and tRNA maturation (105).

Callaghan *et al.* (17) found that the scaffold region is highly unstructured under native conditions and was likely to remain unfolded even within the degradosome. The only exceptions to the unstructured nature of the scaffold are four 10-80 residue long regions of increased structural propensity (17) that correspond to the membrane binding

site of RNase E (106), the protein–RNA interaction site, and the interaction sites for enolase and PNPase (18), respectively. The arginine-rich RNA binding site (ARRBS) is located at amino acids 601-700 and is proposed to somehow enhance RNase E mRNA degradation (105,107). Deletion experiments have demonstrated that association regions for RhlB RNA helicase, enolase and PNPase are located at amino acids 734-738, 739-845 and 844-1045 of the RNase E scaffold, respectively (18). Furthermore, it has been argued that Hfq, an abundant 11.2 kDa RNA-binding protein, can also associate with RNase E, competing with the RhlB RNA helicase for binding in the region of amino acids 734-738 (108).

There is strong evidence that the majority of RNase E binds to the inner cytoplasmic membrane (104,106,109,110). This interaction occurs via amino acid residues 568-582. The phenylalanine at amino acid residue 575 in this α-helix region is key to this binding (106). RNase E proteins lacking this region no longer localize to the membrane, but are found in the cytoplasm (104,106). This same region was previously identified as a short α-helix structured region and proposed to be involved in self-association (17).

Additionally, it has been suggested that RNase E needs to be localized to the inner membrane for normal levels of activity, since protein levels in mutants lacking residues 529-592 are increased compared with strains containing that region (106). Recent work has suggested that membrane binding of RNase E leads to secondary protein structural changes, which cause enzymatic activation, stabilization of folded RNase E, and an increased substrate binding affinity (111).

B. PNPase

PNPase is a 3'-to-5' exonuclease and is a key component of the mRNA degradosome (3,49). PNPase associates with residues 844-1045 of the RNase E scaffold (18). More specifically, scaffold region residues 1021–1061 have been shown to bind PNPase by non-dissociating mass spectrometry, and pull-down assay analysis (17). Although RNase E is localized to the inner membrane, the majority of PNPase molecules have been found in the cytoplasm (104), a result that differs from other degradosome components. These data suggest that only a small fraction of cellular PNPase is bound to RNase E, an unsurprising conclusion due to the 5-10 fold excess of PNPase compared to RNase E in exponentially growing cells (104).

Additionally, PNPase binds directly to the RhlB helicase (112) in addition to its binding to the scaffold domain, suggesting that multiple associations occur to form or strengthen the degradosome complex. PNPase has also been shown to be a member of the polyadenylation complex through binding to both PAP I and Hfq (113), which will be discussed in greater detail later in this chapter.

C. RhlB

RhlB is a DEAD box ATP-dependent RNA helicase (56,114-116) that associates with the RNase E-based degradosome through an interaction with amino acid residues 734-738 of the C-terminal scaffold of RNase E (17,18,104). RhlB unwinds double-stranded RNA by employing ATP hydrolysis (114). It has been suggested that RhlB works in the degradosome to unwind RNA structures that inhibit PNPase exonuclease activity (56). Purified RhlB has been shown *in vitro* to have significantly increased ATPase activity

when complexed with RNase E, compared to when RhlB is on its own (17,18,115), suggesting that the interaction with RNase E stimulates RhlB activity. The majority of RhlB has also been shown to localize to the cellular membrane when the C-terminus of RNase E is present (104), confirming the interaction with the RNase E scaffold. RhlB has also been suggested to physically interact with PNPase in addition to the RNase E scaffold (117).

D. Enolase

Enolase is a glycolytic enzyme associated with the RNase E-based degradosome (56) through an interaction with the residues 739-845 of the RNase E scaffold (17,18). Its exact role in mRNA degradation is unknown. The majority of enolase has been found localized to the membrane when RNase E is membrane bound (104), confirming the physical interaction of RhlB with the RNase E scaffold.

E. Hfq

Hfq is a ubiquitous and abundant 11.2 kDa RNA-binding protein that exists *in vivo* as a hexamer. It has been argued that Hfq can also associate with RNase E, competing with the RhlB RNA helicase for binding in the region of amino acids 734-738 (108). Hfq plays a major role in sRNA degradation by RNase E (99,118). Hfq has also been shown to be part of a polyadenylation complex with PNPase and PAP I (113), a role which will be discussed below.

POLYADENYLATION IN *E. COLI*

Polyadenylation at the 3' terminus of a transcript is a key mechanism in mRNA metabolism in both Eukaryota and Bacteria, but it appears to function very differently in the two domains. In Eukaryota, the addition of a poly(A) tail provides stability to prevent 3'-to-5' degradation and promotes more efficient translation (119-121). In contrast, bacterial polyadenylation has been shown to be involved in marking transcripts for degradation (122-126).

It has been hypothesized that since *E. coli* does not have a 5'→3' exonuclease, nor can most of its exonucleases degrade through secondary structures, that the addition of poly(A) tails by PAP I or PNPase to the 3' end of the mRNAs aids in the ability to degrade the secondary structure of mRNAs (53). In addition, it is unknown, but proposed that multiple rounds of polyadenylation and exonucleolytic degradation may be necessary before these inhibitory secondary structures are completely degraded (127).

Interestingly, although mRNA transcripts were originally believed to be the only substrates for polyadenylation, in *E.* coli rRNAs, tRNAs, sRNAs, and defective tRNAs can all be substrates for polyadenylation as well (69,126,128,129). It has been observed that the polyadenylation of tRNAs and sRNAs generates shorter tails than those found on mRNA transcripts.

Enzymes involved in *E. coli* mRNA Polyadenylation

Polyadenylation in *E. coli* is carried out primarily by poly(A) polymerase I (PAP I), but also involves the action of polynucleotide phosphorylase (PNPase) as the second

poly(A) polymerase. While there is much known about these two enzymes and their roles in polyadenylation, the exact mechanism by which PAP I and PNPase identify and select their RNA substrates for polyadenylation is still not completely understood.

A. PAP I

PAP I was first purified from *E. coli* in 1962 (130), but it was not until thirty years later that it was shown to be responsible for the addition of poly(A) tails onto the *lpp* transcript, the first direct evidence of PAP I function *in vivo* (131). At that time *pcnB*, the structural gene for PAP I, was also identified (132). Since then, PAP I has been shown to add poly(A) tails *in vivo* that exclusively contain adenosine residues. These PAP I-generated poly(A) tails are normally between 10 and 40 nucleotides in length (125). However, tail lengths are reduced by 3'→5' exonucleases such as RNase II and PNPase (60,125,133,134). *In vivo,* the homopolymeric tails are found on mRNA decay products or on full-length transcripts after Rho-independent transcription terminators (60,113,135,136), suggesting that Rho-independent transcription terminators, with their structure of a stable hairpin loop followed by a short U-rich single-stranded region (137), likely function as *in vivo* polyadenylation signals. In fact, over 80% of poly(A) tails are normally found after Rho-independent transcription terminators (113).

Deletion of the *pcnB* gene leads to a 90% decrease in intracellular poly(A) tail levels (136). Taken together, these data suggest that PAP I is responsible for the majority of all polyadenylation within the cell. Surprisingly, the PAP I overproduction was shown to be toxic (136). Recently, it has been demonstrated that the toxicity of

overproduction of PAP I is related to the polyadenylation of mature tRNAs and the concomitant inhibition of protein synthesis (129).

PAP I has also been shown to be associated with or localized to the inner membrane during exponential growth, but it appears to be released from the inner membrane as cells enter stationary phase (138,139). This release upon entry into stationary phase has been shown to be dependent on the adapter protein SprE (RssB) (139). Data showing that a PAP I leader-GFP fusion that contained the first 24 amino acid residues of PAP I localized to the inner membrane (138) suggests that the PAP I interaction with the inner membrane is dependent on some feature of the PAP I protein leader region. Additionally, evidence from immunoprecipitation of PAP I-GFP suggests that RNase E and the degradosome components are physically associated with PAP I, and that this interaction is SprE-dependent during stationary phase (140). However, to date, there has been no direct evidence of any interaction between the functions of PAP I or RNase E-based degradosome, other than that known association of polyadenylation aiding in mRNA degradation. In addition, it should be noted that PAP I is present in the cell at very low levels (30-50 molecules per cell) (113). An examination of a link between PAP I function and the presence of the RNase E-based degradosome will be discussed in Chapter 3.

B. PNPase

The evidence that a PAP I deletion mutant was not completely defective in polyadenylation led to the search for a second poly(A) polymerase (141). The *f310* gene was initially identified as the structural gene for a second poly(A) polymerase (142), but

later work disproved this hypothesis (143). Subsequently, PNPase was identified as the second poly(A) polymerase (50). Although PNPase is a 3'→5' exonuclease and is a component of the mRNA degradosome (3,49), depending on the inorganic phosphate levels, PNPase can work either exonucleolytically or biosynthetically *in vitro* and *in vivo* (50,144). Subsequently, PNPase has also been identified in several other prokaryotes as the primary poly(A) polymerase in cases where PAP I is not present or the PAP I paralogue lacks poly(A) polymerase activity (145,146).

When PNPase functions as a poly(A) polymerase, it adds adenosine-rich heteropolymeric tails (50). These tails contain all four nucleotides, with compositions of more than 50% adenosine residues (50). While it was suggested that the presence of non-A nucleosides resulted from occasional PAP I misincorporation (147,148), heteropolymeric tails were eliminated in PNPase mutants of *E. coli*, suggesting that PNPase was actually responsible for these tails (50). In agreement with this data, strains with higher levels of PNPase have higher levels of heteropolymeric tails (60). It was also observed that PNPase, unlike PAP I, does not add tails after secondary structures such as Rho-independent transcription terminators but rather adds tails near the 5' termini of mRNA transcripts (60).

C. Hfq

Another protein involved in polyadenylation in *E. coli* is Hfq, an abundant 11.2 kDa RNA-binding protein. Hfq has been shown to be extensively involved in the function of sRNAs, stabilizing the sRNAs and aiding in their base pairing with target RNAs (149-152). However, it is still unclear exactly how Hfq brings a sRNA and its target RNA

together. Additionally, Hfq has been shown to have an affinity for single-stranded A/U rich RNA regions (153), similar to RNase E, suggesting that Hfq can compete with and block cleavages by RNase E (154).

Mutation of the *hfq* gene reduces the ability of PAP I to add poly(A) tails to transcripts after Rho-independent transcription terminators, even though intracellular PAP I protein levels remain unchanged (113). Total poly(A) levels are lower in Hfq mutants and the poly(A) tails observed are shorter, even when PNPase, RNase II or RNase E are also missing, demonstrating that the shortened tails are not the result nucleolytic degradation (113).

The Polyadenylation Complex

The existence of a polyadenylation complex containing PAP I, Hfq, and PNPase was proposed based on experimental evidence demonstrating physical interactions among PAP I, PNPase and Hfq (113). Co-purification of both PNPase and Hfq occurs under native conditions with histidine-tagged PAP I, as well as the co-immunoprecipitation of PAP I, PNPase, and Hfq under native conditions using PNPase or Hfq antibodies (113). This data suggests the existence of a multiprotein complex that is required for the polyadenylation of mRNAs with Rho-independent transcription terminators.

On a related note, it was observed that in a *pnp* mutant, PAP I adds poly(A) tails primarily to breakdown products rather than full-length transcripts with Rho-independent transcription terminators (113), suggesting a possible interaction between PNPase and PAP I function. Since the primary role of PNPase in *E. coli* is as a member of the

degradosome and as a 3'→5' exonuclease (3,49), this potential PNPase/PAP I interaction could imply a link between PAP I mediated-polyadenylation and the functions of the degradosome. This question will be examined further in Chapter 3.

Polyadenylation levels in *E. coli*

In 1992, Cao and Sarkar (131) found that 1.3% of the total RNA was polyadenylated in exponentially growing *E. coli* by measuring pulse-labeled RNA bound to oligo(dT)-cellulose. However, it was later shown that ~90% of the ORFs in exponentially growing cells were polyadenylated to some degree by PAP I employing genome-wide macroarray analysis of polyadenylated transcripts in wild-type and *pcnB*$^-$ strains of *E. coli* (135). This result demonstrated a more global role for PAP I in the cell than previously thought. It is now hypothesized that only small percentage of total RNA transcripts are polyadenylated at any given time, but that the majority of transcripts are able to be substrates for polyadenylation.

Furthermore, there also seems to be a direct correlation between the nature of the transcription terminator and the enzyme responsible for the addition of poly(A) tails. It was observed from the macroarray analysis that the majority of mRNAs polyadenylated by PAP I were terminated in a Rho-independent manner (135). In contrast, the macroarray analysis suggested that transcripts lacking a Rho-independent transcription terminator were not substrates for PAP I (135).

Transcripts deemed primarily substrates of either PAP I or PNPase are found to have at least 60% homopolymeric tails or heteropolymeric tails, respectively (113,135). The composition varies among transcripts, but is reproducible for a specific transcript.

For example *ompA* has been shown to have around 77% homopolymeric tails (135), while the *trxA* mRNA tails have been shown to be 100% heteropolymeric (113).

Areas of polyadenylation needing further study

Although much is known about polyadenylation and its role in mRNA degradation in *E. coli*, there are still many questions that need to be answered. How polyadenylation is signaled, what is the timing of polyadenylation in RNA turnover, what functional or physical interactions occur with the major processing endonuclease RNase E, and are the ORFs within a polycistronic operon polyadenylated in a similar manner are just a few of the questions unanswered with regards to polyadenylation in *E. coli*.

A. Polyadenylation Signals

It remains unclear precisely what signals PAP I or PNPase to add a tail to a particular substrate. The presence or absence of a Rho-independent transcription terminator could determine which polyadenylation enzyme is used (60,113,135,136), but it is still unknown what the exact requirements, if any, are for that signal and how the signal is recognized. It is also still unclear if there is any physical interaction between PAP I and the secondary structure of the Rho-independent transcription terminator.

B. Timing of Polyadenylation

It also remains unclear at what point after transcription polyadenylation occurs. It was proposed that poly(A) tails mark the transcript for immediate degradation (124). However, this idea needs to be reexamined more fully in light of evidence that suggests

a larger role than previously thought for PAP I and polyadenylation in the cell. The possibility of polyadenylation occurring simultaneously with processing raises the question of how quickly a poly(A) tail signals that a particular transcript should be degraded. Is stability of polyadenylated transcripts consistent among the full-length transcripts, processed transcripts, and breakdown products? *In vivo* evidence suggests that PAP I-added tails are only found on mRNA decay products or after Rho-independent transcription terminators (60,113,136). These results could suggest that poly(A) tails have two slightly different functions and may be recognized by different enzymes at different stages of the decay pathway. The idea of two functions for PAP I could be supported by the evidence that in *pnp* mutants, PAP I adds poly(A) tails primarily to breakdown products rather than full-length mRNAs containing Rho-independent transcription terminators (113). However, it has yet to be determined precisely what percentage of the poly(A) tails added by PAP I are added to breakdown products versus full-length transcripts under wild-type conditions. Perhaps PAP I requires interaction with PNPase and the degradosome to function effectively as a poly(A) polymerase for full-length transcripts.

C. Interaction with the RNase E-based degradosome

It also remains to be determined what are the exact physical interactions of PAP I or the polyadenylation complex with RNase E or the components of the RNase E-based degradosome. The answer to this question could explain the preference of PAP I for polyadenylation after Rho-independent transcription terminators, since it has been shown that RNase E removes such substrates from a variety of primary tRNA

transcripts (33). The question of an PAP I interaction with the degradosome will be addressed in Chapter 3.

D. Polyadenylation of polycistronic transcripts

Experimental polyadenylation studies, until now, have only examined the polyadenylation of mono- or dicistronic transcripts, but have not looked at the polyadenylation of large polycistronic transcripts. It was observed from macroarray analysis that many ORFs within a polycistronic transcript showed polyadenylation patterns that were directly related to the transcription terminator of the operon (135), suggesting that the transcription terminator of a polycistronic transcript may be a polyadenylation signal for an entire operon. Thus, in a polycistronic transcript terminated in Rho-independent fashion, processed transcripts of the operon were predominantly substrates for PAP I, while processed units of a polycistronic transcript terminating in Rho-dependent manner were predominantly substrates for PNPase (135). However, this observation has yet to be examined in-depth to determine if the polyadenylation profiles of the processed ORF transcripts are actually similar to each other. This question will be addressed in Chapter 3 through the examination of the polyadenylation of the large polycistronic *rpsJ* operon.

THE *RPSJ* OPERON IN *E. COLI*

The *E. coli* ribosome is composed of the 5S, 16S, and 23S rRNAs together with more than 50 ribosomal proteins (r-proteins) (155). The r-proteins S1 to S21 assemble onto the 16S rRNA to makeup the 30S small ribosomal subunit, while the L1 through L36 r-

proteins assemble together with the 5S and 23S rRNAs to form the 50S large ribosomal subunit. Interestingly, 26 of the genes for the more than 50 r-proteins are transcribed by three transcriptional units clustered together—the *rpsJ* (or *S10*) operon, the *rplN* (or *spc*) operon, and the *rpsM* (or *α*) operon. Chapters 2 and 3 will include an in-depth examination of the processing and polyadenylation, respectively, of the *rpsJ* operon.

The *rpsJ* operon

The *rpsJ* operon is a 5.2 kilobase polycistronic transcript made up of 11 genes (Fig. 1.4) (156,157). The genes and their encoded ribosomal proteins are as follows: *rpsJ* (S10), *rplC* (L3), *rplD* (L4), *rplW* (L23), *rplB* (L2), *rpsS* (S19), *rplV* (L22), *rpsC* (S3), *rplP* (L16), *rpmC* (L29), and *rpsQ* (S17). All 11 genes encode 30S or 50S ribosomal subunit proteins. Additionally, the *rpsJ* transcript has a highly structured 5' untranslated region (UTR) and a 3' Rho-independent transcription terminator.

Cellular Control of Ribosomal Operons

The cell uses a vast amount of energy in producing and maintaining ribosome content, so it has a vast network of regulatory mechanisms to tightly control ribosome production. The foundation of cellular control of rRNA and r-proteins is to maintain a balance of one-to-one ratio of rRNA to each r-protein to make functional ribosomes and also to not use excess cellular energy making more ribosomes than necessary. Overproduction of one of any components would be a great waste to the cell, while underproduction of any of these components would result in many incomplete and nonfunctional ribosomes. As such, the cell has been shown to tightly regulate the

transcription and translation of its r-protein operons. [See (158-160) for extensive reviews on the topic of ribosomal operons and their autogenous control.] In this dissertation, for the sake of brevity, only the autogenous control of the *rpsJ* operon and its proteins will be discussed.

Cellular Control of the *rpsJ* Operon

The *rpsJ* operon has been well-studied over the past 30 years, and has been shown to have complex auto-regulation feedback loops for both of its transcription and translation through direct interactions of the L4 protein (*rplD*), the third gene in the *rpsJ* operon, with the 5′ UTR of the polycistronic transcript (161-166). The 5’ UTR has been identified as containing two hairpin regions, HD and HE, which are responsible for transcriptional and translational control (161-164,166,167). The HD loop is necessary for L4/NusA activity and thus essential for transcriptional control, while the HE loop, which has homology to 23S rRNA, is where termination occurs and is essential to both transcriptional and translational control. Different nucleotides of HE hairpin are necessary for translational and transcriptional control (166), in that mutations of the region have been shown to abolish one without the loss of the other.

A. Direct Control of *rpsJ* transcript levels via the L4 protein

One mechanism that helps control *rpsJ* transcript levels is through L4 protein levels (168,169). In this mechanism, excess L4 protein, together with the NusA protein, will recognize and bind specific nucleotides in the hairpin loops of the 5′-UTR of *rpsJ* causing transcriptional termination, which leads to decreased protein concentrations of

all the operon's proteins in the cell (161-164,166). Additionally, L4 interaction with the hairpin is thought to sequester the Shine-Delgarno sequence and the ribosomal entry site, preventing translation (160,170).

B. Indirect Control of *rpsJ* transcript levels via the S10 protein

The second mechanism by which the *rpsJ* operon is controlled is through S10 protein concentrations. S10 (formerly known as NusE), is encoded by the *rpsJ* gene and is essential to the cellular viability. In this mechanism, which has yet to be fully elucidated, excess S10, together with NusB and other antitermination factors (171-173), promote antitermination of the seven *rrn* operons, allowing more rRNA to be transcribed. These rRNAs, together with the r-proteins, will then form mature ribosomes, directly leading to a decrease in excess r-proteins in the cell (172-174).

Processing of the *rpsJ* Operon

To date, processing of the large polycistronic *rpsJ* operon has not been examined. It is generally assumed that the *rpsJ* operon transcript it is processed into smaller, more manageable pieces, like other large polycistronic transcripts, but this hypothesis has never been directly tested. This hypothesis will be examined and discussed more fully in Chapter 2.

Polyadenylation of the *rpsJ* Operon

Macroarray data has suggested that at least some of the transcripts in the *rpsJ* operon are polyadenylated (135). However, this phenomenon has not been examined in detail,

nor has it been established if all ORFs within a polycistronic transcript are polyadenylated in the same manner. This question will be examined and discussed in Chapter 3 of this dissertation.

FIGURES

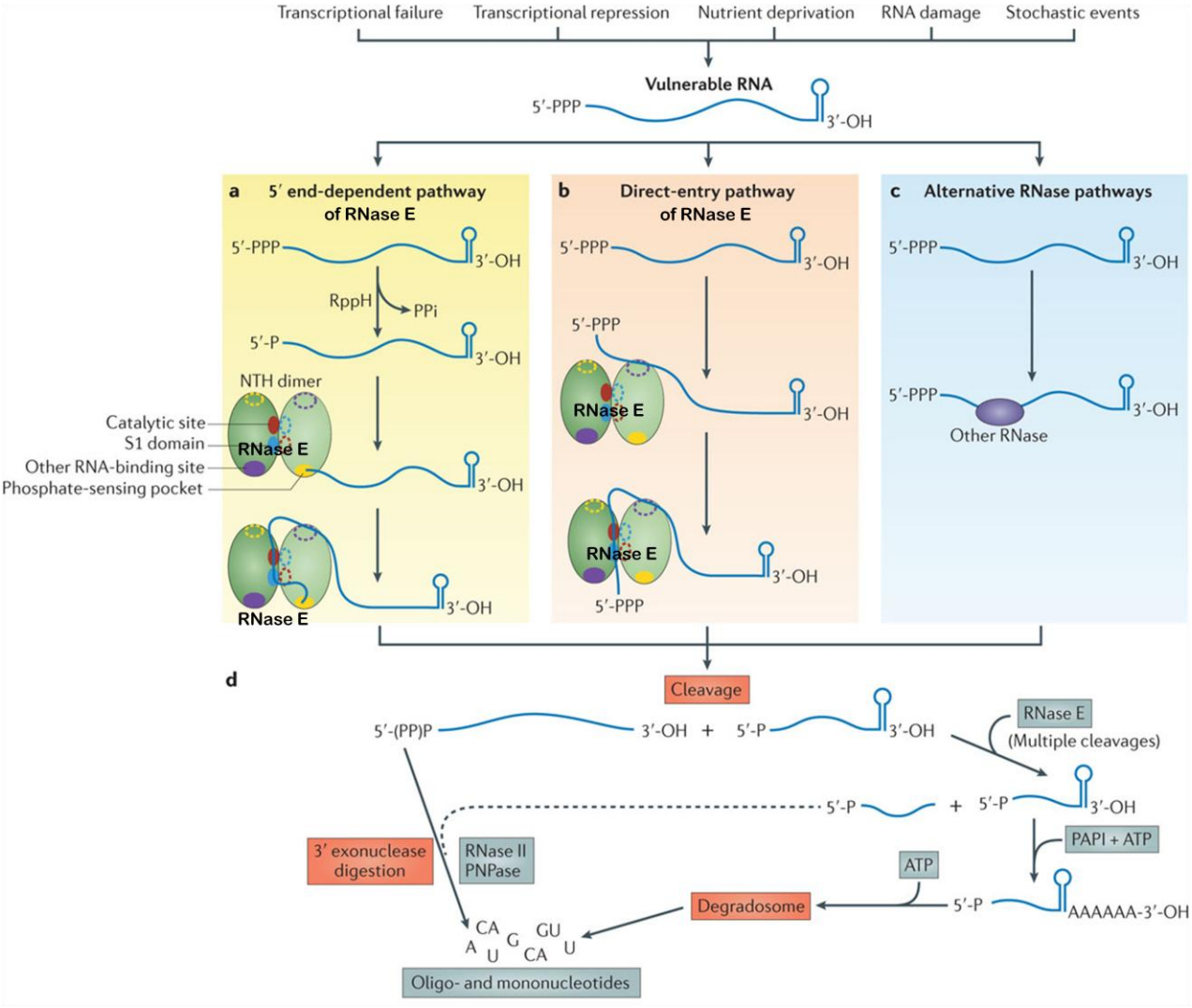

Figure 1.1. Model of mRNA decay pathways in *E. coli*. This figure shows the currently proposed pathways of mRNA decay and is modified from an extensive review on the topic (175).

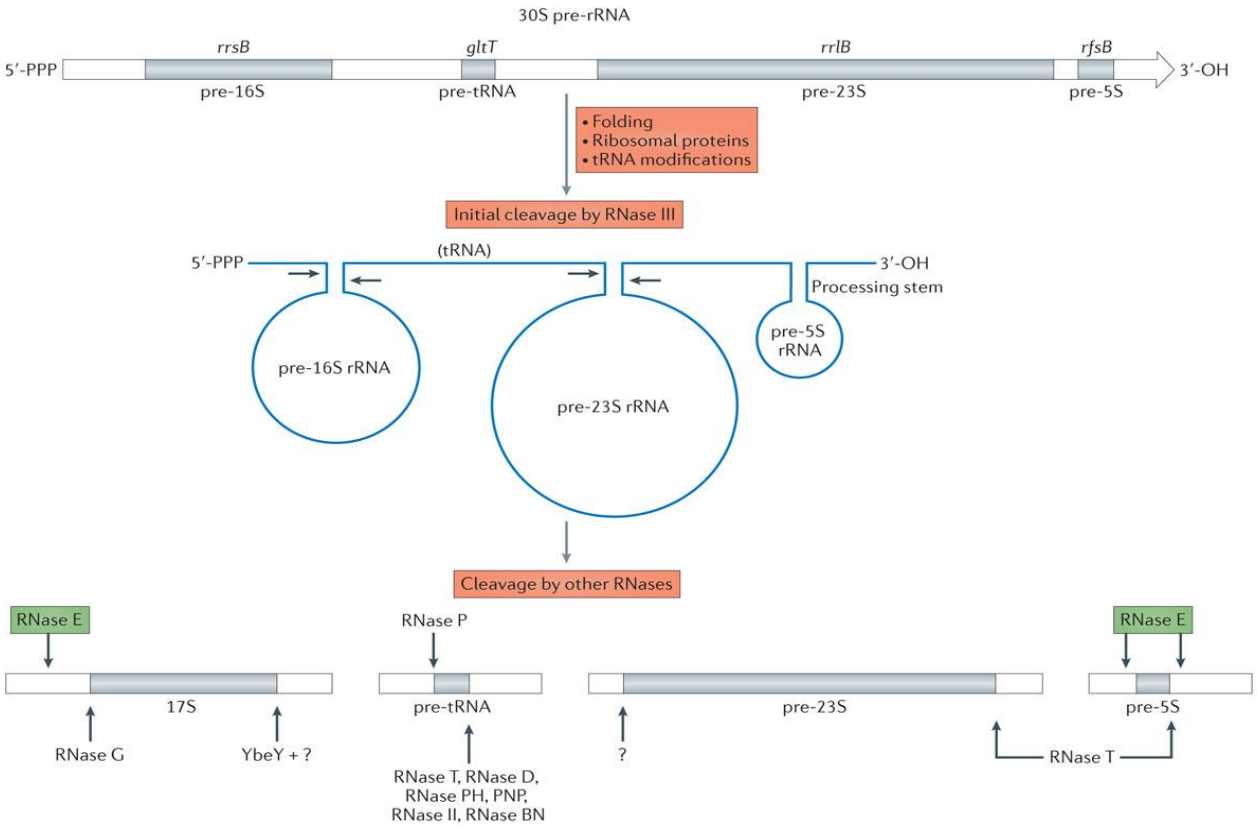

Figure 1.2. Model of rRNA processing pathways in *E. coli*. This figure shows the currently proposed pathways of rRNA processing and is from an extensive review on the topic (175).

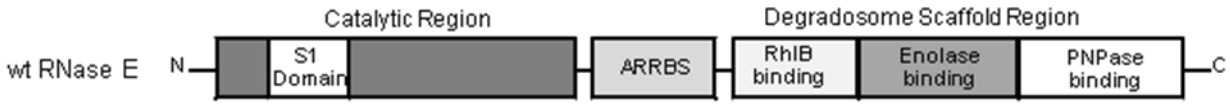

Figure 1.3. Schematic of wild-type RNase E protein. The areas labeled on the degradosome scaffold region indicate the associated binding site of the various proteins listed in the boxes. The S1 RNA binding domain and Arginine-rich RNA binding site (ARRBS) are also shown.

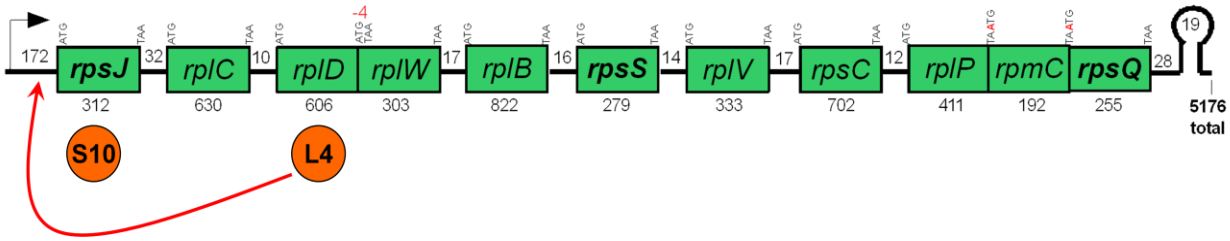

Figure 1.4. The *rpsJ* transcript. Two of the eleven encoded proteins are shown. Nucleotide lengths of the 5' UTR, each gene, intercistronic regions and the stem-loop terminator are shown above.

REFERENCES

1. Kushner, S.R. (2002) mRNA decay in *Escherichia coli* comes of age. *J. Bacteriol.*, **184**, 4658-4665.
2. Deutscher, M.P. (2006) Degradation of RNA in bacteria: comparison of mRNA and stable RNA. *Nucleic Acids Res.*, **34**, 659-666.
3. Donovan, W.P. and Kushner, S.R. (1986) Polynucleotide phosphorylase and ribonuclease II are required for cell viability and mRNA turnover in *Escherichia coli* K-12. *Proc. Natl. Acad. Sci. USA*, **83**, 120-124.
4. Carpousis, A.J. (2007) The RNA degradosome of *Escherichia coli*: an mRNA-degrading machine assembled on RNase E. *Annu. Rev. Microbiol.*, **61**, 71-87.
5. McDowall, K.J., Lin-Chao, S. and Cohen, S.N. (1994) A+U content rather than a particular nucleotide order determines the specificity of RNase E cleavage. *J. Biol. Chem.*, **269**, 10790-10796.
6. Mackie, G.A. (1992) Secondary structure of the mRNA for ribosomal protein S20. Implications for cleavage by ribonuclease E. *J. Biol. Chem.*, **267**, 1054-1061.
7. Stead, M.B., Marshburn, S., Mohanty, B.K., Mitra, J., Pena Castillo, L., Ray, D., van Bakel, H., Hughes, T.R. and Kushner, S.R. (2011) Analysis of *Escherichia coli* RNase E and RNase III activity *in vivo* using tiling microarrays. *Nucleic Acids Res.*, **39**, 3188-3203.
8. Misra, T.K. and Apirion, D. (1979) RNase E, an RNA processing enzyme from *Escherichia coli*. *J. Biol. Chem.*, **254**, 11154-11159.
9. Apirion, D. and Lassar, A.B. (1978) A conditional lethal mutant of *Escherichia coli* which affects the processing of ribosomal RNA. *J. Biol. Chem.*, **253**, 1738-1742.

10. Li, Z., Pandit, S. and Deutscher, M.P. (1999) RNase G (CafA protein) and RNase E are both required for the 5' maturation of 16S ribosomal RNA. *EMBO J.*, **18**, 2878-2885.

11. Ow, M.C., Liu, Q., Mohanty, B.K., Andrew, M.E., Maples, V.F. and Kushner, S.R. (2002) RNase E levels in *Escherichia coli* are controlled by a complex regulatory system that involves transcription of the *rne* gene from three promoters. *Mol. Microbiol.*, **43**, 159-171.

12. Lin-Chao, S., Wei, C.L. and Lin, Y.T. (1999) RNase E is required for the maturation of *ssrA* RNA and normal *ssrA* RNA peptide-tagging activity. *Proc. Natl. Acad. Sci. USA*, **96**, 12406-12411.

13. Callaghan, A.J., Marcaida, M.J., Stead, J.A., McDowall, K.J., Scott, W.G. and Luisi, B.F. (2005) Structure of *Escherichia coli* RNase E catalytic domain and implications for RNA turnover. *Nature*, **437**, 1187-1191.

14. Koslover, D.J., Callaghan, A.J., Marcaida, M.J., Garman, E.F., Martick, M., Scott, W.G. and Luisi, B.F. (2008) The crystal structure of the *Escherichia coli* RNase E apoprotein and a mechanism for RNA degradation. *Structure*, **16**, 1238-1244.

15. Callaghan, A.J., Redko, Y., Murphy, L.M., Grossmann, J.G., Yates, D., Garman, E., Ilag, L.L., Robinson, C.V., Symmons, M.F., McDowall, K.J. *et al.* (2005) "Zn-link": a metal-sharing interface that organizes the quaternary structure and catalytic site of the endoribonuclease, RNase E. *Biochemistry*, **44**, 4667-4675.

16. Kaberdin, V.R., Miczak, A., Jakobsen, J.S., Lin-Chao, S., McDowall, K.J. and von Gabain, A. (1998) The endoribonucleolytic N-terminal half of *Escherichia coli* RNase E is evolutionarily conserved in *Synechocystis sp.* and other bacteria but

not the C-terminal half, which is sufficient for degradosome assembly. *Proc. Natl. Acad. Sci. USA*, **95**, 11637-11642.

17. Callaghan, A.J., Aurikko, J.P., Ilag, L.L., Gunter Grossmann, J., Chandran, V., Kuhnel, K., Poljak, L., Carpousis, A.J., Robinson, C.V., Symmons, M.F. *et al.* (2004) Studies of the RNA degradosome-organizing domain of the *Escherichia coli* ribonuclease RNase E. *J. Mol. Biol.*, **340**, 965-979.
18. Vanzo, N.F., Li, Y.S., Py, B., Blum, E., Higgins, C.F., Raynal, L.C., Krisch, H.M. and Carpousis, A.J. (1998) Ribonuclease E organizes the protein interactions in the *Escherichia coli* RNA degradosome. *Genes Dev.*, **12**, 2770-2781.
19. Carpousis, A.J., Luisi, B.F. and McDowall, K.J. (2009) Endonucleolytic initiation of mRNA decay in *Escherichia coli*. *Prog. Mol. Biol. Transl. Sci.*, **85**, 91-135.
20. Deana, A., Celesnik, H. and Belasco, J.G. (2008) The bacterial enzyme RppH triggers messenger RNA degradation by 5' pyrophosphate removal. *Nature*, **451**, 355-358.
21. Kime, L., Jourdan, S.S., Stead, J.A., Hidalgo-Sastre, A. and McDowall, K.J. (2010) Rapid cleavage of RNA by RNase E in the absence of 5' monophosphate stimulation. *Mol. Microbiol.*, **76**, 590-604.
22. Baker, K.E. and Mackie, G.A. (2003) Ectopic RNase E sites promote bypass of 5'-end-dependent mRNA decay in *Escherichia coli*. *Mol. Microbiol.*, **47**, 75-88.
23. Luciano, D.J., Hui, M.P., Deana, A., Foley, P.L., Belasco, K.J. and Belasco, J.G. (2012) Differential control of the rate of 5'-end-dependent mRNA degradation in *Escherichia coli*. *J. Bacteriol.*, **194**, 6233-6239.

24. Okada, Y., Wachi, M., Hirata, A., Suzuki, K., Nagai, K. and Matsuhashi, M. (1994) Cytoplasmic axial filaments in *Escherichia coli* cells: possible function in the mechanism of chromosome segregation and cell division. *J. Bacteriol.*, **176**, 917-922.

25. Wachi, M., Umitsuki, G., Shimizu, M., Takada, A. and Nagai, K. (1999) *Escherichia coli cafA* gene encodes a novel RNase, designated as RNase G, involved in processing of the 5' end of 16S rRNA. *Biochem. Biophys. Res. Commun.*, **259**, 483-488.

26. Briant, D.J., Hankins, J.S., Cook, M.A. and Mackie, G.A. (2003) The quaternary structure of RNase G from *Escherichia coli*. *Mol. Microbiol.*, **50**, 1381-1390.

27. Lee, K., Bernstein, J.A. and Cohen, S.N. (2002) RNase G complementation of rne null mutation identifies functional interrelationships with RNase E in *Escherichia coli*. *Mol. Microbiol.*, **43**, 1445-1456.

28. Ow, M.C., Perwez, T. and Kushner, S.R. (2003) RNase G of *Escherichia coli* exhibits only limited functional overlap with its essential homologue, RNase E. *Mol. Microbiol.*, **49**, 607-622.

29. Tamura, M., Lee, K., Miller, C.A., Moore, C.J., Shirako, Y., Kobayashi, M. and Cohen, S.N. (2006) RNase E maintenance of proper FtsZ/FtsA ratio required for nonfilamentous growth of *Escherichia coli* cells but not for colony-forming ability. *J. Bacteriol.*, **188**, 5145-5152.

30. Chung, D.H., Min, Z., Wang, B.C. and Kushner, S.R. (2010) Single amino acid changes in the predicted RNase H domain of *Escherichia coli* RNase G lead to complementation of RNase E deletion mutants. *RNA*, **16**, 1371-1385.

31. Kim, K.S. and Lee, Y. (2004) Regulation of 6S RNA biogenesis by switching utilization of both sigma factors and endoribonucleases. *Nucleic Acids Res.*, **32**, 6057-6068.

32. Mohanty, B.K. and Kushner, S.R. (2007) Ribonuclease P processes polycistronic tRNA transcripts in *Escherichia coli* independent of ribonuclease E. *Nucleic Acids Res.*, **35**, 7614-7625.

33. Mohanty, B.K. and Kushner, S.R. (2008) Rho-independent transcription terminators inhibit RNase P processing of the *secG leuU* and *metT* tRNA polycistronic transcripts in *Escherichia coli*. *Nucleic Acids Res.*, **36**, 364-375.

34. Dunn, J.J. and Studier, F.W. (1973) T7 early RNAs and *Escherichia coli* ribosomal RNAs are cut from large precursor RNAs *in vivo* by ribonuclease 3. *Proc. Natl. Acad. Sci. USA*, **70**, 3296-3300.

35. Portier, C., Dondon, L., Grunberg-Manago, M. and Regnier, P. (1987) The first step in the functional inactivation of the *Escherichia coli* polynucleotide phosphorylase messenger is a ribonuclease III processing at the 5' end. *EMBO J.*, **6**, 2165-2170.

36. Meng, W. and Nicholson, A.W. (2008) Heterodimer-based analysis of subunit and domain contributions to double-stranded RNA processing by *Escherichia coli* RNase III in vitro. *Biochem. J.*, **410**, 39-48.

37. Babitzke, P. and Kushner, S.R. (1991) The Ams (altered mRNA stability) protein and ribonuclease E are encoded by the same structural gene of *Escherichia coli*. *Proc. Natl. Acad. Sci. USA*, **88**, 1-5.

38. Li, Y. and Altman, S. (2003) A specific endoribonuclease, RNase P, affects gene expression of polycistronic operon mRNAs. *Proc. Natl. Acad. Sci. USA*, **100**, 13213-13218.

39. Perwez, T. and Kushner, S.R. (2006) RNase Z in *Escherichia coli* plays a significant role in mRNA decay. *Mol. Microbiol.*, **60**, 723-737.

40. Dutta, T. and Deutscher, M.P. (2009) Catalytic properties of RNase BN/RNase Z from *Escherichia coli*: RNase BN is both an exo- and endoribonuclease. *J. Biol. Chem.*, **284**, 15425-15431.

41. Asha, P.K., Blouin, R.T., Zaniewski, R. and Deutscher, M.P. (1983) Ribonuclease BN: identification and partial characterization of a new tRNA processing enzyme. *Proc. Natl. Acad. Sci. USA*, **80**, 3301-3304.

42. Ohtani, N., Haruki, M., Morikawa, M., Crouch, R.J., Itaya, M. and Kanaya, S. (1999) Identification of the genes encoding Mn2+-dependent RNase HII and Mg2+-dependent RNase HIII from *Bacillus subtilis*: classification of RNases H into three families. *Biochemistry*, **38**, 605-618.

43. Otsuka, Y. and Yonesaki, T. (2005) A novel endoribonuclease, RNase LS, in *Escherichia coli*. *Genetics*, **169**, 13-20.

44. Koga, M., Otsuka, Y., Lemire, S. and Yonesaki, T. (2011) *Escherichia coli rnlA* and *rnlB* compose a novel toxin-antitoxin system. *Genetics*, **187**, 123-130.

45. Subbarayan, P.R. and Deutscher, M.P. (2001) *Escherichia coli* RNase M is a multiply altered form of RNase I. *RNA*, **7**, 1702-1707.

46. Deutscher, M.P. (1993) Promiscuous exoribonucleases of *Escherichia coli*. *J. Bacteriol.*, **175**, 4577-4583.

47. Jarrige, A.-C., Brechemier-Baey, D., Mathy, N., Duche, O. and Portier, C. (2002) Mutational analysis of polynucleotide phosphorylase from *Escherichia coli*. *J. Mol. Biol.*, **321**, 397-409.

48. Briani, F., Del Favero, M., Capizzuto, R., Consonni, C., Zangrossi, S., Greco, C., De Gioia, L., Tortora, P. and Deho, G. (2007) Genetic analysis of polynucleotide phosphorylase structure and functions. *Biochimie*, **89**, 145-157.

49. Carpousis, A.J., Van Houwe, G., Ehretsmann, C. and Krisch, H.M. (1994) Copurification of *E. coli* RNAase E and PNPase: evidence for a specific association between two enzymes important in RNA processing and degradation. *Cell*, **76**, 889-900.

50. Mohanty, B.K. and Kushner, S.R. (2000) Polynucleotide phosphorylase functions both as a 3' - 5' exonuclease and a poly(A) polymerase in *Escherichia coli*. *Proc. Natl. Acad. Sci. USA*, **97**, 11966-11971.

51. Arraiano, C.M., Yancey, S.D. and Kushner, S.R. (1988) Stabilization of discrete mRNA breakdown products in *ams pnp rnb* multiple mutants of *Escherichia coli* K-12. *J. Bacteriol.*, **170**, 4625-4633.

52. Guarneros, G. and Portier, C. (1991) Different specificities of ribonuclease II and polynucleotide phosphorylase in 3'mRNA decay. *Biochimie*, **73**, 543-549.

53. Spickler, C. and Mackie, G.A. (2000) Action of RNase II and polynucleotide phosphorylase against RNAs containing stem-loops of defined structure. *J. Bacteriol.*, **182**, 2422-2427.

54. Nurmohamed, S., Vaidialingam, B., Callaghan, A.J. and Luisi, B.F. (2009) Crystal structure of *Escherichia coli* polynucleotide phosphorylase core bound to RNase

E, RNA and manganese: implications for catalytic mechanism and RNA degradosome assembly. *J. Mol. Biol.*, **389**, 17-33.

55. Shi, Z., Yang, W.Z., Lin-Chao, S., Chak, K.F. and Yuan, H.S. (2008) Crystal structure of *Escherichia coli* PNPase: central channel residues are involved in processive RNA degradation. *RNA*, **14**, 2361-2371.

56. Py, B., Higgins, C.F., Krisch, H.M. and Carpousis, A.J. (1996) A DEAD-box RNA helicase in the *Escherichia coli* RNA degradosome. *Nature*, **381**, 169-172.

57. Coburn, G.A., Miao, X., Briant, D.J. and Mackie, G.A. (1999) Reconstitution of a minimal RNA degradosome demonstrates functional coordination between a 3' exonuclease and a DEAD-box RNA helicase. *Genes Dev.*, **13**, 2594-2603.

58. De Lay, N. and Gottesman, S. (2011) Role of polynucleotide phosphorylase in sRNA function in *Escherichia coli*. *RNA*, **17**, 1172-1189.

59. Andrade, J.M., Pobre, V., Matos, A.M. and Arraiano, C.M. (2012) The crucial role of PNPase in the degradation of small RNAs that are not associated with Hfq. *RNA*, **18**, 844-855.

60. Mohanty, B.K. and Kushner, S.R. (2000) Polynucleotide phosphorylase, RNase II and RNase E play different roles in the *in vivo* modulation of polyadenylation in *Escherichia coli*. *Mol. Microbiol.*, **36**, 982-994.

61. Kelly, K.O. and Deutscher, M.P. (1992) The presence of only one of five exoribonucleases is sufficient to support the growth of *Escherichia coli*. *J. Bacteriol.*, **174**, 6682-6684.

62. Frazao, C., McVey, C.E., Amblar, M., Barbas, A., Vonrhein, C., Arraiano, C.M. and Carrondo, M.A. (2006) Unravelling the dynamics of RNA degradation by ribonuclease II and its RNA-bound complex. *Nature*, **443**, 110-114.

63. Cannistraro, V.J. and Kennell, D. (1994) The processive reaction mechanism of ribonuclease II. *J. Mol. Biol.*, **243**, 930-943.

64. Kelly, K.O. and Deutscher, M.P. (1992) Characterization of *Escherichia coli* RNase PH. *J. Biol. Chem.*, **267**, 17153-17158.

65. Vincent, H.A. and Deutscher, M.P. (2006) Substrate recognition and catalysis by the exoribonuclease RNase R. *J. Biol. Chem.*, **281**, 29769-29775.

66. Jacob, A.I., Kohrer, C., Davies, B.W., RajBhandary, U.L. and Walker, G.C. (2013) Conserved bacterial RNase YbeY plays key roles in 70S ribosome quality control and 16S rRNA maturation. *Mol. Cell*, **49**, 427-438.

67. Ge, Z., Mehta, P., Richards, J. and Karzai, A.W. (2010) Non-stop mRNA decay initiates at the ribosome. *Mol. Microbiol.*, **78**, 1159-1170.

68. Andrade, J.M., Hajnsdorf, E., Regnier, P. and Arraiano, C.M. (2009) The poly(A)-dependent degradation pathway of *rpsO* mRNA is primarily mediated by RNase R. *RNA*, **15**, 316-326.

69. Li, Z., Reimers, S., Pandit, S. and Deutscher, M.P. (2002) RNA quality control: degradation of defective transfer RNA. *EMBO J.*, **21**, 1132-1138.

70. Cheng, Z.F. and Deutscher, M.P. (2003) Quality control of ribosomal RNA mediated by polynucleotide phosphorylase and RNase R. *Proc. Natl. Acad. Sci. USA*, **100**, 6388-6393.

71. Warner, J.R. (2013) YbeY: the jealous tailor. *Mol. Cell*, **49**, 422-423.

72. Cairrao, F., Cruz, A., Mori, H. and Arraiano, C.M. (2003) Cold shock induction of RNase R and its role in the maturation of the quality control mediator SsrA/tmRNA. *Mol. Microbiol.*, **50**, 1349-1360.

73. Cairrao, F. and Arraiano, C.M. (2006) The role of endoribonucleases in the regulation of RNase R. *Biochem. Biophys. Res. Commun.*, **343**, 731-737.

74. Andrade, J.M., Cairrao, F. and Arraiano, C.M. (2006) RNase R affects gene expression in stationary phase: regulation of *ompA*. *Mol. Microbiol.*, **60**, 219-228.

75. Chen, C. and Deutscher, M.P. (2005) Elevation of RNase R in response to multiple stress conditions. *J. Biol. Chem.*, **280**, 34393-34396.

76. Ghosh, S. and Deutscher, M.P. (1999) Oligoribonuclease is an essential component of the mRNA decay pathway. *Proc. Natl. Acad. Sci. USA*, **96**, 4372-4377.

77. Datta, A.K. and Niyogi, K. (1975) A novel oligoribonuclease of *Escherichia coli*. II. Mechanism of action. *J. Biol. Chem.*, **250**, 7313-7319.

78. Niyogi, S.K. and Datta, A.K. (1975) A novel oligoribonuclease of *Escherichia coli*. I. Isolation and properties. *J. Biol. Chem.*, **250**, 7307-7312.

79. Yu, D. and Deutscher, M.P. (1995) Oligoribonuclease is distinct from the other known exoribonucleases of *Escherichia coli*. *J. Bacteriol.*, **177**, 4137-4139.

80. Zuo, Y. and Deutscher, M.P. (2001) Exoribonuclease superfamilies: structural analysis and phylogenetic distribution. *Nucleic Acids Res.*, **29**, 1017-1026.

81. Viswanathan, M., Dower, K.W. and Lovett, S.T. (1998) Identification of a potent DNase activity associated with RNase T of *Escherichia coli*. *J. Biol. Chem.*, **273**, 35126-35131.

82. Cudny, H. and Deutscher, M.P. (1988) 3' processing of tRNA precursors in ribonuclease-deficient *Escherichia coli*. Development and characterization of an *in vitro* processing system and evidence for a phosphate requirement. *J. Biol. Chem.*, **263**, 1518-1523.

83. Cudny, H. and Deutscher, M.P. (1980) Apparent involvement of ribonuclease D in the 3' processing of tRNA precursors. *Proc. Natl. Acad. Sci. USA*, **77**, 837-841.

84. Cudny, H., Zaniewski, R. and Deutscher, M.P. (1981) *Escherichia coli* RNase D. Catalytic properties and substrate specificity. *J. Biol. Chem.*, **256**, 5633-5637.

85. Cudny, H., Zaniewski, R. and Deutscher, M.P. (1981) *Escherichia coli* RNase D. Purification and structural characterization of a putative processing nuclease. *J. Biol. Chem.*, **256**, 5627-5632.

86. Deutscher, M.P., Marshall, G.T. and Cudny, H. (1988) RNase PH: an *Escherichia coli* phosphate-dependent nuclease distinct from polynucleotide phosphorylase. *Proc. Natl. Acad. Sci. USA*, **85**, 4710-4714.

87. Ishii, R., Nureki, O. and Yokoyama, S. (2003) Crystal structure of the tRNA processing enzyme RNase PH from *Aquifex aeolicus*. *J. Biol. Chem.*, **278**, 32397-32404.

88. Choi, J.M., Park, E.Y., Kim, J.H., Chang, S.K. and Cho, Y. (2004) Probing the functional importance of the hexameric ring structure of RNase PH. *J. Biol. Chem.*, **279**, 755-764.

89. Zhou, Z. and Deutscher, M.P. (1997) An essential function for the phosphate-dependent exoribonucleases RNase PH and polynucleotide phosphorylase. *J. Bacteriol.*, **179**, 4391-4395.

90. Redko, Y. and Condon, C. (2010) Maturation of 23S rRNA in *Bacillus subtilis* in the absence of Mini-III. *J. Bacteriol.*, **192**, 356-359.

91. Li, Z., Pandit, S. and Deutscher, M.P. (1998) 3' exoribonucleolytic trimming is a common feature of the maturation of small, stable RNAs in *Escherichia coli*. *Proc. Natl. Acad. Sci. USA*, **95**, 2856-2861.

92. Kelly, K.O., Reuven, N.B., Li, Z. and Deutscher, M.P. (1992) RNase PH is essential for tRNA processing and viability in RNase-deficient *Escherichia coli* cells. *J. Biol. Chem.*, **267**, 16015-16018.

93. Dutta, T., Malhotra, A. and Deutscher, M.P. (2012) Exoribonuclease and endoribonuclease activities of RNase BN/RNase Z both function *in vivo*. *J. Biol. Chem.*, **287**, 35747-35755.

94. Kushner, S.R. (2004) mRNA decay in prokaryotes and eukaryotes: different approaches to a similar problem. *IUBMB Life*, **56**, 585-594.

95. Bandyra, K.J., Bouvier, M., Carpousis, A.J. and Luisi, B.F. (2013) The social fabric of the RNA degradosome. *Biochim. Biophys. Acta*, **1829**, 514-522.

96. Schuck, A., Diwa, A. and Belasco, J.G. (2009) RNase E autoregulates its synthesis in *Escherichia coli* by binding directly to a stem-loop in the *rne* 5' untranslated region. *Mol. Microbiol.*, **72**, 470-478.

97. Diwa, A.A. and Belasco, J.G. (2002) Critical features of a conserved RNA stem-loop important for feedback regulation of RNase E synthesis. *J. Biol. Chem.*, **277**, 20415-20422.

98. Jain, C. and Belasco, J.G. (1995) RNase E autoregulates its synthesis by controlling the degradation rate of its own mRNA in *Escherichia coli*: unusual sensitivity of the *rne* transcript to RNase E activity. *Genes Dev.*, **9**, 84-96.

99. Masse, E., Escorcia, F.E. and Gottesman, S. (2003) Coupled degradation of a small regulatory RNA and its mRNA targets in *Escherichia coli*. *Genes Dev.*, **17**, 2374-2383.

100. Lalaouna, D., Simoneau-Roy, M., Lafontaine, D. and Masse, E. (2013) Regulatory RNAs and target mRNA decay in prokaryotes. *Biochim. Biophys. Acta*, **1829**, 742-747.

101. Py, B., Causton, H., Mudd, E.A. and Higgins, C.F. (1994) A protein complex mediating mRNA degradation in *Escherichia coli*. *Mol. Microbiol.*, **14**, 717-729.

102. Miczak, A., Kaberdin, V.R., Wei, C.L. and Lin-Chao, S. (1996) Proteins associated with RNase E in a multicomponent ribonucleolytic complex. *Proc. Natl. Acad. Sci. USA*, **93**, 3865-3869.

103. Prud'homme-Genereux, A., Beran, R.K., Iost, I., Ramey, C.S., Mackie, G.A. and Simons, R.W. (2004) Physical and functional interactions among RNase E, polynucleotide phosphorylase and the cold-shock protein, CsdA: evidence for a 'cold shock degradosome'. *Mol. Microbiol.*, **54**, 1409-1421.

104. Liou, G.G., Jane, W.N., Cohen, S.N., Lin, N.S. and Lin-Chao, S. (2001) RNA degradosomes exist *in vivo* in *Escherichia coli* as multicomponent complexes associated with the cytoplasmic membrane via the N-terminal region of ribonuclease E. *Proc. Natl. Acad. Sci. USA*, **98**, 63-68.

105. Ow, M.C., Liu, Q. and Kushner, S.R. (2000) Analysis of mRNA decay and rRNA processing in *Escherichia coli* in the absence of RNase E-based degradosome assembly. *Mol. Microbiol.*, **38**, 854-866.

106. Khemici, V., Poljak, L., Luisi, B.F. and Carpousis, A.J. (2008) The RNase E of *Escherichia coli* is a membrane-binding protein. *Mol. Microbiol.*, **70**, 799-813.

107. Lopez, P.J., Marchand, I., Joyce, S.A. and Dreyfus, M. (1999) The C-terminal half of RNase E, which organizes the *Escherichia coli* degradosome, participates in mRNA degradation but not rRNA processing *in vivo*. *Mol. Microbiol.*, **33**, 188-199.

108. Ikeda, Y., Yagi, M., Morita, T. and Aiba, H. (2011) Hfq binding at RhlB-recognition region of RNase E is crucial for the rapid degradation of target mRNAs mediated by sRNAs in *Escherichia coli*. *Mol. Microbiol.*, **79**, 419-432.

109. Miczak, A., Srivastava, R.A. and Apirion, D. (1991) Location of the RNA-processing enzymes RNase III, RNase E and RNase P in the *Escherichia coli* cell. *Mol. Microbiol.*, **5**, 1801-1810.

110. Taghbalout, A. and Rothfield, L. (2007) RNase E and the other constituents of the RNA degradosome are components of the bacterial cytoskeleton. *Proc. Natl. Acad. Sci. USA*, **104**, 1667-1672.

111. Murashko, O.N., Kaberdin, V.R. and Lin-Chao, S. (2012) Membrane binding of *Escherichia coli* RNase E catalytic domain stabilizes protein structure and increases RNA substrate affinity. *Proc. Natl. Acad. Sci. USA*, **109**, 7019-7024.

112. Lin, P.H. and Lin-Chao, S. (2005) RhlB helicase rather than enolase is the beta-subunit of the *Escherichia coli* polynucleotide phosphorylase (PNPase)-exoribonucleolytic complex. *Proc. Natl. Acad. Sci. USA*, **102**, 16590-16595.

113. Mohanty, B.K., Maples, V.F. and Kushner, S.R. (2004) The Sm-like protein Hfq regulates polyadenylation dependent mRNA decay in *Escherichia coli*. *Mol. Microbiol.*, **54**, 905-920.

114. Kalman, M., Murphy, H. and Cashel, M. (1991) *rhlB*, a new *Escherichia coli* K-12 gene with an RNA helicase-like protein sequence motif, one of at least five such possible genes in a prokaryote. *New Biol.*, **3**, 886-895.

115. Chandran, V., Poljak, L., Vanzo, N.F., Leroy, A., Miguel, R.N., Fernandez-Recio, J., Parkinson, J., Burns, C., Carpousis, A.J. and Luisi, B.F. (2007) Recognition and cooperation between the ATP-dependent RNA helicase RhlB and ribonuclease RNase E. *J. Mol. Biol.*, **367**, 113-132.

116. Iost, I. and Dreyfus, M. (2006) DEAD-box RNA helicases in *Escherichia coli*. *Nucleic Acids Res.*, **34**, 4189-4197.

117. Liou, G.G., Chang, H.Y., Lin, C.S. and Lin-Chao, S. (2002) DEAD box RhlB RNA helicase physically associates with exoribonuclease PNPase to degrade double-stranded RNA independent of the degradosome-assembling region of RNase E. *J. Biol. Chem.*, **277**, 41157-41162.

118. Aiba, H. (2007) Mechanism of RNA silencing by Hfq-binding small RNAs. *Curr. Opin. Microbiol.*, **10**, 134-139.

119. Caponigro, G. and Parker, R. (1996) Mechanism and control of mRNA turnover in *Saccharomyces cerevisiae*. *Microbiol. Rev.*, **60**, 233-249.

120. Ryan, K. and Bauer, D.L. (2008) Finishing touches: post-translational modification of protein factors involved in mammalian pre-mRNA 3' end formation. *Int. J Biochem. Cell Biol.*, **40**, 2384-2396.

121. Ross, J. (1996) Control of messenger RNA stability in higher eukaryotes. *Trends Genet.*, **12**, 171-175.

122. Hajnsdorf, E., Braun, F., Haugel-Nielsen, J. and Régnier, P. (1995) Polyadenylylation destabilizes the *rpsO* mRNA of *Escherichia coli*. *Proc. Natl. Acad. Sci. USA*, **92**, 3973-3977.

123. Coburn, G.A. and Mackie, G.A. (1996) Differential sensitivities of portions of the mRNA for ribosomal protein S20 to 3'-exonucleases is dependent on oligoadenylation and RNA secondary structure. *J. Biol. Chem.*, **271**, 15776-15781.

124. Li, Z., Pandit, S. and Deutscher, M.P. (1998) Polyadenylation of stable RNA precursors *in vivo*. *Proc. Natl. Acad. Sci. USA*, **95**, 12158-12162.

125. O'Hara, E.B., Chekanova, J.A., Ingle, C.A., Kushner, Z.R., Peters, E. and Kushner, S.R. (1995) Polyadenylylation helps regulate mRNA decay in *Escherichia coli*. *Proc. Natl. Acad. Sci. USA*, **92**, 1807-1811.

126. Xu, F., Lin-Chao, S. and Cohen, S.N. (1993) The *Escherichia coli pcnB* gene promotes adenylylation of antisense RNAI of ColE1-type plasmids in vivo and degradation of RNAI decay intermediates. *Proc. Natl. Acad. Sci. USA*, **90**, 6756-6760.

127. Coburn, G.A. and Mackie, G.A. (1998) Reconstitution of the degradation of the mRNA for ribosomal protein S20 with purified enzymes. *J. Mol. Biol.*, **279**, 1061-1074.

128. Mohanty, B.K., Maples, V.F. and Kushner, S.R. (2012) Polyadenylation helps regulate functional tRNA levels in *Escherichia coli*. *Nucleic Acids Res.*, **40**, 4589-4603.

129. Mohanty, B.K. and Kushner, S.R. (2013) Deregulation of poly(A) polymerase I in *Escherichia coli* inhibits protein synthesis and leads to cell death. *Nucleic Acids Res.*, **41**, 1757-1766.

130. August, J.T., Ortiz, P.J. and Hurwitz, J. (1962) Ribonucleic acid-dependent ribonucleotide incorporation. I. Purification and properties of the enzyme. *J. Biol. Chem.*, **237**, 3786-3793.

131. Cao, G.J. and Sarkar, N. (1992) Poly(A) RNA in *Escherichia coli*: nucleotide sequence at the junction of the *lpp* transcript and the polyadenylate moiety. *Proc. Natl. Acad. Sci. USA*, **89**, 7546-7550.

132. Cao, G.-J. and Sarkar, N. (1992) Identification of the gene for an *Escherichia coli* poly(A) polymerase. *Proc. Natl. Acad. Sci. USA*, **89**, 10380-10384.

133. Aiso, T., Yoshida, H., Wada, A. and Ohki, R. (2005) Modulation of mRNA stability participates in stationary-phase-specific expression of ribosome modulation factor. *J. Bacteriol.*, **187**, 1951-1958.

134. Cao, G.J., Kalapos, M.P. and Sarkar, N. (1997) Polyadenylated mRNA in *Escherichia coli*: Modulation of poly(A) levels by polynucleotide phosphorylase and ribonuclease II. *Biochimie*, **79**, 211-220.

135. Mohanty, B.K. and Kushner, S.R. (2006) The majority of *Escherichia coli* mRNAs undergo post-transcriptional modification in exponentially growing cells. *Nucleic Acids Res.*, **34**, 5695-5704.

136. Mohanty, B.K. and Kushner, S.R. (1999) Analysis of the function of *Escherichia coli* poly(A) polymerase I in RNA metabolism. *Mol. Microbiol.*, **34**, 1094-1108.

137. Lesnik, E.A., Sampath, R., Levene, H.B., Henderson, T.J., McNeil, J.A. and Ecker, D.J. (2001) Prediction of Rho-independent transcriptional terminators in *Escherichia coli*. *Nucleic Acids Res.*, **29**, 3583-3594.

138. Jasiecki, J. and Wegrzyn, G. (2005) Localization of *Escherichia coli* poly(A) polymerase I in cellular membrane. *Biochem. Biophys. Res. Commun.*, **329**, 598-602.

139. Carabetta, V.J., Mohanty, B.K., Kushner, S.R. and Silhavy, T.J. (2009) The response regulator SprE (RssB) modulates polyadenylation and mRNA stability in *Escherichia coli*. *J. Bacteriol.*, **191**, 6812-6821.

140. Carabetta, V.J., Silhavy, T.J. and Cristea, I.M. (2010) The response regulator SprE (RssB) is required for maintaining poly(A) polymerase I-degradosome association during stationary phase. *J. Bacteriol.*, **192**, 3713-3721.

141. Kalapos, M.P., Cao, G.J., Kushner, S.R. and Sarkar, N. (1994) Identification of a second poly(A) polymerase in *Escherichia coli*. *Biochem. Biophys. Res. Commun.*, **198**, 459-465.

142. Cao, G.J., Pogliano, J. and Sarkar, N. (1996) Identification of the coding region for a second poly(A) polymerase in *Escherichia coli*. *Proc. Natl. Acad. Sci. USA*, **93**, 11580-11585.

143. Mohanty, B.K. and Kushner, S.R. (1999) Residual polyadenylation in poly(A) polymerase I (*pcnB*) mutants of *Escherichia coli* does not result from the activity encoded by the *f310* gene. *Mol. Microbiol.*, **34**, 1109-1119.

144. Soreq, H. and Littauer, U.Z. (1977) Purification and characterization of polynucleotide phosphorylase from *Escherichia coli*. Probe for the analysis of 3' sequences of RNA. *J. Biol. Chem.*, **252**, 6885-6888.

145. Rott, R., Zipor, G., Portnoy, V., Liveanu, V. and Schuster, G. (2003) RNA polyadenylation and degradation in cyanobacteria are similar to the chloroplast but different from *Escherichia coli*. *J. Biol. Chem.*, **278**, 15771-15777.

146. Sohlberg, B., Huang, J. and Cohen, S.N. (2003) The *Streptomyces coelicolor* polynucleotide phosphorylase homologue, and not the putative poly(A) polymerase, can polyadenylate RNA. *J. Bacteriol.*, **185**, 7273-7278.

147. Yehudai-Resheff, S. and Schuster, G. (2000) Characterization of the *E.coli* poly(A) polymerase: nucleotide specificity, RNA-binding affinities and RNA structure dependence. *Nucleic Acids Res.*, **28**, 1139-1144.

148. Sippel, A.E. (1973) Purification and characterization of adenosine triphosphate: ribonucleic acid adenyltransferase from *Escherichia coli*. *Eur. J. Biochem.*, **37**, 31-40.

149. Vogel, J. and Luisi, B.F. (2011) Hfq and its constellation of RNA. *Nat. Rev. Microbiol.*, **9**, 578-589.

150. Zhang, A., Wassarman, K.M., Ortega, J., Steven, A.C. and Storz, G. (2002) The Sm-like Hfq protein increases OxyS RNA interaction with target mRNAs. *Mol. Cell*, **9**, 11-22.

151. Waters, L.S. and Storz, G. (2009) Regulatory RNAs in bacteria. *Cell*, **136**, 615-628.

152. Panja, S. and Woodson, S.A. (2012) Hfq proximity and orientation controls RNA annealing. *Nucleic Acids Res.*, **40**, 8690-8697.

153. Kajitani, M., Kato, A., Wada, A., Inokuchi, Y. and Ishihama, A. (1994) Regulation of the *Escherichia coli hfq* gene encoding the host factor for phage Q beta. *J. Bacteriol.*, **176**, 531-534.

154. Mackie, G.A. (2000) Stabilization of circular *rpsT* mRNA demonstrates the 5'-end dependence of RNase E action *in vivo*. *J. Biol. Chem.*, **275**, 25069-25072.

155. Lindahl, L. and Zengel, J.M. (1982) Expression of ribosomal genes in bacteria. *Adv. Genet.*, **21**, 53-121.

156. Zurawski, G. and Zurawski, S.M. (1985) Structure of the *Escherichia coli* S10 ribosomal protein operon. *Nucleic Acids Res.*, **13**, 4521-4526.

157. Lindahl, L., Post, L., Zengel, J., Gilbert, S.F., Strycharz, W.A. and Nomura, M. (1977) Mapping of ribosomal protein genes by *in vitro* protein synthesis using DNA fragments of lambdafus3 transducing phage DNA as templates. *J. Biol. Chem.*, **252**, 7365-7383.

158. Nomura, M., Gourse, R. and Baughman, G. (1984) Regulation of the synthesis of ribosomes and ribosomal components. *Annu. Rev. Biochem.*, **53**, 75-117.

159. Squires, C.L. and Zaporojets, D. (2000) Proteins shared by the transcription and translation machines. *Annu. Rev. Microbiol.*, **54**, 775-798.

160. Nomura, M. (1999) Regulation of ribosome biosynthesis in *Escherichia coli* and *Saccharomyces cerevisiae*: diversity and common principles. *J. Bacteriol.*, **181**, 6857-6864.

161. Li, X., Lindahl, L. and Zengel, J.M. (1996) Ribosomal protein L4 from *Escherichia coli* utilizes nonidentical determinants for its structural and regulatory functions. *RNA*, **2**, 24-37.

162. Zengel, J.M. and Lindahl, L. (1996) A hairpin structure upstream of the terminator hairpin required for ribosomal protein L4-mediated attenuation control of the S10 operon of *Escherichia coli*. *J. Bacteriol.*, **178**, 2383-2387.

163. Sha, Y., Lindahl, L. and Zengel, J.M. (1995) RNA determinants required for L4-mediated attenuation control of the S10 r-protein operon of *Escherichia coli*. *J. Mol. Biol.*, **245**, 486-498.

164. Sha, Y., Lindahl, L. and Zengel, J.M. (1995) Role of NusA in L4-mediated attenuation control of the S10 r-protein operon of *Escherichia coli*. *J. Mol. Biol.*, **245**, 474-485.

165. Nomura, M., Yates, J.L., Dean, D. and Post, L.E. (1980) Feedback regulation of ribosomal protein gene expression in *Escherichia coli*: structural homology of ribosomal RNA and ribosomal protein MRNA. *Proc. Natl. Acad. Sci. USA*, **77**, 7084-7088.

166. Allen, T., Shen, P., Samsel, L., Liu, R., Lindahl, L. and Zengel, J.M. (1999) Phylogenetic analysis of L4-mediated autogenous control of the S10 ribosomal protein operon. *J. Bacteriol.*, **181**, 6124-6132.

167. Freedman, L.P., Zengel, J.M., Archer, R.H. and Lindahl, L. (1987) Autogenous control of the S10 ribosomal protein operon of *Escherichia coli*: genetic dissection of transcriptional and posttranscriptional regulation. *Proc. Natl. Acad. Sci. USA*, **84**, 6516-6520.

168. Lindahl, L., Archer, R. and Zengel, J.M. (1983) Transcription of the S10 ribosomal protein operon is regulated by an attenuator in the leader. *Cell*, **33**, 241-248.

169. Zengel, J.M., Mueckl, D. and Lindahl, L. (1980) Protein L4 of the *E. coli* ribosome regulates an eleven gene r protein operon. *Cell*, **21**, 523-535.

170. Yates, J.L. and Nomura, M. (1980) *E. coli* ribosomal protein L4 is a feedback regulatory protein. *Cell*, **21**, 517-522.

171. Mason, S.W., Li, J. and Greenblatt, J. (1992) Direct interaction between two *Escherichia coli* transcription antitermination factors, NusB and ribosomal protein S10. *J. Mol. Biol.*, **223**, 55-66.

172. Mason, S.W. and Greenblatt, J. (1991) Assembly of transcription elongation complexes containing the N protein of phage lambda and the *Escherichia coli* elongation factors NusA, NusB, NusG, and S10. *Genes Dev.*, **5**, 1504-1512.

173. Das, A., Ghosh, B., Barik, S. and Wolska, K. (1985) Evidence that ribosomal protein S10 itself is a cellular component necessary for transcription antitermination by phage lambda N protein. *Proc. Natl. Acad. Sci. USA*, **82**, 4070-4074.

174. Das, A. (1993) Control of transcription termination by RNA-binding proteins. *Annu. Rev. Biochem.*, **62**, 893-930.

175. Mackie, G.A. (2013) RNase E: at the interface of bacterial RNA processing and decay. *Nat. Rev. Microbiol.*, **11**, 45-57.

CHAPTER 2

RNASE E IS THE MAJOR ENDONUCLEASE RESPONSIBLE FOR PROCESSING THE POLYCISTRONIC *RPSJ* MESSENGER RNA TRANSCRIPT IN *ESCHERICHIA COLI*[1]

[1] Kristen B. Mildenhall, Bijoy K. Mohanty, and Sidney R. Kushner. To be submitted to J. Bacteriol.

ABSTRACT

The processing and decay of RNA species in *Escherichia coli* involves the complex interaction of endonucleases and exonucleases. As such, most studies have only dealt with the analysis of either mono- or dicistronic mRNAs. In this study, the processing/decay of the large polycistronic *rpsJ* transcript (containing 11 ORFs) has been examined. Our data suggest that RNase E is the major enzyme involved in the initial processing of the *rpsJ* transcript and is responsible for the removal of the 3' Rho-independent transcription terminator. Our results also indicate that the 5' untranslated region of the *rpsJ* transcript remains intact in wild-type cells. Additionally, the processing pattern of the *rpsJ* transcript suggests a role for additional endonucleases in secondary cleavages. Interestingly, the cell appears to maintain fixed ratios of each ORF transcript within the polycistronic *rpsJ* operon, despite changes in the processing of the full-length transcript in RNase E mutants. These results indicate greater flexibility for the cell to control the ribosomal protein levels at the transcript level than previously observed.

INTRODUCTION

The processing or decay of mRNAs in *Escherichia coli* is performed by a combination of endonucleases and 3'→5' exonucleases. The processing pathways are often a complex combination of primary and secondary endonucleolytic cleavages, along with exonucleolytic degradation of initial cleavage products. To date, other than a preliminary analysis of the *in vivo* turnover of the *trp* operon (1), no one has systematically examined the processing of a large polycistronic mRNA operon, despite the general assumption that these large transcripts are processed into smaller, more manageable species. Addressing the issue of processing of the large mRNA transcripts is especially pertinent for the ribosomal protein transcripts, as they are predominately found in large polycistronic operons. One such large polycistronic transcript is the *rpsJ* transcript (Fig. 2.1).

The *rpsJ* transcript is a 5.2 kb polycistronic transcript made up of 11 genes, all of which encode either 30S or 50S ribosomal subunit proteins (2,3). The *rpsJ* transcript has a highly structured 5' untranslated region (UTR) and a 3' Rho-independent transcription terminator (Fig. 2.2). The *rpsJ* operon has been well-studied and has been shown to have complex auto-regulation feedback of its transcription and translation through direct interaction of the L4 protein (*rplD*), the third gene in the *rpsJ* operon with the 5′ UTR of the polycistronic transcript (4-9).

Ribosomal proteins (r-proteins) are encoded in a one-to-one ratio to each other and to the 16S, 23S, and 5S rRNAs. The foundation of the cell's control of its rRNA and r-proteins is to maintain one-to-one balance of rRNA to each r-protein such that only

mature ribosomes are formed. Therefore the cell tightly regulates the transcription and translation of many of its r-protein operons (10-12).

Preliminary polyadenylation data of the *rpsJ* transcript suggested that this large polycistronic transcript was highly processed. Since RNase E is the major enzyme involved in initiating RNA processing and decay in *E. coli* (13), we hypothesized that this enzyme was responsible for the initial processing of the *rpsJ* transcript. To test this hypothesis, the processing patterns of the *rpsJ* transcript in various endonuclease and exonuclease mutants were examined and compared with a wild-type control using northern blots. These data demonstrated that RNase E was the primary endonuclease responsible for *rpsJ* transcript processing and the removal of the 3' Rho-independent transcription terminator. Furthermore, our results also indicate that other endonucleases are involved in a series of secondary cleavages.

MATERIALS AND METHODS

Bacterial Strains and Growth

All the strains and plasmids used in this study are listed in Table 2.1. They are all isogenic derivatives of MG1693. The *rne-1* allele encodes a temperature-sensitive mutation that functionally inactivates RNase E at 44^{o}C (14), while the *rnpA49* allele encodes a temperature-sensitive mutation that functionally inactivates the protein subunit of RNase P at 44^{o}C (15).

Bacterial strains were grown under one of three conditions: For experiments with temperature-sensitive mutations (*rne-1* or *rnpA49*), all strains were grown under similar conditions at 30°C with shaking at 225 rpm in Luria broth supplemented with thymine

(50 µg/ml) and streptomycin (20 mg/mL), chloramphenicol (20 mg/mL) or kanamycin (25 mg/mL), where appropriate, until they reached a cell density of approximately 1 x 10^8/ml (50 Klett units above background, no. 42 green filter). Subsequently, the cultures were shifted to the non-permissive temperature of 44°C for 1 hour. Cultures were diluted with pre-warmed growth medium as needed to maintain them in exponential growth (Klett 50-90) and were subsequently harvested at approximately 60 Klett units above background.

For experiments not involving strains with temperature-sensitive mutations, strains were grown at 37°C with shaking at 225 rpm in Luria broth supplemented with thymine (50 µg/ml) and antibiotics, where appropriate, until they reached a cell density of approximately 60 Klett units above background.

For experiments employing minimal medium, MG1693 and SK3564 (*rne∆1018/rng-219)* were grown at 37°C with shaking at 225 rpm in M9 medium supplemented with thymine (50 µg/ml) and additional supplements of 0.1% glucose for MG1693 and 0.75% glucose and 1% casamino acids for SK3564, until they reached a cell density of approximately 60 Klett units above background.

Optimization of M9 Minimal Medium

To obtain more comparable growth rates between MG1693 (wild-type) and SK3564 (*rne∆1018/rng-219)*, various concentrations of glucose and casmino acid supplements were tested as additions to the M9 medium. For these experiments, 5 mL aliquots of M9 medium supplemented with various concentrations of glucose were inoculated with 100uL of SK3564 and grown overnight at 37°C with shaking. Subsequently, readings

were taken to determine which concentration of glucose led to the highest cell density. Once the optimal glucose concentration had been determined, the experiment was repeated using the optimal concentration of glucose and varying concentration of casamino acids. Optimal concentrations for SK3564 were determined to be 0.75% glucose and 1% casamino acids (data not shown).

Bacterial Growth Curves in Rich and Minimal Media

To determine the differences in growth rates between MG1693 (wild-type) and SK3564 (*rne∆1018/rng-219)* in the various media, the strains were grown in Luria broth or M9 minimal medium as described above. Measurements under both growth conditions were taken every 30 minutes. Cells were diluted with pre-warmed growth medium as needed to maintain in exponential growth (Klett 50-90). Growth curves were replicated in triplicate and values averaged and then plotted.

RNA Isolation and Northern Analysis

Total RNA was isolated from various exponentially growing strains as described previously (16,17) under the growth conditions described above. The quality of RNA samples was checked by agarose gel electrophoresis and then quantified using a Nanodrop® ND-2000c spectrophotometer. Polyacrylamide northern analysis was carried out as described previously (18).

Glyoxyl agarose northern analysis was conducted using samples prepared with NorthernMax®-Gly sample loading dye (Ambion) and electrophoresis in a 1.5% agarose gel in BPTE buffer run at 80 volts for approximately 4.5 hours. Gel transfer and

subsequent steps were conducted as previously described (18). Formaldehyde agarose northern analysis was conducted as described previously (19). To analyze the processing pattern of the *rpsJ* transcript, the northern blots were probed with γ-P^{32}-end-labeled oligonucleotides labeled using T4 PNK (NEB) that were specific for different regions of interest of the *rpsJ* operon. The various oligonucleotide probes used are listed in Table 2.2. Quantification of band intensities was calculated using ImageQuant TL 7.0 software (GE Healthcare).

***rpsJ* mRNA Half-lives**

To determine the chemical half-lives of the *rpsJ* transcript, rifampicicin/naladixic acid was added to exponentially growing cells at the time of the temperature shift to 44°C as described previously (16,17). Time points were taken at 0, 1, 2, 4, 8, and 16 minutes. RNA was isolated and run on a 1.5% glyoxyl agarose northern as described above. Blots were probed and examined as described above.

RNA Isolation for Tiling Arrays

Strains were grown under conditions described above. Total RNA was isolated as described previously (16,17). The quality of RNA samples was checked by agarose gel electrophoresis and then quantified using a Nanodrop® ND-2000c spectrophotometer. The RNA was then labeled, fragmented, and hybridized to the tiling array, as described previously (13). These MG1655 based genome arrays were tiled using 60 nucleotide length probes containing 20 base pair overlaps at each end with both strands completely represented and manufactured by Agilent Technologies (Palo Alto, CA,

USA) as described previously (13). Results were viewed using the Integrated Genome Browser (20).

RESULTS

Northern Analysis of *rpsJ* transcript processing

To identify the full-length transcript of the *rpsJ* operon and examine its processing *in vivo*, polyacrylamide and agarose northern blots of RNA isolated from isogenic strains lacking various endonucleases were compared using a probe that hybridized to the 3' terminus of the *rpsJ* ORF, the first gene of the operon (Fig. 2.3). A transcript ~5.4 kb was present in every strain. Accumulation of the full-length transcript was seen in the RNase E mutant (Fig. 2.3, lane 4), with a 3.8-fold increase in full-length transcript compared to the wild-type control. In contrast, there was no increase in either the full-length transcript or decay intermediates in the RNase Z or RNase G deletion mutants (Fig. 2.3, lanes 2, 5). The wild-type strain appeared to have more processed fragments 3kb and smaller than the RNase E mutant (Fig. 2.3, lanes 1, 4).

This experiment was subsequently repeated using a RNase E deletion mutant (*rne*Δ*1018/rng-219*) and a RNase III deletion mutant (*rnc-14*). As shown in Fig. 2.4, there was less of the full-length *rpsJ* transcript in the RNase III mutant than the wild-type control. The increase of the full-length *rpsJ* transcript in the *rne*Δ*1018/rng-219* mutant was comparable to what was seen with the *rne-1* allele (Fig. 2.3, lane 4).

Analysis of the *rpsJ* mRNA in various RNase E mutants.

Since it was clear that RNase E played a major role in the processing or decay of the full-length *rpsJ* transcript (Figs. 2.3, 2.4), the fate of the transcript in strains carrying different *rne* alleles was analyzed. In this experiment, an RNase E truncation mutation lacking the degradosome scaffold region (*rne*Δ*645*), a newly isolated temperature-sensitive allele (*rne-117*), and a multiple mutant carrying *rne-1* along with mutations in RNase II and polynucleotide phosphorylase were examined (Fig. 2.5). A probe that hybridized to the 5' UTR of the *rpsJ* transcript was utilized. The largest increase in the full-length transcript occurred in the *rne-1 pnp-7 rnb-500* triple mutant (Fig. 2.15, lane 5).

Surprisingly, in all of the mutants, there were a series of decay intermediates that had retained the 5' UTR but had been shortened from the 3' terminus (Fig. 2.5). When the experiment was repeated with a probe for the 3' Rho-independent transcription terminator, increased levels of the full-length transcript were again observed in three of the four RNase E mutants. Unexpectedly, the amount of the full-length transcript present decreased in the *rne-1 pnp-7 rnb-500* mutant (Fig. 2.6, lane 5). Some additional decay intermediates were observed, particularly in the *rne*Δ*1018/rng-219* strain (Fig. 2.6). In addition, there was a very large increase in a ~200bp fragment that represented the Rho-independent transcription terminator (Fig. 2.6).

Interestingly, only the *rne-1 pnp-7 rnb-500* strain showed stabilization of the full-length transcript compared to wild-type when the 5' UTR region was present (Fig. 2.5, lane 5), whereas transcripts containing the 3' stem-loop did not show any stabilization compared to wild-type for the *rne-1 pnp-7 rnb-500* (Fig. 2.6, lane 5). The *rne*Δ*645* scaffold mutant strain did not have any significant effect on full-length transcript

accumulation but did appear to have a difference on the fragment pattern of fragments less than 3kb (Figs. 2.5, 2.6, lane 2).

Analysis of *rpsJ* transcript fragments using additional hybridization probes

In order to determine if there was a distinct cleavage pattern of the *rpsJ* transcript, we initially examined polyacrylamide and agarose northern blots in various RNase E mutant strains using probes for five genes within the operon (Figs. 2.7 and 2.8). Subsequently, agarose northern analysis of wild-type versus the *rne-1* strain was also performed with probes for the remaining six genes of the operon (Fig. 2.9).

As expected, every probe showed an accumulation of the full-length *rpsJ* operon transcript in the *rne-1* and *rne*Δ*1018/rng-219* mutants (Table 2.3), in agreement with the results seen for the terminal regions (Figs. 2.5, 2.6). It is also important to note that the stabilization of the full-length transcript seen in the *rne-1 pnp-7 rnb-500* strain with the 5' UTR probe was not seen for any of the other regions probed, including the *rpsJ* probe just downstream of the 5' UTR region (Fig. 2.7A).

The RNase E mutant strains showed a build-up of various fragments for each region probed, ranging in size from ~5kb to ~500bp (Figs. 2.7, 2.9). Each region probed had a different and complex fragment pattern. In contrast, the only region affected in the polyacrylamide northern (which separates only ~700 bp transcripts or less), was for the *rpsQ* probed regions (Fig. 2.8D), which showed build-up of smaller size fragments, similar to what was seem for the 3' transcription terminator probe.

Effect of PAP I on *rpsJ* transcript processing

To determine if polyadenylation had any effect on the processing and/or decay of the full-length *rpsJ* operon transcript or its 3' terminus, the transcript profiles in strains carrying various combinations of RNase E and PAP I mutations were compared using a probe specific for the Rho-independent transcription terminator. The data obtained (Fig. 2.10) demonstrated that PAP I did not have a significant effect on the stability of the full-length transcript, as none of the double mutant strains defective in RNase E and PAP I showed any dramatic difference from the single RNase E mutants. There was some stabilization of smaller fragments in the *rne-1* Δ*pcnB* strain compared to the *rne-1* single mutant (Fig. 2.10). The deletion of *pcnB* in the *rne-1 pnp-7 rnb-500* strain appeared to significantly stabilize a number of smaller fragments present (Fig 2.10, lane 8).

Developing growth conditions to obtain comparable generation times for MG1693 and SK3564

It is well established that the ribosome content of cells is directly related to growth rate (21). Therefore, to eliminate any growth dependent effects on ribosome concentrations, and thus r-protein concentrations, we attempted to obtain comparable doubling times between the MG1693 (wild-type control) and SK3564 (*rne*Δ*1018/rng-219*) mutant strain employing M9 minimal medium with glucose as the carbon source. It was determined through OD_{600} measurements of a series of overnight cultures that M9 medium supplemented with 0.75% glucose and 1% casamino acids was optimal for SK3564 growth (data not shown). The wild-type MG1693 was grown at a lower concentration of the same carbon source (0.1% glucose) without any casamino acids to obtain a

comparable growth rate. When grown in M9 minimal medium supplemented with thymine, glucose, and casamino acids, MG1693 had a doubling time of 70-75 minutes, while SK3564 had a doubling time of 100-115 minutes. The doubling times of the strains grown in Luria broth supplemented with thymine were approximately 30 minutes for MG1693 versus 98-102 minutes for SK3564.

Tiling Array Analysis for *rne-1*

To examine the effects of RNase E on the *rpsJ* operon transcript in its entirety, a tiling array was performed for the *rne-1* strain versus the MG1693 wild-type control. In contrast to northern analysis, the array did not show any significant difference in the transcript levels of the *rpsJ* operon under the different conditions (Fig. 2.11A). This is in agreement, however, with the *rne∆1018/rng-219* arrays previously published (13), which also demonstrated no steady-state RNA level changes occurred for the *rpsJ* operon. The *rne∆1018/rng-219* strain was grown at 37°C and has been proposed to be a good substitute for the *rne-1* allele (22). Our results showed that the profile of the *rne-1* versus *rne∆1018/rng-219* array did not differ dramatically, which confirmed the idea that the *rne∆1018/rng-219* strain may be a good alternative to the temperature-sensitive *rne-1* allele.

Interestingly, however, one obvious difference between the *rne-1* and the *rne∆1018/rng-219* strains related to decreased levels of the 5′ and 3′ regions of 16S rRNA in all seven *rrn* operons (Fig. 2.11B). This result was in contrast to what was observed in the *rnc-14* and *rne∆1018/rng-219* arrays previously published (Fig.

2.11B)(13). However, the array pattern at the 3' end of the 23S rRNA was similar in all the strains tested (Fig. 2.11B).

Additionally, as opposed to the *rpsJ* results, the *rplN* and *rpsM* ribosomal protein operons that are directly downstream of the *rpsJ* operon did show an increase in steady-state levels in the *rne-1* and *rne*Δ*1018/rng-219* arrays (Fig. 2.11A).

Tiling Array Analysis for *rne*Δ*1018/rng-219* in Minimal Medium

To eliminate any growth dependent effects from the tiling arrays on the ribosomal concentrations and r-protein concentrations, the *rne*Δ*1018/rng-219* tiling array was repeated using RNA isolated from the strain grown in minimal medium as described in the previous section. We were particularly interested in carrying out this experiment because both our *rne-1* array results and the previously published *rne*Δ*1018/rng-219* array results from our laboratory (13) did not show any significant difference in *rpsJ* transcript levels in MG1693 versus SK3564 when the strains were grown in Luria broth. These result were in striking contrast to the northern analysis data presented in Figs. 2.3-2.7, 2.9.

However, even when MG1693 and SK3564 were grown in minimal medium with comparable generation times there was not any significant difference in the *rpsJ* polycistronic transcript levels between the two strains (Fig. 2.12). We did observe increased levels of the downstream *rplN* and *rpsM* ribosomal protein operons (Fig. 2.12).

Northern Blot analysis of MG1693 AND SK3564 grown in minimal medium

Northern blot analysis was performed for the wild-type and *rne∆1018/rng-219* strains grown in minimal medium to determine if accumulation of the full-length transcript was still seen in the RNase E mutant when the strains were grown with comparable generation times. Agarose northern blots of wild-type and *rne∆1018/rng-219* strains were compared using probes for 5' UTR and the *rpsS* gene (Fig. 2.13) and various intercistronic regions of the *rpsJ* operon transcript (Fig. 2.14). Accumulation of the full-length transcript was still observed in the *rne∆1018/rng-219* mutant (Fig. 2.13), with a 2.1-fold and 3.5-fold increase in full-length transcript compared to wild-type when probed with the *rpsS* and 5' UTR probes, respectively. Similar results were obtained with the intercistronic probes (Fig. 2.14).

Chemical half-lives of the 5' *rpsJ* UTR

To determine the stability of the *rpsJ* full-length transcript in the *rne-1* mutant compared to the wild-type control, the chemical half-life of the full-length transcript was examined. Blots were probed for the 5' UTR of the *rpsJ* transcript (Fig. 2.15). The half-life of the full-length *rpsJ* transcript in SK5665 (*rne-1*) was 3.86 ± 0.89 minutes, and 2.2 ± 0.56 minutes for MG1693 (wild-type). Surprisingly, full-length *rpsJ* transcript levels increased up until 2 minutes for the wild-type control and 4 minutes for *rne-1* strain prior to decreasing (Fig. 2.15).

To determine if the increase in the amount of the *rpsJ* transcript was some type of experimental artifact, we used previously isolated RNA from an *rne-1* strain that had been used for other half-life experiments that had not shown this behavior. In this

experiment an agarose northern blot and was probed for regions of the *rpsJ* and *rplN* operons and the monocistronic *adhE* transcript (Fig. 2.16). As we had observed in Fig. 2.15, the amount of the full-length *rpsJ* transcript increased until ~ 4 minutes before decreasing. This increase for several minutes before decreasing was also seen for the large polycistronic *rplN* polycistronic transcript (Fig. 2.16) and *rpsM* polycistronic transcript (data not shown), whereas the monocistronic *adhE* transcript did not display this effect (Fig. 2.16).

DISCUSSION

RNase E processes the full-length *rpsJ* transcript

The results presented here demonstrate that the *rpsJ* operon is a large polycistronic operon that is processed into smaller discrete fragments (Figs. 2.3-2.10, 2.13, 2.14). Accumulation of full-length and processed products in various RNase E mutants suggests that RNase E is the primary endonuclease responsible for this processing. Even when growth rates were adjusted to be comparable using minimal medium, inactivation of RNase E still was observed to stabilize the full-length transcript (Fig. 2.12).

Additionally, the analysis of the processing pattern of the RNase E scaffold mutant (*rneΔ645*) indicated a potential role for the scaffold domain, mainly in processing medium-sized fragments (less than 2kb). This result also suggested that only the catalytic domain of RNase E is critical for the initial cleavages or removal of the Rho-independent transcription terminator from the *rpsJ* transcript (Figs. 2.5-2.7, lane 2).

The lack of significant build-up of full-length or intermediates in RNase Z and RNase G mutants (Fig. 2.3) or RNase III mutants (Fig. 2.4) eliminated these endonucleases as primary processing enzymes.

RNase E is likely responsible for the removal of the 3' Rho-independent transcription terminator

The 5' UTR region was present on many processing fragments in the wild-type background (Fig. 2.5), while the 3' stem-loop was predominately found on the full-length transcript (Fig. 2.6). This observation strongly suggested that the removal of the 3' stem-loop as an early step in normal *rpsJ* processing. Additionally, in the *rne-1* mutant the presence of the 3' stem-loop on fragments of varying sizes (Fig. 2.6 lane 4), with a strong accumulation of the ~200 bp fragment, suggested that RNase E was the primary enzyme responsible for stem-loop removal and its subsequent degradation, and that perhaps stem-loop removal is an early or rate-limiting step. The fact that the *rne-1 pnp-7 rnb-500* strain does not seem to have any change in the accumulation of the ~200 bp fragment compared to the *rne-1* single mutant, suggested that these two exonucleases do not play a major role in stem-loop degradation.

On the other hand, the 5' UTR pattern in the *rne-1* strain did not seem to indicate any significant role of RNase E in removal of the 5' UTR (Fig. 2.5). Failure to remove the 5' UTR may be important because the 5' UTR exerts both transcriptional and translational control on the entire operon (4,23).

Loss of RNase E stabilizes the full-length *rpsJ* transcript

Analysis of the chemical half-life of full-length *rpsJ* transcript (Fig. 2.15) suggested that not only does RNase E process the *rpsJ* full-length transcript, but that the lack of RNase E also stabilized the full-length *rpsJ* transcript. The observation that the abundance of full-length transcript continued to increase for 2-4 minutes after the equilibration of the rifampicicin/naladixic acid seen for *rpsJ* operon transcripts (Figs. 2.15A, 2.16A) is likely due to the completion of transcription of the large polycistronic transcript that took place between the addition and equilibration of the rifampicicin/naladixic acid. This is normally not seen in shorter transcripts, such as *adhE* (Fig. 2.16C), but this increase was also observed when the same northern blot was striped and reprobed for the *rplN* operon transcript *(*Fig. 2.16B) and the *rpsM* operon transcript (data not shown), the other large polycistronic ribosomal protein operons in the cell. It could also be a phenomenon that is specifically related to ribosomal protein transcripts.

Individual transcript ratios for the *rpsJ* operon transcript are maintained despite changes in its processing

The tiling array analysis of the *rne-1* mutant and the *rne∆1018/rng-219* grown in rich or minimal medium conditions both showed that the *rpsJ* operon steady-state levels were unchanged, even when conditions were adjusted to allow for comparable growth rates (Figs. 2.11, 2.12). At first glance, this result conflicts with the northern blot analysis that demonstrates a strong stabilization of the full-length transcript under the same conditions (Figs. 2.7 lane 3, 2.13). However, since the RNA is fragmented during the array procedure, the array inherently lacks the ability to detect differences if the cellular

concentration of each mRNA fragment is maintained; in other words, the tiling arrays cannot detect processing without breakdown or decay of a fragment more than 40 nucleotides in length.

Therefore, our result strongly suggested that the cell maintains the individual transcript ratios of each gene in the polycistronic *rpsJ* operon, despite changes in the processing of the full-length transcript in RNase E mutants. This result was supported by the lack of the strong banding pattern around 3kb in the *rne* mutants that is observed in the wild-type strain (Figs. 2.4 lane 2, 2.6 lane 3, 2.10AB). Our hypothesis is in agreement with the known tight cellular control of the r-protein operons and indicates greater flexibility and adaptation of the cell in controlling the ribosomal protein levels at the transcript level than previously observed. However, the maintenance of steady-state levels was not observed with any of the arrays for the *rplN* and *rpsM* operons that are directly downstream of the *rpsJ* operon (Figs. 2.11A, 2.12), a result that is still unclear.

The *rpsJ* operon transcript is a substrate for other endonucleolytic cleavages when RNase E is missing

The lack of complete build-up of full-length product or disappearance of intermediates in the RNase E mutants (Figs. 2.3-2.10, 2.13, 2.14) strongly suggested secondary cleavages by other endonucleases. The processing fragment pattern is very complex even when probed for other gene regions or intercistronic regions of the polycistronic transcript (Figs. 2.7, 2.10, 2.14), suggesting several other secondary players.

The processing pattern in the *rne-1 pnp-7 rnb-500* mutant showed a slight build-up of processed fragments (Figs. 2.5-2.7, lane 5), but the pattern was largely

unchanged from the *rne-1* single mutant (Table 2.3). These results indicated that these two major exonucleases only have a minor degradative role in the overall processing of the *rpsJ* operon transcript.

The overall lack of change in the full-length transcript profile of double mutant strains defective in *rne-1* Δ*pcnB* strain compared to the *rne-1* single mutant suggested that polyadenylation is not playing a significant role in the absence of RNase E. This is not surprising, as RNase E is the major endonuclease which acts on polyadenylated substrates. The stabilization of smaller fragments in the *rne-1* Δ*pcnB* strain and the *rne-1 pnp-7 rnb-500* Δ*pcnB* compared to the *rne-1* single mutant (Fig. 2.10), suggested that polyadenylation may still be playing a role in the stability of the smaller fragments even when RNase E is missing.

TABLES AND FIGURES

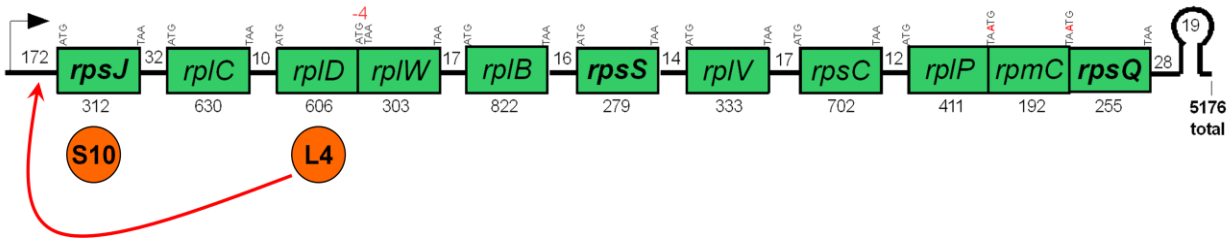

Figure 2.1. The *rpsJ* transcript. Two of the eleven encoded proteins are shown. Nucleotide lengths of the 5' UTR, each gene, intercistronic regions and the stem-loop terminator are shown above.

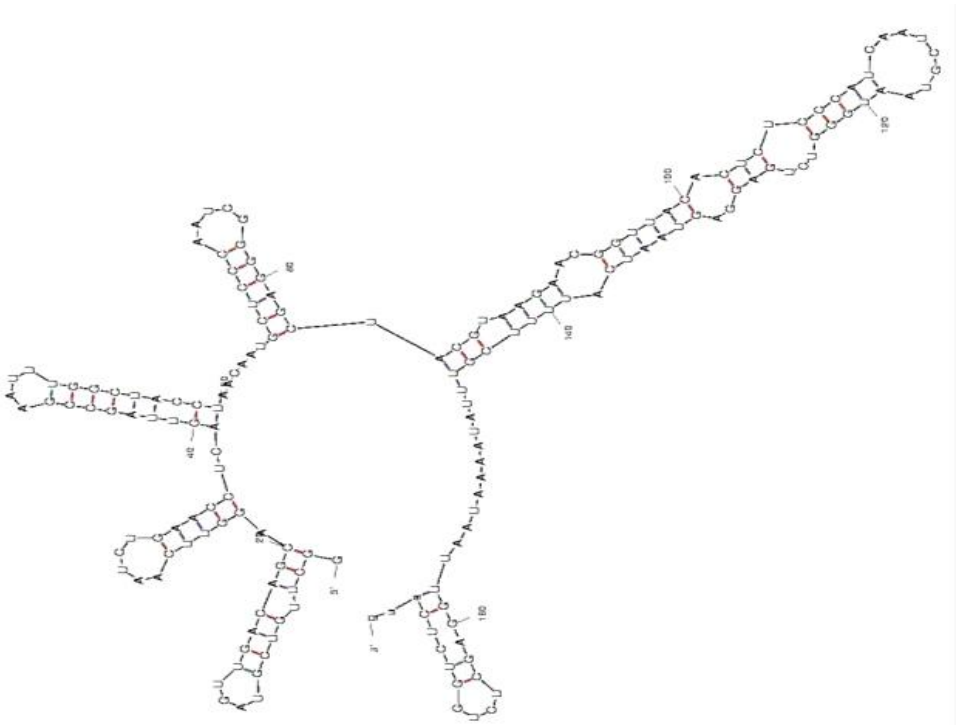

A. 5’ Untranslated Region (UTR)

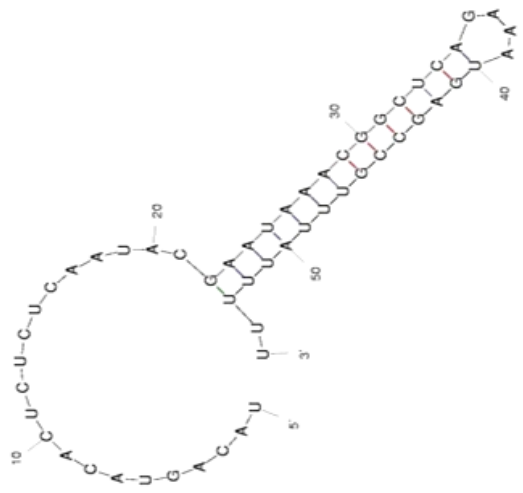

B. 3’ Rho-independent transcription terminator

Figure 2.2. The 5’ UTR and 3’ Rho-independent transcription terminator of the rpsJ operon. The 5’ UTR and 3’ Rho-independent transcription terminator sequences were folded using the m-fold program (24).

Table 2.1. List of bacterial strains and plasmids used in this study. RNase = ribonuclease, PAP I = poly(A)polymerase I, PNPase= polynucleotide phosphorylase.

Strains	**Genotype**	**Endo-nuclease(s) missing**	**Exo-nuclease(s) or other missing**	**Reference Or Source**
MG1693	*thyA715 rph-1*	none	none	*E. coli* Genetic Stock Center
SK2538	*rng::cat thyA715 rph-1*	RNase G	none	(25)
SK2685	*rne*Δ*1018::bla srlD300::*Tn*10 recA56 thyA715 rph-1* pDHK6 (*rne*Δ*645 Sp/Sm*^{R})	RNase E scaffold domain	none	(26)
SK3543	*rne*Δ*1018::bla srlD300::*Tn*10 recA56 thyA715 rph-1* pDHK28 (*rng*Δ*219* low copy *Km*^{R})	RNase E (*rng-219* present in its place)	none	(22)
SK3564	*rne*Δ*1018::bla* Δ*pcnB::apr srlD300::*Tn*10 recA56 thyA715 rph-1* pDHK30 (*rng*Δ*219* single copy *Sp/Sm*^{R})	RNase E (*rng-219* present in its place)	None **Other:** PAP I	(22)
SK3642	*rne*Δ*1018::bla* Δ*pcnB::apr srlD300::*Tn*10 recA56 thyA715 rph-1* pMOK13 (*rne-1* low copy *Cm*^{R})	RNase E (ts)	**Other:** PAP I	DuBose and Kushner, unpublished results.
SK3645	*rne*Δ*1018::bla srlD300::*Tn*10 recA56 thyA715 rph-1* pDHK30 (*rng*Δ*219* single copy Sp/*Sm*^{R})	RNase E (*rng-219* present in its place)		DuBose and Kushner, unpublished results.
SK3750	*rne*Δ*1018::bla srlD300*::Tn*10 recA56 thyA715 rph-1* pUGK49 (*rne-117 low copy Km*^{R})	RNase E (ts)	none	Reyes-Darius, Perwez, and Kushner, unpublished results.
SK4161	*rne-1* Δ*rnz::apr* Δ*mazEFG::kan thyA715 rph-1*	RNase E (ts) RNase Z MazEFG (toxin-antitoxin system)	none	Richter-Roche and Kushner, unpublished results.
SK4455	*rnc-14::*ΔTn*10 thyA715 rph-1*	RNase III	none	(13)
SK4484	*rne-1 rng::cat rnlA2::kan rnz*Δ*::apr rpsD296::*Tn*10 rnpA49 thyA715 rph-1*	RNase E (ts) RNase G RNase Z RNase LS RNase P (ts)	none	Maples and Kushner, unpublished results.

SK5665	*rne-1 thyA715 rph-1*	RNase E (ts)	none	(27)
SK5704	*rne-1 pnp-7 rnb-500 thyA715 rph-1*	RNase E (ts)	PNPase RNase II	(27)
SK8901	*rne-1 pnp-7 rnb-500* ∆*pcnB::apr thyA715 rph-1*	RNase E (ts)	PNPase RNase II **Other:** PAP I	(17)
SK9705	*rne*∆*1018::bla srlD300::*Tn*10 recA56 thyA715 rph-1* pQLK26 (*rne*+ 6-8copy *Km*^{R})	None	None	(28)
SK9937	*rne*∆*1018::bla srlD300::*Tn*10 recA56 thyA715 rph-1* pMOK13 (*rne-1* 6-8copy *Cm*^{R})	RNase E (ts)	None	(28)
SK9795	*rnz*∆*500::kan thyA715 rph-1*	RNase Z	none	(29)

Table 2.2. Oligonucleotide probes used in this study.

Name	**Sequence**
rpsJ UTR	5'-CTCCTCAGACCCATTACGATTG-3'
3' rpsJ	5'-AACCCAGGCTGATCTGCACG-3'
5' rplC	5'-GTTACTGGGATAGAAACGCCGTC-3'
rplC-rplD intercistronic	5'-TCCATTGCTATCTCCTTACG-3'
5' rplD	5'-AATCACGACCGAAGGTAGTTTCG-3'
5' rplW	5'-AGAAACGTGCGGTGCACGCA-3'
rplW-rplB intercistronic	5'-CATTGTATTACTCCTCCGACT-3'
5' rplB	5'-AACTACGTGGCGACGACCCG-3'
rplB-rpsS intercistronic	5'-CATGGCTTATCCTCTAAAATT-3'
3' rpsS	5'-CTTCGCTTTTTTATCAGCAG-3'
rpsS-rplV intercistronic	5'-CATCTCTTCCTCCTACCTTA-3'
5' rplV	5'-ACCTTCTGAGCAGAAGAACGAGC-3'
rplV-rpsC intercistronic	5'-ATTGCTAGTCTCCAGAGTCT-3'
5' rpsC	5'-AGCCAGTTCCTTAGTCAGGTAC-3'
rpsC-rplP intercistronic	5'-ACATCAGCGACGCTCCTTAT-3'
3' *rplP*	5'-CATCACCGTCTTAGTTACAAAGG-3'
5' *rpmC*	5'-ACTTGCAGCCTGCATACGCAGG-3'
5' *rpsQ*	5'-ACGCGACCTTGCAGAGTACGG-3'
rpsQ stem-loop	5'-CCGTTTATTCGTATTGAGAGAG-3'
5' *rplN*	5'-GTTCAGCATAGTCTGTTCTTGG-3'
adhE	5'-CTTCACCGATCAGAATCTTG-3'

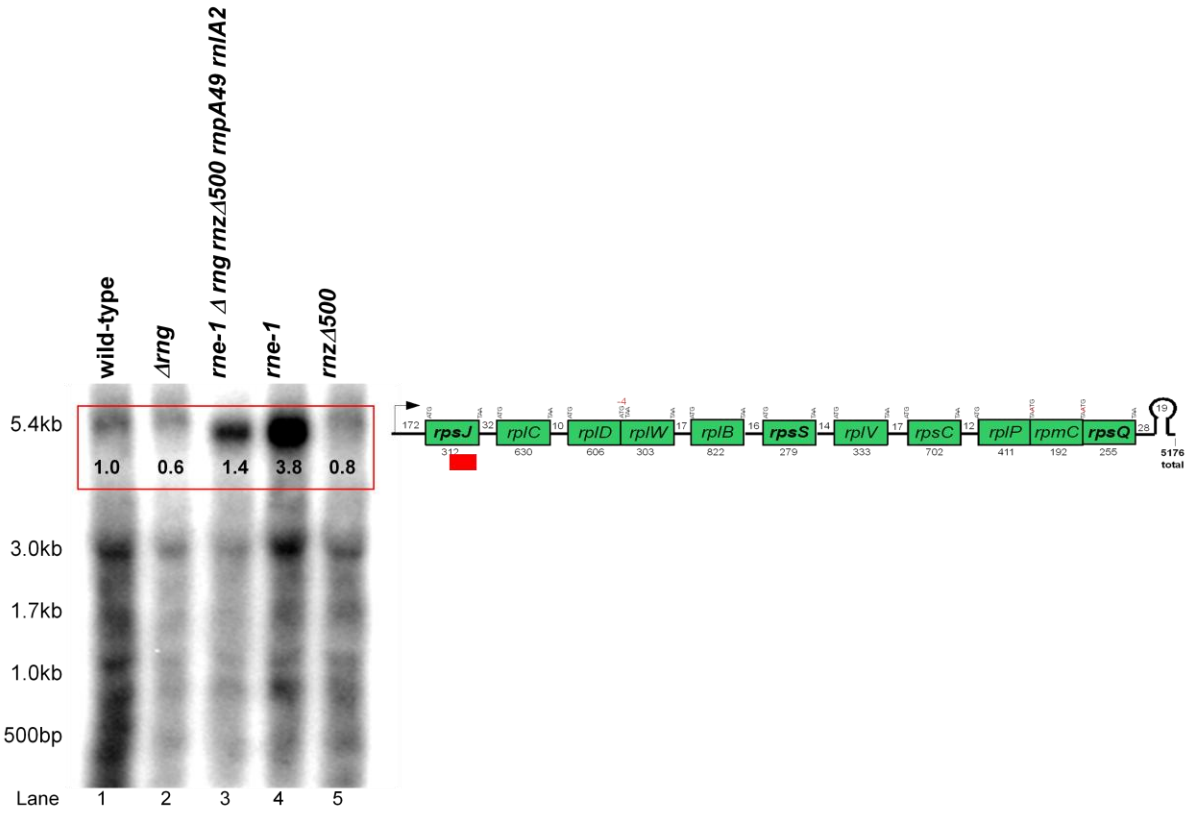

Figure 2.3. Agarose northern blot of endonuclease mutants probed with 3' *rpsJ* probe. Cells were initially grown at 30°C prior to shifting to 44°C for 1hr. RNA was run on a 1.5% glyoxyl agarose gel. Strains were as follows: MG1693 (wild-type), SK2538 (Δ*rng*), SK4484 (*rne-1* Δ*rng rnz*Δ*500 rnpA49 rnlA2*), SK5665 (*rne-1*), and SK9795 (*rnz*Δ*500*) in Lanes 1-5, respectively. Quantification of the full-length transcript was calculated with wild-type set at 1.0 and is shown in each lane. The sizes of the various transcripts based on a sizing ladder (RiboRuler^{TM}, Fermentas) are shown to the left of the blot.

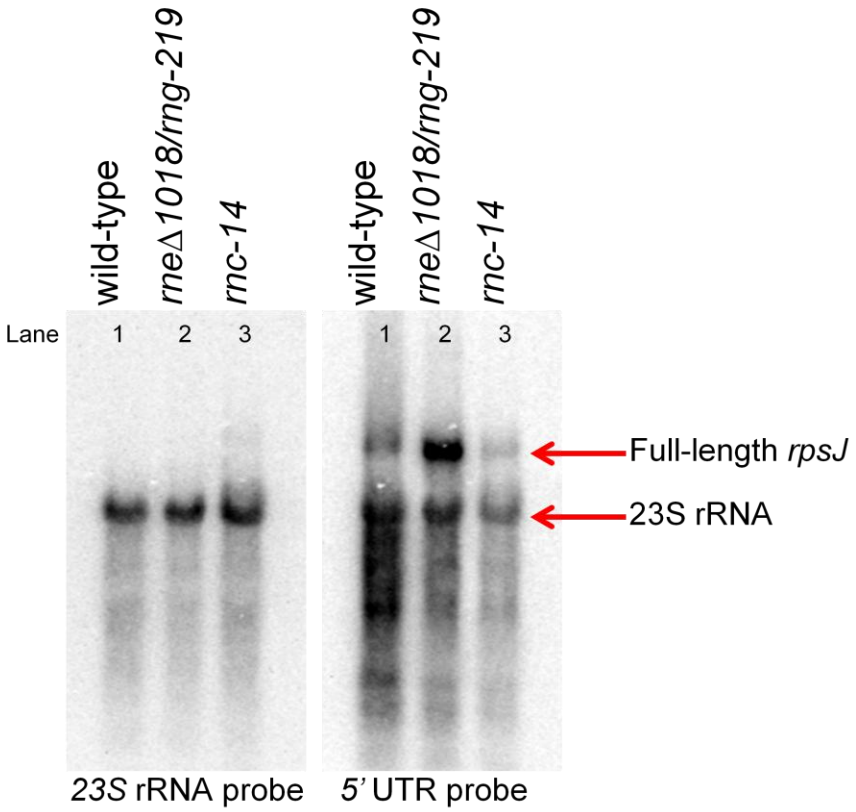

Figure 2.4. RNase III is not involved in *rpsJ* processing

Cells were grown at 37°C. RNA was run on a 1.2% formaldehyde agarose gel. Strains were as follows: MG1693 (wild-type), SK3564 (*rneΔ1018/rng-219*), and SK4455 (*rnc-14*) in Lanes 1-3, respectively.

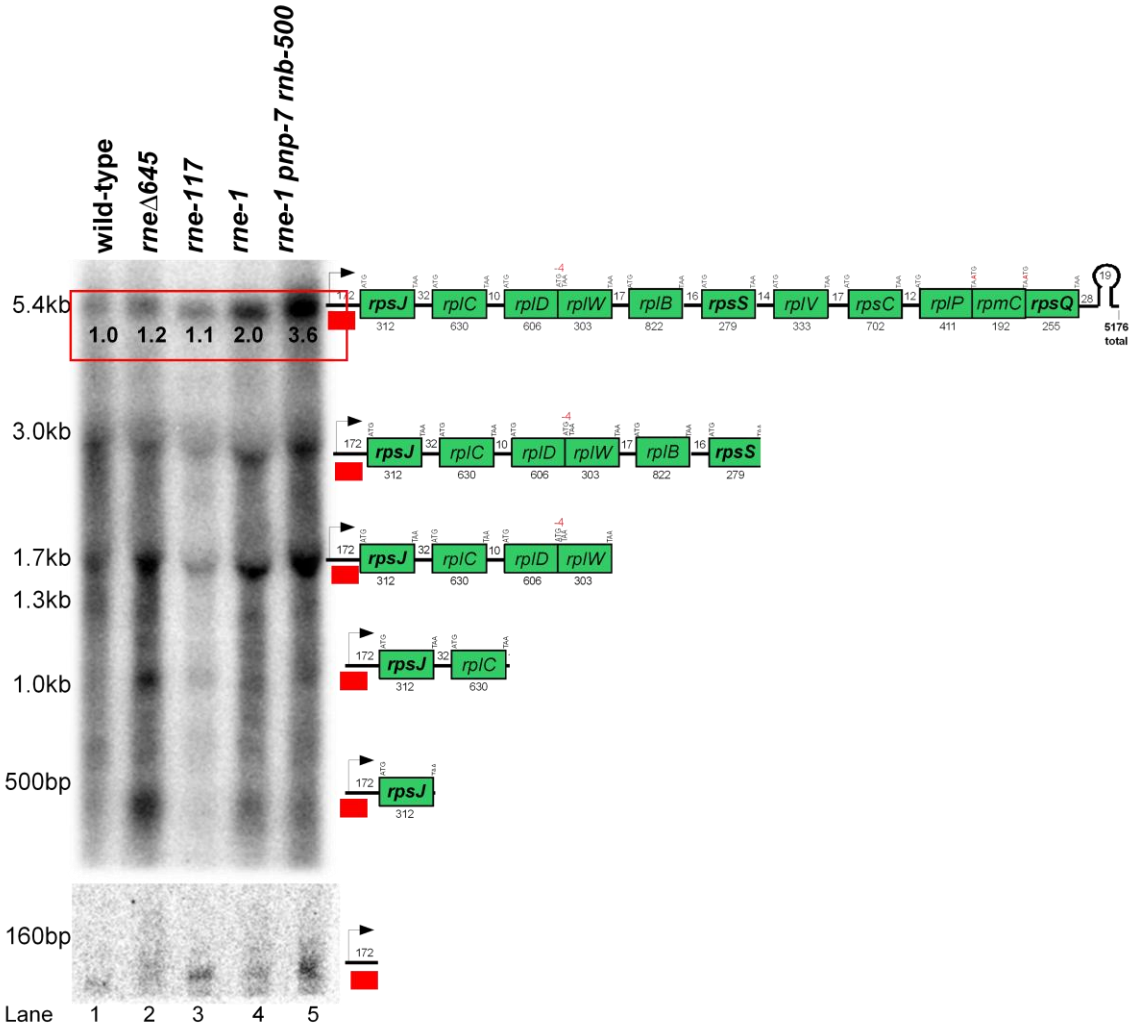

Figure 2.5. Agarose and polyacrylamide northern blots of various RNase E mutants probed with 5′ *rpsJ* UTR probe. Cells were initially grown at 30°C prior to shifting to 44°C for 1hr. RNA was run on a 1.5% glyoxyl agarose gel (top) or a 6% urea polyacrylamide gel (bottom). Strains were as follows: MG1693 (wild-type), SK2685 (*rneΔ645*), SK3750 (*rne-117*), SK5665 (*rne-1*), and SK5704 (*rne-1 pnp-7 rnb-500*) in Lanes 1-5, respectively. Quantification of the full-length transcript was calculated with wild-type set at 1.0 and is shown in each lane. Predicted structures for the various *rpsJ* transcripts are shown to the right of the blot. The sizes of the various transcripts based on a sizing ladder (RiboRuler^{TM}, Fermentas) are shown to the left of the blot.

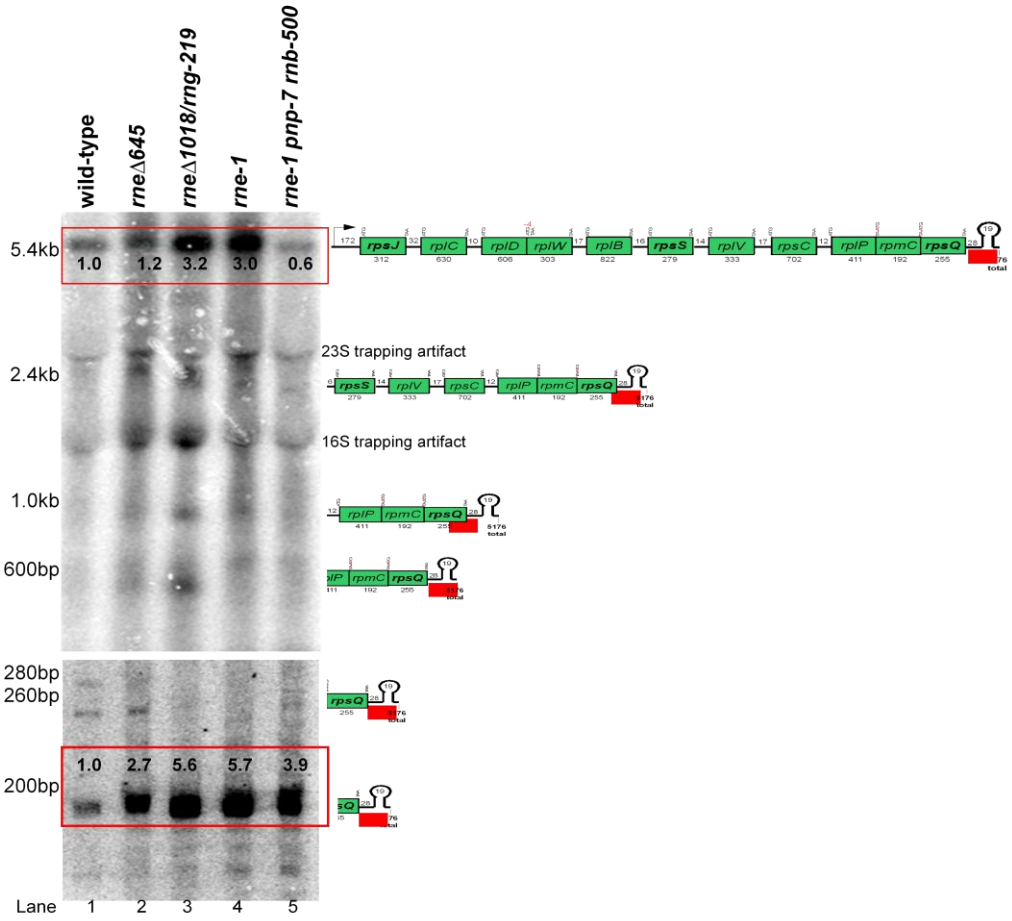

Figure 2.6. Agarose and polyacrylamide northern blots of various RNase E mutants probed with the 3′ Rho-independent transcription terminator probe. Cells were initially grown at 30°C prior to shifting to 44°C for 1hr. RNA was run on a 1.5% glyoxyl agarose gel (top) or a 6% urea polyacrylamide gel (bottom). Strains were as follows: MG1693 (wild-type), SK2685 (*rne*Δ*645*), SK3564 (*rne*Δ*1018/rng-219*), SK5665 (*rne-1*), and SK5704 (*rne-1 pnp-7 rnb-500*) in Lanes 1-5, respectively. Quantifications of the full-length transcript and the ~200 bp fragment were calculated with wild-type set at 1.0 and are shown in each lane. Predicted structures for the various *rpsJ* transcripts are shown to the right of the figure. The sizes of the various transcripts based on a sizing ladder (RiboRuler^{TM}, Fermentas) are shown to the left of the blot.

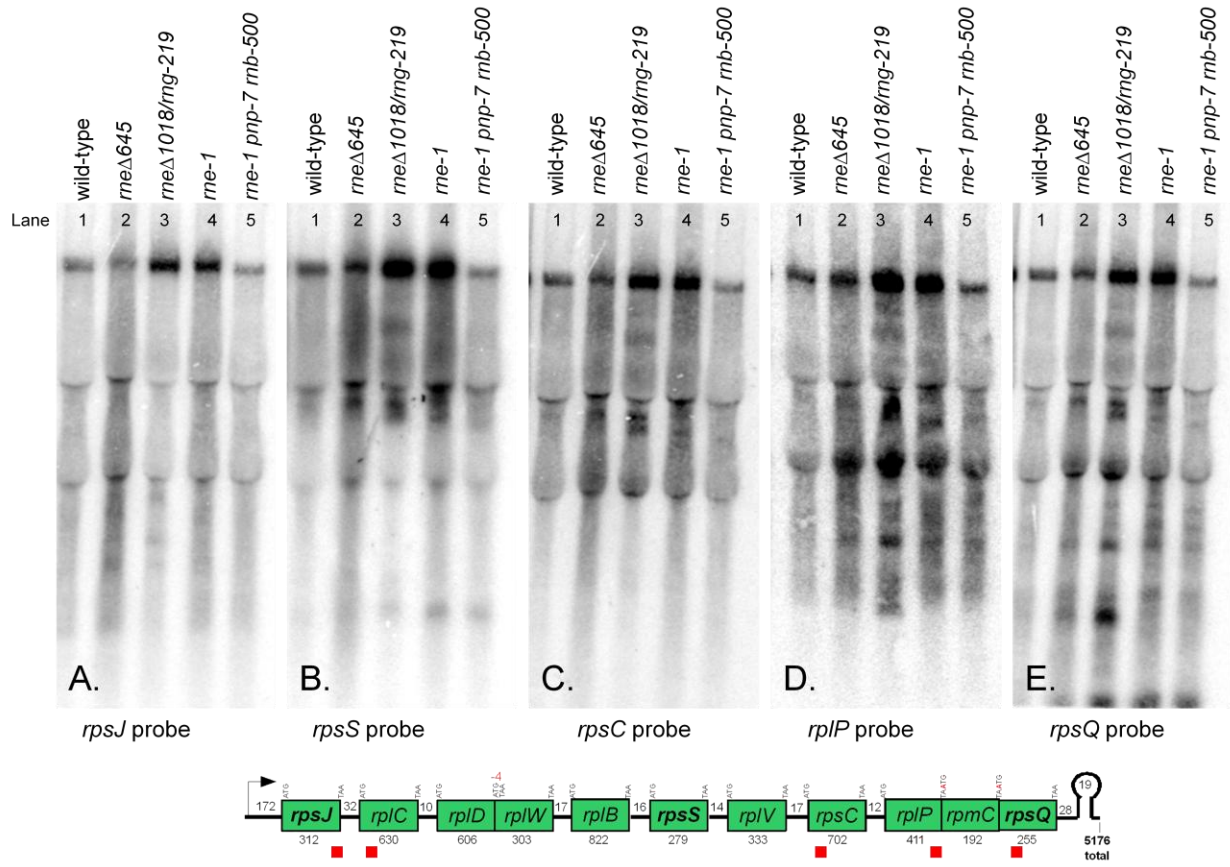

Figure 2.7. Agarose northern blots of endondonuclease or endo/exonuclease mutants probed for *rpsJ*, *rpsS*, *rpsC*, *rplP*, and *rpsQ*. Cells were initially grown at 30°C prior to shifting to 44°C for 1hr. RNA was run on a 1.5% glyoxyl agarose gel. Strains were as follows: MG1693 (wild-type), SK2685 (*rne*Δ*645*), SK3564 (*rne*Δ*1018/rng-219*), SK5665 (*rne-1*), and SK5704 (*rne-1 pnp-7 rnb-500*) in Lanes 1-5, respectively.

Table 2.3. Quantification of full-length transcript levels for agarose northern blots in various RNase E mutants. Quantification of the full-length transcript of blots shown in Figs. 2.5, 2.6 and 2.7 with wild-type set at 1.0.

	Wild-type	***rne*∆*645***	***rne*∆*1018/ rng-219***	***rne-1***	***rne-1 pnp-7 rnb-500***
5' UTR	1.0	1.2	ND	2.0	3.6
rpsJ	1.0	1.0	2.8	2.2	0.6
rpsS	1.0	0.9	3.3	2.8	0.6
rpsC	1.0	0.7	2.9	2.3	0.5
rplP	1.0	1.4	4.0	2.8	0.8
rpsQ	1.0	1.2	3.4	2.4	0.7
stem-loop	1.0	1.2	3.2	3.0	0.6

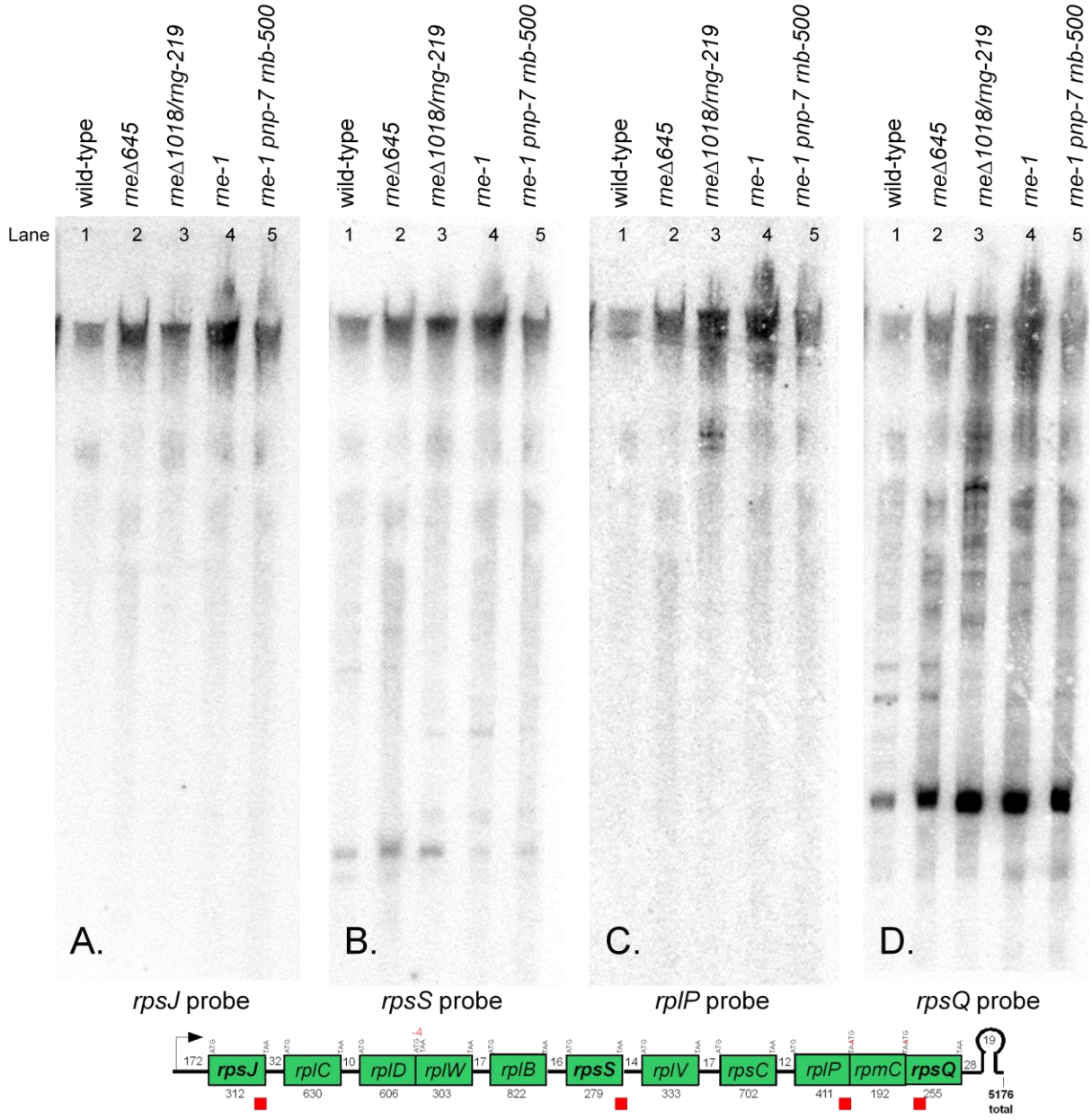

Figure 2.8. Polyacrylamide northern blots of various RNase E mutants probed for *rpsJ*, *rpsS*, *rplP*, and *rpsQ*. Cells were initially grown at 30°C prior to shifting to 44°C for 1hr. RNA was run on a 6% urea polyacrylamide gel. Strains were as follows: MG1693 (wild-type), SK2685 (*rneΔ645*), SK3564 (*rneΔ1018/rng-219*), SK5665 (*rne-1*), and SK5704 (*rne-1 pnp-7 rnb-500*) in Lanes 1-5, respectively.

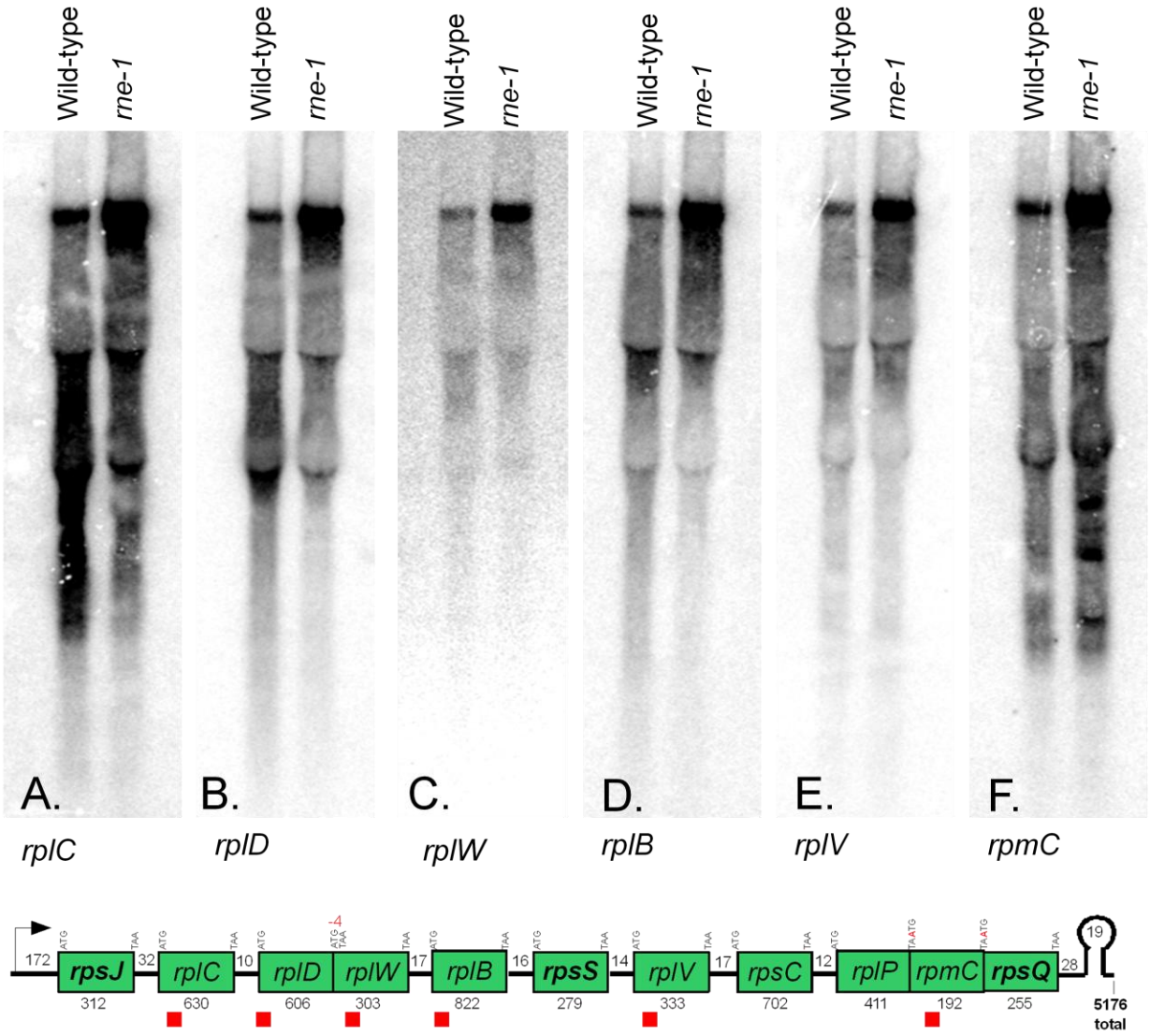

Figure 2.9. Agarose northern blots of wild-type and *rne-1* strains probed for *rplC*, *rplD*, *rplW*, *rplB*, *rplV*, and *rpmC*. Cells were initially grown at 30°C prior to shifting to 44°C for 1hr. RNA was run on a 1.5% glyoxyl agarose gel. Strains were MG1693 (wild-type) and SK5665 (*rne-1*) in Lanes 1 and 2, respectively.

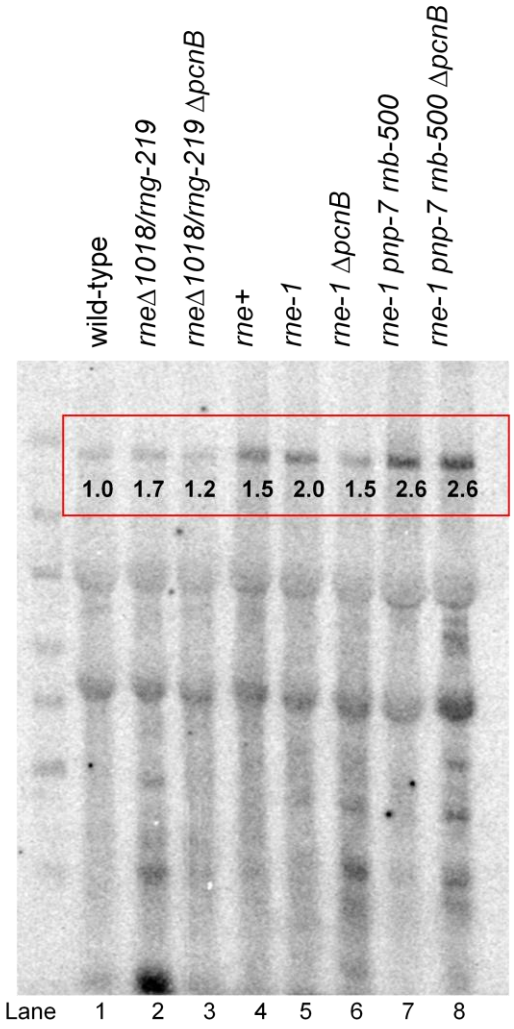

Figure 2.10. Agarose northern blot of various RNase E mutants in the presence or absence of poly(A) polymerase I (PAP I). Cells were initially grown at 30°C with shift to 44°C for 1hr. RNA was run on a 1.5% glyoxyl agarose gel and the northern blot was probed with the oligonucleotide used in Fig. 2.6. Strains were as follows: MG1693 (wild-type), SK3543 (*rneΔ1018/rng-219*), SK3645 (*rneΔ1018/rng-219 ΔpcnB*), SK9704 (*rne+*), SK9937(*rne-1*), SK3642 (*rne-1 ΔpcnB*), SK5704 (*rne-1 pnp-7 rnb-500*), SK8901 (*rne-1 pnp-7 rnb-500 ΔpcnB*) in Lanes 1-8, respectively. Quantification of the full-length transcript was calculated with wild-type set at 1.0 and is shown in each lane.

A.

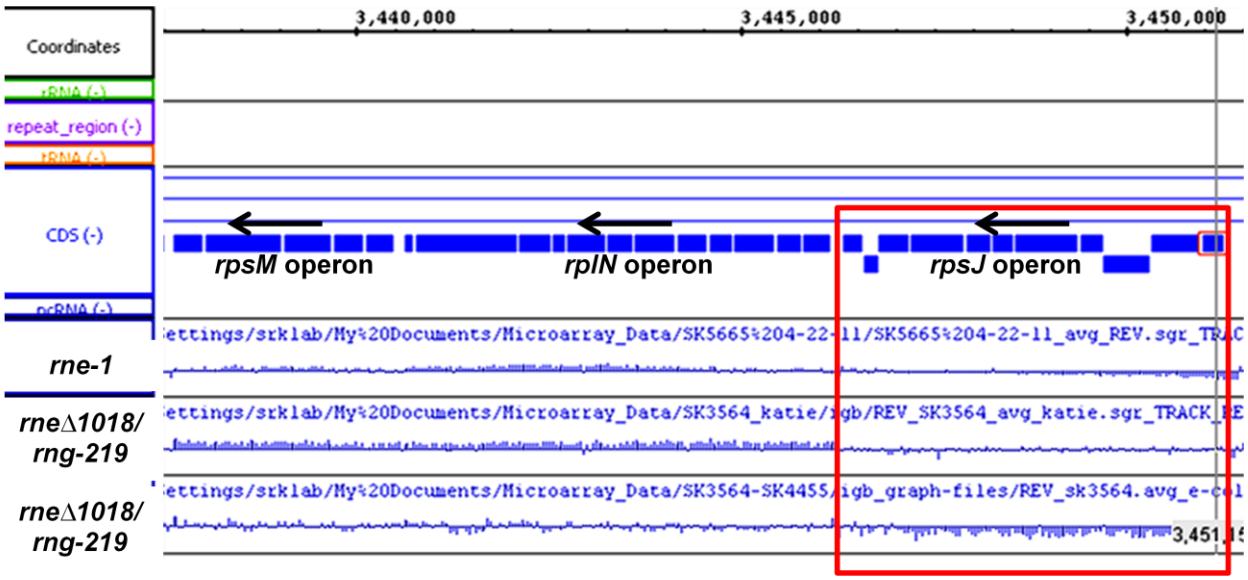

B.

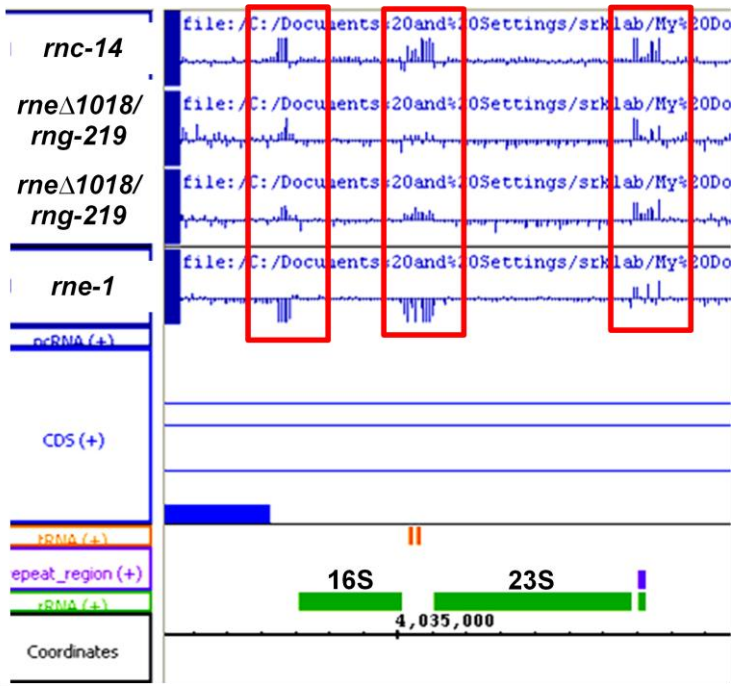

Figure 2.11. Differences in the *rpsJ* operon and the 16S rRNA in the *rne-1* array.

Changes in the steady-state levels of the genes that are involved in the *rpsJ* (panel A) and *rrn* (panel B) operons. The *rnc-14* and *rneΔ1018/rng-219* array (bottom in A, top in B) were previously published (13). The *rneΔ1018/rng-219* (top in A, bottom in B) was

previously analyzed in this laboratory (Bowden and Kushner, unpublished results.) The *rne-1* array was performed as part of this study. The image presented was obtained from a screen shot of the Integrated Genome Browser program (20). Gene or operon names appear above or below the operons that encode them, which indicate their location in the genome relative to nucleotide coordinates, as displayed in the center of the graph. Black arrows indicate the direction of transcription. The array data is displayed as vertical lines representing the log2 ratio of fluorescence between the mutant and wild-type strains.

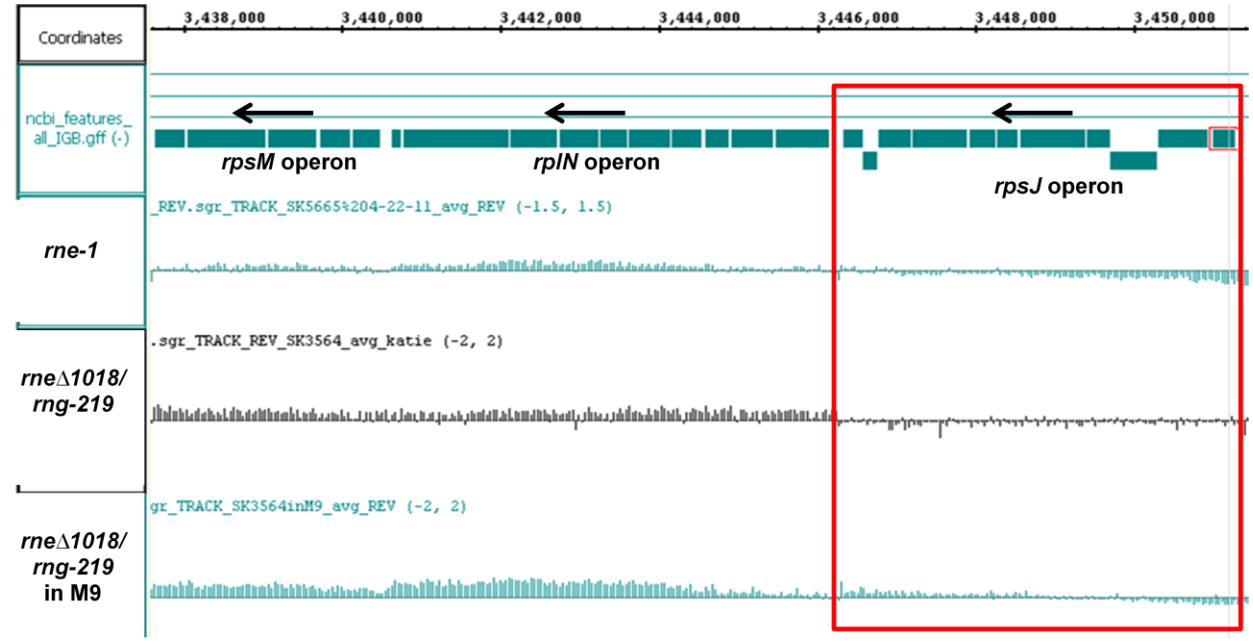

Figure 2.12. Microarray comparison for the *rpsJ* ribosomal operon when strains were grown at comparable growth rates. Changes in the steady-state levels of the genes that are involved in the *rpsJ* operon. The *rne-1* array was performed as part of this study and is also shown in Fig. 2.11. The *rneΔ1018/rng-219* was previously analyzed in this laboratory (Bowden and Kushner, unpublished results.) The *rneΔ1018/rng-219* in M9 medium array was performed as part of this study. The image presented was obtained from a screen shot of the Integrated Genome Browser program (20). Operon names appear above or below the operons that encode them, which indicate their location in the genome relative to nucleotide coordinates, as displayed in the center of the graph. Black arrows indicate the direction of transcription. The array data is displayed as vertical lines representing the log2 ratio of fluorescence between the mutant and wild-type strains.

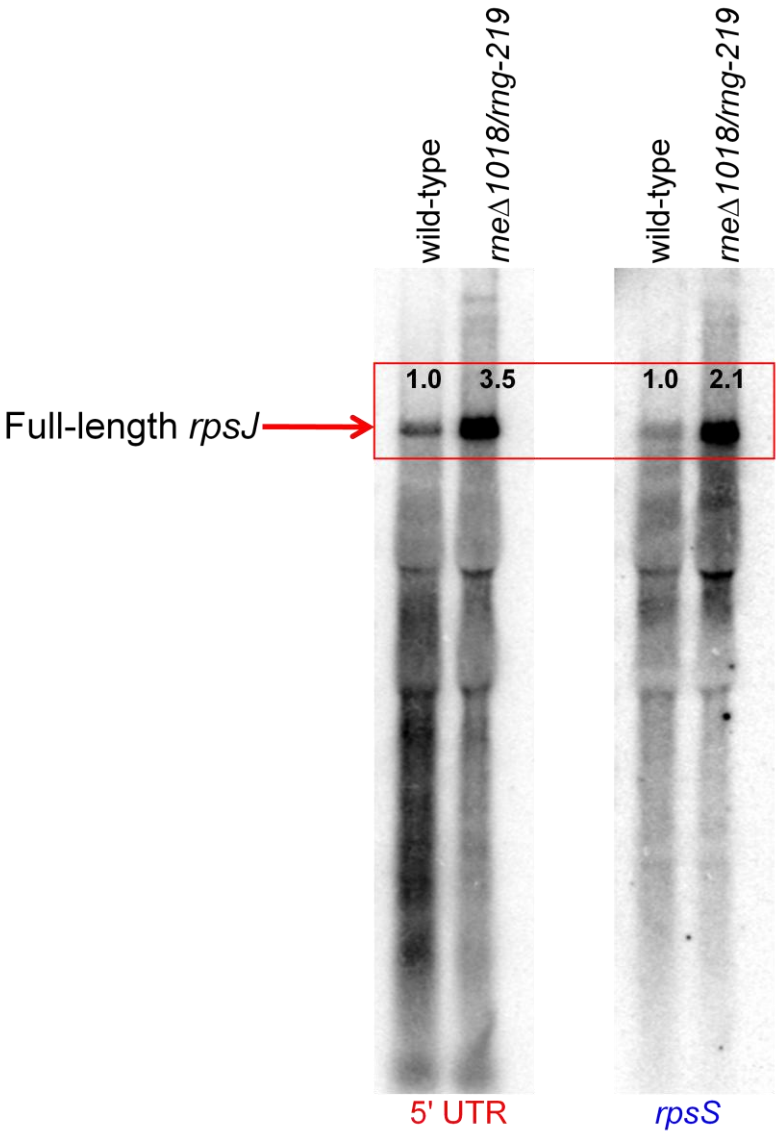

Figure 2.13. Analysis of *rpsJ* transcript from strains grown at comparable growth rates in minimal medium. Cells were grown at 37°C. RNA was run on a 1.5% glyoxyl agarose gel. Strains were MG1693 (wild-type) and SK3564 (*rneΔ1018/rng-219*) in Lanes 1 and 2, respectively.

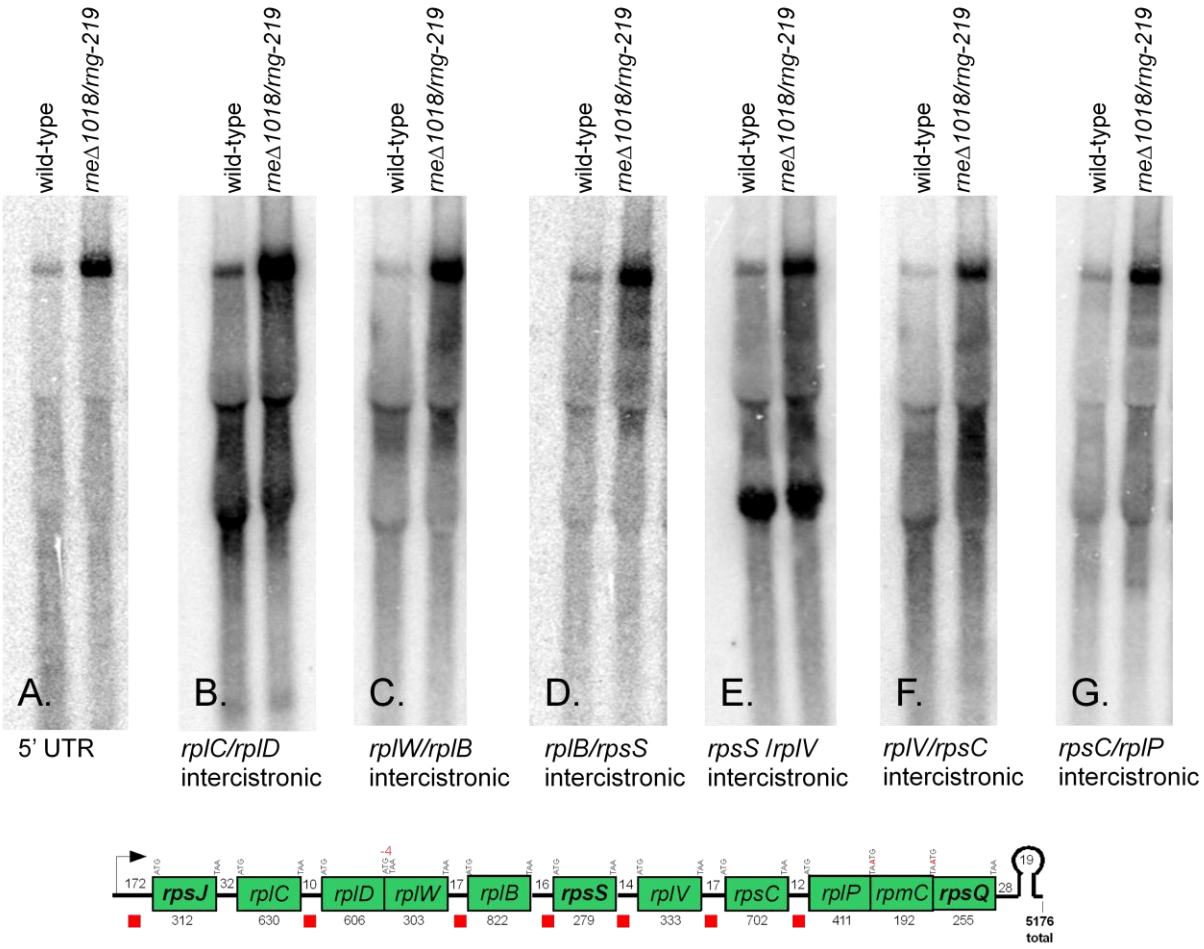

Figure 2.14. Agarose northern blots of wild-type and *rneΔ1018/rng-219* strains grown in M9 minimal medium and probed for several intercistronic regions. Cells were grown at 37°C. RNA was run on a 1.5% glyoxyl agarose gel. Strains were MG1693 (wild-type) and SK3564 (*rneΔ1018/rng-219*) in Lanes 1 and 2, respectively.

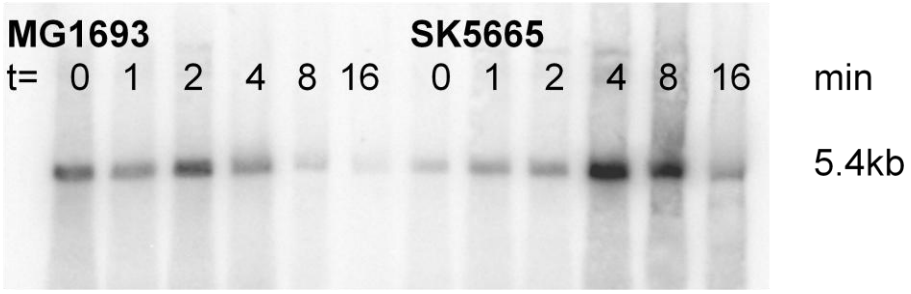

Figure 2.15. Chemical half-lives of the full-length *rpsJ* transcript. The calculated half-life of the full-length *rpsJ* transcript was 2.2 ± 0.56 minutes for MG1693 (wild-type) and 3.86 ± 0.89 minutes for SK5665 (*rne-1*). Cells were initially grown at 30°C with shift to 44°C for 1hr. RNA was run on a 1.5% glyoxyl agarose gel.

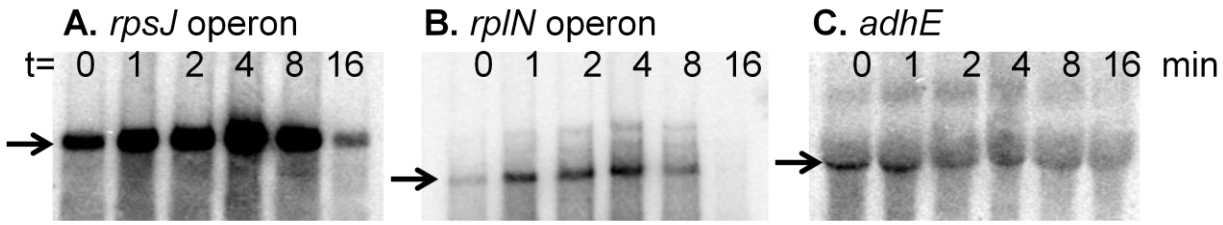

Figure 2.16. Chemical half-lives of the *rpsJ* operon transcript, the *rplN* operon transcript, and *adh* transcript in SK4161. Cells were initially grown at 30°C with shift to 44°C for 1hr. RNA from SK4161 (*rne-1* ∆*rnz::apr* ∆*mazEFG*) was run on a 1.5% glyoxyl agarose gel. Arrows indicate the full-length transcript of 5.2 kb, 5.6 kb, and 3.0 kb for *rpsJ*, *rplN*, and *adhE*, respectively.

REFERENCES

1. Morse, D.E., Mosteller, R.D. and Yanofsky, C. (1969) Dynamics of synthesis, translation, and degradation of *trp* operon messenger RNA in *E. coli*. *Cold Spring Harb. Symp. Quant. Biol.*, **34**, 725-740.
2. Zurawski, G. and Zurawski, S.M. (1985) Structure of the *Escherichia coli* S10 ribosomal protein operon. *Nucleic Acids Res.*, **13**, 4521-4526.
3. Lindahl, L., Post, L., Zengel, J., Gilbert, S.F., Strycharz, W.A. and Nomura, M. (1977) Mapping of ribosomal protein genes by *in vitro* protein synthesis using DNA fragments of lambdafus3 transducing phage DNA as templates. *J. Biol. Chem.*, **252**, 7365-7383.
4. Li, X., Lindahl, L. and Zengel, J.M. (1996) Ribosomal protein L4 from *Escherichia coli* utilizes nonidentical determinants for its structural and regulatory functions. *RNA*, **2**, 24-37.
5. Zengel, J.M. and Lindahl, L. (1996) A hairpin structure upstream of the terminator hairpin required for ribosomal protein L4-mediated attenuation control of the S10 operon of *Escherichia coli*. *J. Bacteriol.*, **178**, 2383-2387.
6. Sha, Y., Lindahl, L. and Zengel, J.M. (1995) RNA determinants required for L4-mediated attenuation control of the S10 r-protein operon of *Escherichia coli*. *J. Mol. Biol.*, **245**, 486-498.
7. Sha, Y., Lindahl, L. and Zengel, J.M. (1995) Role of NusA in L4-mediated attenuation control of the S10 r-protein operon of *Escherichia coli*. *J. Mol. Biol.*, **245**, 474-485.

8. Nomura, M., Yates, J.L., Dean, D. and Post, L.E. (1980) Feedback regulation of ribosomal protein gene expression in *Escherichia coli*: structural homology of ribosomal RNA and ribosomal protein MRNA. *Proc. Natl. Acad. Sci. USA*, **77**, 7084-7088.

9. Allen, T., Shen, P., Samsel, L., Liu, R., Lindahl, L. and Zengel, J.M. (1999) Phylogenetic analysis of L4-mediated autogenous control of the S10 ribosomal protein operon. *J. Bacteriol.*, **181**, 6124-6132.

10. Nomura, M., Gourse, R. and Baughman, G. (1984) Regulation of the synthesis of ribosomes and ribosomal components. *Annu. Rev. Biochem.*, **53**, 75-117.

11. Squires, C.L. and Zaporojets, D. (2000) Proteins shared by the transcription and translation machines. *Annu. Rev. Microbiol.*, **54**, 775-798.

12. Nomura, M. (1999) Regulation of ribosome biosynthesis in *Escherichia coli* and *Saccharomyces cerevisiae*: diversity and common principles. *J. Bacteriol.*, **181**, 6857-6864.

13. Stead, M.B., Marshburn, S., Mohanty, B.K., Mitra, J., Pena Castillo, L., Ray, D., van Bakel, H., Hughes, T.R. and Kushner, S.R. (2011) Analysis of *Escherichia coli* RNase E and RNase III activity *in vivo* using tiling microarrays. *Nucleic Acids Res.*, **39**, 3188-3203.

14. Babitzke, P. and Kushner, S.R. (1991) The Ams (altered mRNA stability) protein and ribonuclease E are encoded by the same structural gene of *Escherichia coli*. *Proc. Natl. Acad. Sci. USA*, **88**, 1-5.

15. Schedl, P. and Primakoff, P. (1973) Mutants of *Escherichia coli* thermosensitive for the synthesis of transfer RNA. *Proc. Natl. Acad. Sci. USA*, **70**, 2091-2095.

16. Mohanty, B.K., Giladi, H., Maples, V.F. and Kushner, S.R. (2008) Analysis of RNA decay, processing, and polyadenylation in *Escherichia coli* and other prokaryotes. *Methods Enzymol.*, **447**, 3-29.

17. O'Hara, E.B., Chekanova, J.A., Ingle, C.A., Kushner, Z.R., Peters, E. and Kushner, S.R. (1995) Polyadenylylation helps regulate mRNA decay in *Escherichia coli*. *Proc. Natl. Acad. Sci. USA*, **92**, 1807-1811.

18. Mohanty, B.K. and Kushner, S.R. (2007) Ribonuclease P processes polycistronic tRNA transcripts in *Escherichia coli* independent of ribonuclease E. *Nucleic Acids Res.*, **35**, 7614-7625.

19. Stead, M.B., Agrawal, A., Bowden, K.E., Nasir, R., Mohanty, B.K., Meagher, R.B. and Kushner, S.R. (2012) RNAsnap: a rapid, quantitative and inexpensive, method for isolating total RNA from bacteria. *Nucleic Acids Res.*, **40**, e156.

20. Nicol, J.W., Helt, G.A., Blanchard, S.G., Jr., Raja, A. and Loraine, A.E. (2009) The Integrated Genome Browser: free software for distribution and exploration of genome-scale datasets. *Bioinformatics*, **25**, 2730-2731.

21. Bremer, H. and Dennis, P. (1996) In Neidhardt, F. C., Curtiss III, R., Ingraham, J. L., Lin, E. C. C., Low, K. B., Magasanik, B., Reznikoff, W. S., Riley, M., Schaechter, M. and Umbarger, H. E. (eds.), *Escherichia coli and Salmonella*. 2nd ed. ASM Press, Washington, DC, pp. 1553-1569.

22. Chung, D.H., Min, Z., Wang, B.C. and Kushner, S.R. (2010) Single amino acid changes in the predicted RNase H domain of *Escherichia coli* RNase G lead to complementation of RNase E deletion mutants. *RNA*, **16**, 1371-1385.

23. Lindahl, L. and Zengel, J.M. (1979) Operon-specific regulation of ribosomal protein synthesis in *Escherichia coli*. *Proc. Natl. Acad. Sci. USA*, **76**, 6542-6546.

24. Zuker, M. (2003) Mfold web server for nucleic acid folding and hybridization prediction. *Nucleic Acids Res.*, **31**, 3406-3415.

25. Ow, M.C., Perwez, T. and Kushner, S.R. (2003) RNase G of *Escherichia coli* exhibits only limited functional overlap with its essential homologue, RNase E. *Mol. Microbiol.*, **49**, 607-622.

26. Ow, M.C. and Kushner, S.R. (2002) Initiation of tRNA maturation by RNase E is essential for cell viability in *E. coli*. *Genes Dev.*, **16**, 1102-1115.

27. Arraiano, C.M., Yancey, S.D. and Kushner, S.R. (1988) Stabilization of discrete mRNA breakdown products in *ams pnp rnb* multiple mutants of *Escherichia coli* K-12. *J. Bacteriol.*, **170**, 4625-4633.

28. Ow, M.C., Liu, Q. and Kushner, S.R. (2000) Analysis of mRNA decay and rRNA processing in *Escherichia coli* in the absence of RNase E-based degradosome assembly. *Mol. Microbiol.*, **38**, 854-866.

29. Perwez, T. and Kushner, S.R. (2006) RNase Z in *Escherichia coli* plays a significant role in mRNA decay. *Mol. Microbiol.*, **60**, 723-737.

CHAPTER 3

POLYADENYLATION OF MESSENGER RNAS BY POLY(A) POLYMERASE I IN *ESCHERICHIA COLI* IS LINKED TO THE PRESENCE OF AN INTACT RNASE E-BASED DEGRADOSOME[1]

[1] Kristen B. Mildenhall, Dae-hwan Chung, Bijoy K. Mohanty, and Sidney R. Kushner. To be submitted to Nucleic Acids Research.

ABSTRACT

In *Escherichia coli*, poly(A) polymerase I (PAP I) has been shown to account for 90% of the poly(A) tails that are added to mRNAs, rRNAs, and pre-tRNAs. Here we show that the polyadenylation of mRNAs by PAP I is directly linked to an intact RNase E-based degradosome. The polyadenylation profiles of specific mRNA transcripts (*lpp, rpsJ* and *rpsQ*) changed dramatically both in the location of the tails and in their nucleotide composition when the scaffold region of the RNase E protein was deleted. Specifically, in the absence of degradosome assembly, the majority of the tails for specific mRNA transcripts were heteropolymeric and were added by polynucleotide phosphorylase (PNPase). The polyadenylation profiles of PNPase mutants encoding either a non-functional PNPase, or enzymes with either reduced degradative activity or severely reduced biosynthetic activity were also examined to determine the possible role of PNPase in PAP I-mediated polyadenylation. Our data suggest the existence of a more extensive polyadenylation complex and a more direct link between mRNA degradation and polyadenylation than previously envisioned. Additionally, since RNase E and PAP I have both been previously demonstrated to be associated with the inner membrane during exponential growth, it appears that polyadenylation of mRNAs by PAP I likely occurs at the inner membrane.

INTRODUCTION

Polyadenylation at the 3' termini of mRNAs is an important post-transcriptional event in both eukaryotes and prokaryotes. In eukaryotes, the addition of poly(A) tails increases mRNA stability by preventing both 5'→ 3' and 3'→ 5' degradation and promotes more efficient translation (1-3). In contrast, polyadenylation of bacterial mRNAs, as demonstrated in *Escherichia coli,* leads to relatively short tails that are appear to target the mRNAs for more rapid degradation (4-9).

In *E. coli,* less than 2% of total RNA is polyadenylated at one time, however, more than 80% of the mRNA transcripts can be substrates for polyadenylation (10,11). It has been hypothesized that since *E. coli* does not have a 5'→3' exonuclease, nor can most of its exonucleases degrade though secondary structures, that the addition of the poly(A) tails to the 3' end of mRNAs aid in their ability to degrade the secondary structures, particularly Rho-independent transcription terminators that are associated with mRNAs.

Polyadenylation in *E. coli* is carried out by two enzymes, poly(A) polymerase I (PAP I) and polynucleotide phosphorylase (PNPase). PAP I, encoded by *pcnB* (12), is responsible for 90% of polyadenylation and synthesizes short poly(A) tails (1-40 nt) that exclusively contain adenosine residues (7,9,13). However, tail lengths are reduced by 3'→ 5' exonucleases such as RNase II and PNPase (7,14-16). *In vivo,* poly(A) tails are found on both mRNA decay products and full-length transcripts after Rho-independent transcription terminators (9,11,15,17). In fact, over 80% of poly(A) tails are normally located after Rho-independent transcription terminators (17). Over production of PAP I causes cell death, since mature tRNAs become substrates for PAP I, causing a loss of

protein synthesis and cell death (18). However, in exponentially growing cells there are no significant changes in the growth properties of *⊿pcnB* strains (7,9,13).

The second enzyme that can post-transcriptionally add nucleotides onto the 3' ends of mRNAs is PNPase. This enzyme functions both as a 3'→5' exonuclease that degrades RNA using a phosphorolytic mechanism (19) and as a poly(A)-type polymerase that can biosynthetically synthesize long heteropolymeric tails that contain all four nucleotides (20). PNPase adds tails at locations within the mRNA transcripts that are significantly different than those synthesized by PAP I (17,20). Of particular interest is the fact that PNPase has been shown to form complexes with both PAP I (17) and RNase E (21). However, the exact mechanism by which PNPase functions in the polyadenylation of mRNAs is not clear.

PNPase is also an integral part of the RNase E-based degradosome, a key complex involved in mRNA degradation, which contains PNPase, the RhlB RNA helicase and enolase (21-23) associated with the RNase E scaffold domain. Deletion experiments have demonstrated that association regions for the RhlB RNA helicase, enolase and PNPase are located at amino acids 734-738, 739-845 and 844-1045 of the RNase E scaffold, respectively (24). Furthermore, it has been argued that Hfq, an abundant 11.2 kDa RNA-binding protein, can also associate with RNase E, competing with the RhlB RNA helicase for binding in the region of amino acids 734-738 (25).

Polyadenylation of mRNA transcripts in *E. coli* has also been shown to involve interaction of additional proteins. One protein that has been shown to be involved in PAP I polyadenylation is Hfq. Inactivation of Hfq dramatically reduces the ability of PAP I to add poly(A) tails to transcripts after Rho-independent transcription terminators, even

though intracellular PAP I protein levels remain constant (17). Additionally, total polyadenylation levels are dramatically lower and poly(A) tails observed in an *hfq* mutant are shorter, even when PNPase, RNase II or RNase E are also missing, demonstrating that the shortened tails are not the result of nucleolytic degradation (17). Pull-down and immuno-precipitation experiments have demonstrated physical interactions among PAP I, PNPase and Hfq, suggesting the existence of a multiprotein complex that is required for the polyadenylation of mRNAs with Rho-independent transcription terminators. However, it is important to remember that these proteins are not present in the cell in similar concentrations. PNPase has been shown to be present in large excess relative to RNase E (5-10 fold during exponential phase) (26), while PAP I has only been estimated to have ~32-50 molecules per cell (17).

Although the biological function of the heteropolymeric tails is currently unknown, polyadenylation of mRNAs by PNPase has been observed in a number of other bacteria (27-30). In fact, *E. coli* strains with higher levels of PNPase were observed to have higher levels of heteropolymeric tails (20). It was also shown that PNPase, unlike PAP I, usually does not add tails after secondary structures such as Rho-independent transcription terminators (17,20), although the reasons for the distinction are currently unclear.

Therefore, it was surprising when macroarray analysis of the *E. coli* genome revealed that multiple ORFs within a polycistronic mRNA were targets for polyadenylation (11). For example, with the *rpsJ* polycistronic mRNA, which is over 5,100 nt in length and contains 11 ORFs (Fig. 3.1), polyadenylation of many of its ORFs was detected with the array (11). When initial experiments confirmed that both the first

ORF in the operon (*rpsJ*) and the last ORF (*rpsQ*) were polyadenylated, we decided to examine this phenomenon in greater detail.

Since both Hfq and PNPase, which interact with PAP I, are also associated with the RNase E-based degradosome, we wondered if there was a link between PAP I mediated polyadenylation of mRNAs and the RNase E-based degradosome. Furthermore, if there were a link between polyadenylation and the RNase E-based degradosome, we wanted to determine what components of the degradosome were essential for their interaction. In order to delineate the relationship of these two complexes, if any, the polyadenylation profiles of three ORFs within the polycistronic *rpsJ* operon (*rpsJ*, *rplV*, *rpsQ*) and the transcript for the monocistronic *lpp* mRNA were examined in *E. coli* mutants defective for degradosome assembly or PNPase function along with a wild-type control. Here we show that for transcripts primarily polyadenylated by PAP I, the main components of the degradosome are required for polyadenylation by PAP I. In the absence of an intact degradosome, the majority of the post-transcriptionally added tails were synthesized by PNPase.

MATERIALS AND METHODS

Bacterial Strains and Plasmids

All the strains and plasmids used are listed in Table 1. RNase E partial scaffold deletions were constructed in MG1693 (*thyA715 rph-1*) by P1-mediated transduction using either AC-24 (*rne*Δ*10 zce-726::*Tn*10* Tc^R*)* or AC-26 *(rne*Δ*18 zce-726::*Tn*10* Tc^R*)* (31) as donor strains. The *rne*Δ*10* and *rne*Δ*18* mutations are missing the RNase E scaffold from amino acids 844-1045 and 728-845, respectively, such that PNPase fails

to bind in the *rne*Δ*10* strain while enolase and the RhlB RNA helicase fail to bind in *rne*Δ*18*. AC-24 and AC-26 were the generous gifts of the Carpousis laboratory. MG1693 was provided by the *E. coli* Genetic Stock Center (Yale University). Transductants were confirmed by PCR and DNA sequencing to verify the locations of scaffold deletions.

SK2683 was constructed using a plasmid displacement method. The *rne⊿374* fragment from the 6-8 copy plasmid pMOK16 (32) was transferred into the single copy plasmid pMOK40 (Sm^R/Sp^R) (33) at the *Eco*RI-*Not*I sites and subsequently transformed into SK9714 (32). The covering plasmid (pSBK1) carrying rne^+ was displaced by pWSK129 (34), which had the same origin of DNA replication. Figures of each of the RNase E mutants are shown in Figure 3.2.

Strains were created that carried mutations in the *pnp* gene in which single amino acid substitutions led to alterations in either the 3'→5' exonuclease or polymerization activities, but retained the normal trimeric structure of the PNPase protein *in vivo* (35). The R100D allele lacks both the biosynthetic and degradative activity of PNPase, the N435D has normal biosynthetic activity but severely reduced degradative activity, while the D490N allele has almost normal degradative activity but severely reduced biosynthetic activity (35) (Table 3.2).

Plasmids carrying *pnp* point mutations were constructed in a 6-8 copy vector and under the control of the native *rpsO pnp* promoter as follows: pKMK12 ($rpsO^+$ pnp^+) was first created by *Hin*dIII/*Kpn*I digestion of pKAK7 (36) to excise the native *rpsOpnp* fragment which was subsequently ligated into the *Hin*dIII/*Kpn*I sites of pWSK29 (34). As both pWSK29 and pKAK7 are Ap^R, the ligated plasmid was digested with *Sal*I prior to transformation into DH5α to disrupt any possible pKAK7-derivatives. The pKMK12

plasmid was sequenced using M13R and M13F universal primers to ensure correct junctions.

Next, site directed mutagenesis was performed to create R100D, N435D, or D490N plasmid point mutations using Q5 Site-Directed Mutagenesis Kit (NEB) and the following primer sets to amplify pKMK12 (*rpsO*$^+$ *pnp*$^+$): “R100Dpnp_Fwd2” [CCGCCCG ATTGACCCGCTGTTC], “R100Dpnp_Rev2” [TCAATCAGACGCGCGATC], “N435Dpnp_Fwd2” [CACTGAATCCGACGGTTCCTC], “N435Dpnp_Rev2” [ATTTCAGA CACAACACGTAC], “D490Npnp_Fwd2” [TCACCTGGGCAATATGGACTTC], and “D490Npnp_Rev2” [TCTTCGTCGCCCAAAATG]. The PCR reactions were digested with KLD enzyme mix as directed and subsequently transformed into NEB 5α. Plasmids were isolated from the transformants, sequenced for confirmation, and named pKMK13 (*rpsO*$^+$ *pnp*-R100D), pKMK14 (*rpsO*$^+$ *pnp*-N435D), and pKMK15 (*rpsO*$^+$ *pnp*-D490N).

Following plasmid construction, SK10019 (*pnp⊿683*) (20) was transformed with either pKMK12 (*rpsO*$^+$ *pnp*$^+$), pKMK13 (*rpsO*$^+$ *pnp*-R100D), pKMK14 (*rpsO*$^+$ *pnp*-N435D), pKMK15 (*rpsO*$^+$ *pnp*-D490N), or pWSK29 (vector) to create SK4436, SK4437, SK4438, SK4439, and SK4443, respectively.

The *rne-1* allele encodes a temperature-sensitive mutation that functionally inactivates RNase E at 44^{o}C (37). The *hfq-1* mutation is a deletion/insertion mutation that produces no Hfq protein (17). The *pnp-7* and *pnp⊿683* mutations are a point mutation and chromosomal deletion insertion, respectively, that have been described previously (20,38).

Bacterial growth and doubling times

To obtain growth curves, bacterial strains were grown at 37°C with shaking at 255 rpm in Luria broth supplemented with thymine (50 µg/mL) and streptomycin (20 mg/mL) or ampicillin (200 mg/mL), where appropriate. Measurements were taken every 30 minutes using a Klett-Summerson colorimeter with a green filter (No. 42). Cells were diluted with pre-warmed growth medium as needed to maintain the cultures in exponential growth. Growth curves were done in triplicate and values averaged before the data was plotted.

Pull-down analysis of the RNase E-based degradosome in various mutants

To determine if any of the *pnp* mutations led to alterations in the compositions of the RNase E-based degradosome complex, pull-down assays were performed. Strains were grown at 37°C with shaking at 255 rpm to Klett 80 in Luria broth supplemented with thymine (50 µg/mL) and antibiotic, where appropriate. Cell cultures (50 mL) were collected for protein isolation and quantified as described previously (17). Immuno-precipitations were performed at 4°C by mixing two mg of total protein and PNPase-antibody cross-linked to Pierce Protein A/G magnetic beads (Thermo Scientific; 25 µl) for 1 h in a shaker. The protein–bead complexes were washed three times with RIPA buffer (150mM NaCl, 50 mM Tris-HCl pH 8, 1.0% Nonidet P-40, 0.5% DOC, 0.1% SDS). The immunocomplexes were subsequently eluted from the beads in 40 µl of the SDS-PAGE loading buffer after heating at 55°C for 15 min, followed by boiling for 5 min. For PNPase (2 µl diluted 1:10) and for RNase E (10 µl) immunoprecipitation samples were separated on 7.5% (for RNase E) and 10% (for PNPase) SDS-PAGE gels and

probed with their respective antibodies at a 1:10,000 and 1:2,500 for PNPase (anti-rabbit from A.J. Carpousis laboratory) and RNase E (32), respectively.

Mapping of post-transcriptionally added poly(A) tails

Total RNA was isolated from various exponentially growing strains as described previously (7,39) and treated with DNase I to remove any residual DNA contamination present. The quality of RNA samples was checked by agarose gel electrophoresis and then quantified using a Nanodrop® ND-2000c spectrophotometer. Subsequently, oligo(dT)-dependent cDNAs were obtained for *rpsJ*, *rplV*, *rpsQ*, and *lpp* mRNAs using reverse transcription-PCR with 5' gene-specific and 3' oligo$(dT)_{17}$ primers, as described previously (15,39). The 5' gene-specific primers were as follows: “rpsJ 5' GS” [GTCTGAT CGATCAAGCAACC], “rpsQ 5' GS” [TAATGATCGATAAAATCCGTAC TCTGC], “rplV 5' GS” [AAACTATCGATAAACATCGCCATGCTC], and “lpp366” [GCTACATGGAGATTAACTCAAGCTTGAGGG]. All gene-specific primers contained a *Cla*I site, except for the *lpp* gene-specific primer which contained a *Hin*dIII site, and were designed such that the entire coding sequence of *lpp* and *rpsQ* ORFs and the final 260 and 329 nucleotides of the coding sequence of *rpsJ* and *rplV*, respectively, would be amplified. The cDNAs were all cloned into the *Cla*I/*Xba*I or *Hin*dIII/*Xba*I sites of pWSK29 (34), as described previously (20,39). Preliminary DNA sequencing was performed for MG1693-derived tails using BigDye® Terminator v3.1 Cycle Sequencing kit and an automated sequencer (Applied Biosystems 3730x1 DNA analyzer). All other sequencing was performed by MacrogenUSA using an M13 Reverse primer. Sequences were then analyzed and compared to each specific gene using the online

BLAST blastn program (NCBI) selected for *E. coli* strain MG1655 (taxid:511145) in the NCBI nucleotide collection. Sequence results with tails starting less than three nucleotides following the 5' gene-specific primer sequence were not included to eliminate any mispriming events.

Poly(A) Sizing Assay

Total RNA was isolated from various exponentially growing strains as described previously (7,39). The RNA was treated with DNase I to remove any residual DNA contamination present. The quality of RNA samples was checked by agarose gel electrophoresis and then quantified using a Nanodrop® ND-2000c spectrophotometer. Subsequently, total RNA was 3'-end-labeled with [^{32}P]-pCp and then digested with RNase A and RNase T1 and then separated on a 20% PAGE, as described previously (7,39). A 5'-[^{32}P]-end-labeled oligo(dA) ladder was also run, as described previously (7,39). The gel was exposed to X-ray film overnight.

RESULTS

Polyadenylation profiles of the *rpsJ*, *rplV*, and *rpsQ* transcripts in wild-type *E. coli*

In the macroarray analysis of the *E. coli* transcriptome, it was reported that many of the ORFs within the polycistronic *rpsJ* transcript were subject to polyadenylation (11). In order to confirm that the various ORFs within the *rpsJ* operon were in fact polyadenylated in wild-type *E. coli*, we chose three representative genes from the beginning (*rpsJ*), middle (*rplV*), and end (*rpsQ*) of the polycistronic transcript (Fig. 3.1)

for direct analysis. cDNAs from each ORF were obtained and cloned as described in the Materials and Methods.

As shown in Table 3.3, the majority of the tails associated with the *rpsQ* transcript were homopolymeric indicating that they had been synthesized by PAP I. Additionally, as expected, the majority of the homopolymeric tails had been added after the Rho-independent transcription terminator (Fig. 3.3A), in agreement with previously reported results for the *lpp* mRNA (Fig. 3.4A) (9,20). In the case of the *rpsJ* ORF transcript, almost 50% of the tails associated were homopolymeric (Table 3.3). In contrast, only 20% of the tails associated with the *rplV* transcript were homopolymeric (Table 3.3).

Polyadenylation profiles in strains defective in functional degradosome assembly

The presence of homopolymeric tails on multiple ORFs within the polycistronic *rpsJ* transcript raised the possibility of an association between the polyadenylation reaction of PAP I and the processing of the full-length *rpsJ* transcript by the RNase E-based degradosome. To examine a possible link between PAP I and the RNase E-based degradosome, the polyadenylation profiles of *rpsJ*, *rplV*, and *rpsQ* transcripts were also analyzed in strains defective in functional degradosome assembly. As a positive control, the polyadenylation profile of the *lpp* transcript was also examined, as it has been well-characterized previously (9,20). For these experiments, we employed a complete scaffold mutant (*rne*Δ*374*) which has previously been shown to prevent degradosome formation (32), and two partial scaffold mutants in which either the PNPase scaffold binding region was deleted (*rne*Δ*10*) or the RhlB and Enolase scaffold binding regions

were missing (*rne*Δ*18*) (Fig. 3.2). All three mutants contain a wild-type catalytic region of RNase E, and thus function normally with regards to mRNA decay and tRNA maturation (32).

As shown in Table 3.3, the majority of the tails associated with *rpsJ*, *rpsQ* and *lpp* were heteropolymeric in all three degradosome mutants. It is important to note that the deletion of the entire scaffold region (*rne*Δ*374*) had the most dramatic effect on the polyadenylation profiles with the percentage of homopolymeric tails dropping 2.6-fold for *rpsJ*, 6.5-fold for *rpsQ,* and 3-fold for *lpp* (Table 3.3). Surprisingly, even the prevention of the association of RhlB and enolase with the degradosome led to a significant reduction in the fraction of homopolymeric tails (Table 3.3). Not only was the number of homopolymeric tails dramatically reduced in the absence of degradosome assembly, but the physical location of the tails changed significantly for the *rpsQ* and *lpp* mRNAs in the absence of degradosome assembly (Figs. 3.3, 3.4). In the case of the *lpp* mRNA, the absence of a functional degradosome led to all of the tails being added well upstream of the Rho-independent transcription terminator. However, when we tested the rplV transcript in the *rne*Δ*374* scaffold mutant, it polyadenylation profile was comparable to that observed in the wild-type control (Table 3.3, Fig. 3.5). It should also be noted that the heteropolymeric tails were always significantly longer than the homopolymeric tails (Table 3.3).

Polyadenylation profiles for strains defective in Hfq

Since the Hfq protein has been shown to play a role in polyadenylation of the *lpp* mRNA (17) and it has been suggested that it can also associate with the degradosome (25),

we examined the polyadenylation profiles of the *rpsJ* and *rpsQ* mRNAs in an *hfq-1* mutant. As shown in Table 3.3, the majority of the tails associated with *rpsJ*, *rpsQ* and *lpp* mRNAs were heteropolymeric in the *hfq-1* mutant, indicating that they had been synthesized by PNPase. These results were similar to the result seen in the degradosome mutants and seen previously for the *lpp* mRNA (17).

Analysis of strains carrying point mutations in the gene for PNPase

PNPase has been shown to play an integral role in both the functional degradosome (21) and the polyadenylation complex (17). It was therefore of interest to determine how important the presence of an intact PNPase trimer was to the polyadenylation of various mRNAs. To carry out these experiments, we took advantage of three specific point mutations that had previously been isolated by Jarriage *et al.* (35). The *pnp*-R100D allele encodes a PNPase with normal trimeric structure *in vivo* but no 3'→5' exonuclease and polymerization activities, the N435D-*pnp* allele encodes PNPase with normal trimeric structure *in vivo* and almost biosynthetic normal activity but severely reduced degradative activity, and the D490N-*pnp* allele encodes PNPase with its normal trimeric structure *in vivo* and almost normal degradative activity but severely reduced biosynthetic activity (Table 3.2) (35).

In order to determine if any of these mutants played a role in polyadenylation we constructed a series of low-copy number plasmids carrying these alleles under the control of their native *rpsO pnp* promoter and transformed them into a *pnpΔ683* (20) deletion strain. Strains carrying *pnp*$^{+}$, *pnp*-N435D, and *pnp*-D490N all grew with doubling times of 29.5 $\pm$ 2 minutes (Fig. 3.6). This result was comparable to the

doubling time of MG1693 (data not shown). The strains with the *pnp*-R100D allele or empty vector grew with doubling times of 52.5 ± 2 minutes and 45 ± 2 minutes, respectively. These results were comparable to the growth and doubling time of the *pnp⊿683* strain with no plasmid present (Fig. 3.6).

Pull-down analysis of the RNase E-based degradosome in various mutants

Although it has been shown that all three PNPase point mutants make stable protein *in vivo* (35), we wanted to confirm that these proteins were incorporated in the RNase E-based degradosome. Accordingly, to determine if any mutant strain used prevented proper interaction of PNPase with the RNase E-based degradosome complex, pull-down assays were performed for the wild-type strain, the degradosome mutants (*rne⊿374, rne⊿10, rne⊿18*), the PNPase mutants (*pnp*-R100D, *pnp*-N435D, *pnp*-D490N), and an *hfq-1* mutant strain. The *rne⊿374* degradosome mutant and *pnp⊿683* deletion mutant were used as internal controls, as they have been previously determined to lack interaction of PNPase with RNase E (32)(Mohanty and Kushner, unpublished results). The pull-down analysis demonstrated that all of the PNPase point mutants and the *rne⊿18* mutant retained the interactions between RNase E and PNPase, as expected. Furthermore, the *rne⊿10* mutant strain, which lacks the PNPase binding region of degradosome was defective in degradosome assembly (Fig. 3.7).

Polyadenylation profiles for strains with altered PNPase proteins

To determine if alterations in the PNPase protein affected PAP I polyadenylation, the *rpsJ*, *rpsQ* and *lpp* transcripts from various PNPase mutants were analyzed. As shown

in Table 3.4, almost all of the tails associated with all three transcripts in the *pnp⊿683* deletion strain were homopolymeric indicating that they had been synthesized by PAP I, but the physical location of the tails changed significantly for the *lpp* and *rpsQ* mRNAs in a strain lacking PNPase compared to the wild-type control (Figs. 3.3, 3.4). In the case of both the *rpsQ* and *lpp* mRNAs, the lack of a functional PNPase protein led to all of the tails being added upstream of the Rho-independent transcription terminator (Figs. 3.3C, 3.4C, 3.8AB). This shift was also seen in mutants defective for PNPase without a functional RNase E gene, and both with and without the deletion of the exonuclease RNase II (Fig. 3.9, Table 3.5).

Surprisingly, the absence of a functional protein did not alter the locations of the poly(A) tails for the *rpsJ* transcript (Fig. 3.8C). Similar polyadenylation profiles were observed in strains carrying the *pnp-7* allele as well as mutants in either RNase E (*rne-1*) or the 3'→5' exonuclease, RNase II (*rnb500*) (Table 3.5). The locations of their tails were comparable with the data shown in Table 3.4 and Fig. 3.9, namely tail locations were only shifted if the polyadenylation was directly associated with a Rho-independent transcription terminator.

Polyadenylation profiles for strains defective in PNPase activities

To determine if the physical presence of PNPase in the degradosome complex or partial PNPase enzymatic activity was sufficient for proper PAP I polyadenylation, the *rpsJ*, *rpsQ* and *lpp* transcripts from mutants with an altered PNPase were analyzed. A strain encoding PNPase that retains its normal trimeric structure *in vivo* but lacks both 3'→5' exonuclease and polymerization activities, a strain encoding PNPase which retains its

normal trimeric structure *in vivo* and almost biosynthetic normal activity but has severely reduced degradative activity, and a strain encoding PNPase which retains its normal trimeric structure *in vivo* and almost normal degradative activity but has severely reduced biosynthetic activity (35) were analyzed.

As shown in Table 3.4, almost all of the tails associated with the transcripts examined in both the *pnp*Δ*683* deletion mutant and the inactive *pnp*-R100D mutant were homopolymeric, indicating that they had been synthesized by PAP I. In the case of the *lpp* and *rpsQ* transcripts, the majority of the homopolymeric tails in the PNPase mutants were added within the ORF before the Rho-independent transcription terminator (Fig. 3.8). The profiles of *pnp*-N435D looked more similar to the wild-type control (Table 3.4), but still contained a higher percentage of heteropolymeric tails than observed in wild-type conditions and the tails were located throughout the coding sequence (Fig. 3.8), as opposed to primarily after the Rho-independent transcription terminator in wild-type conditions. Additionally, the profile of the tails added in the *pnp*-D490N mutant strain was predominately heteropolymeric, more similar to the degradosome scaffold mutant than to the wild-type control.

Total poly(A) profiles in various *E. coli* strains

Although the data obtained with the *rpsJ*, *rpsQ* and *lpp* mRNAs demonstrated an important role for degradosome assembly and Hfq in the polyadenylation of specific mRNAs, we wanted to confirm its importance in total polyadenylation in the cell. Accordingly, we examined total poly(A) levels using a poly(A) sizing assay for strains defective in either functional degradosome assembly or defects in PNPase activity.

Total RNA was 3'-end-labeled with [^{32}P]-pCp and then digested with RNase A and RNase T1. Since RNase A cleaves after U and C residues and RNase T1 cleaves after G residues, 3′ poly(A) tails are protected from cleavage and are separated by PAGE, as described in the Materials and Methods. As shown in Fig. 3.10, failure to assemble the degradosome led to a significant reduction in the length and total amount of poly(A) tails in the cell.

DISCUSSION

PAP I polyadenylation depends on an intact degradosome

Examination of specific mRNAs (*rpsJ, rpsQ, lpp)* that are primarily polyadenylated by PAP I in wild-type strains showed that the percentage of homopolymeric tails decreased significantly in the absence of either full degradosome assembly or the Hfq protein (Fig. 3.3). No change was seen in the *rplV* transcript, which was primarily polyadenylated by PNPase I in the wild-type strain (Table 3.3, Fig. 3.5). The significant shift in polyadenylation profiles in the various degradosome mutants (Fig. 3.5), from primarily homopolymeric to primarily heteropolymeric, suggested that PAP I-polyadenylated transcripts require an intact degradosome, since the catalytic function of RNase E was intact in these degradosome mutants (32).

Polyadenylation by PNPase can function independently of an intact degradosome

Examination of the *rplV* transcript, which was primarily polyadenylated by PNPase in the wild-type strain (Table 3.3), showed that the percentage of heteropolymeric remained unchanged in the absence of either full degradosome assembly (Fig. 3.3). This result

strongly suggests that unlike PAP I, the biosynthetic activity of PNPase does not require an intact degradosome and is likely independent of the degradosome/polyadenylation complex interaction.

PAP I added tails are shifted in location in the absence of an intact degradosome

As shown in the contrasting results of Figs. 3.3B and 3.4B compared to Figs. 3A and 4A, failure to assemble an intact degradosome led to a dramatic shift in both the composition and location of the post-transcriptionally PAP I-added homopolymeric tails in the *rpsQ* and *lpp* transcripts. In the wild-type control, the homopolymeric tails of these transcripts were predominately located after the Rho-independent transcription terminator (Figs. 3.3A, 3.4A), while in the degradosome mutant strains (Figs. 3.3B, 3.4B) the homopolymeric tails were located throughout the *lpp* coding sequence.

In fact, it appeared that when the degradosome was missing, PAP I was no longer able to interact or recognize the 3' terminus of the Rho-independent transcription terminator (Fig. 3.4A versus Fig. 3.4B), its preferred substrate in wild-type cells (17). This result was consistent with previously published data for the *lpp* mRNA in an *hfq-1* mutant (17), suggesting Hfq also plays a role in a polyadenylation complex-degradosome interaction.

The physical presence of PNPase in the degradosome is not sufficient for proper PAP I polyadenylation

Since the profile of the *pnp*Δ*683* deletion mutant and the inactive pnp-R100D mutant were experimentally similar (Table 3.4, Fig. 3.8), it would appear that the physical

presence of PNPase in its native trimeric form was not sufficient for wild-type PAP I polyadenylation of mRNAs. The profiles of *pnp*-N435D and *pnp*-D490N mutant strains seen in Table 3.4 were not comparable to what was seen in the wild-type control, especially with regards to the location of the tails (Fig. 3.8), even though PNPase retained partial function *in vivo*. These results suggest that PNPase must not only be physically present in its native trimeric form, but also must have both normal exonucleolytic and biosynthetic activity for wild-type PAP I polyadenylation of mRNAs. Additionally, immunoprecipitation that showed all the PNPase point mutants properly interacted with the degradosome complex (Fig. 3.7) confirms that the effects on polyadenylation in these strains was due to the loss of normal function of PNPase and not any loss of PNPase/degradosome interaction.

PAP I added tails are also shifted in location in the absence of functional PNPase

As expected, in the *pnp*Δ*683* and *pnp*R100D mutant strains, there were only a small number of tails that were not homopolymeric (Table 3.4). The few that did appear were dramatically shorter in length (Table 3.4), suggestive of either experimental artifacts or a rare misincorporation of a single nucleotide by PAP I. The elimination of heteropolymeric tails was consistent with previous work showing that deletion or inactivation of PNPase eliminated heteropolymeric tailing (15,17,20).

Furthermore, there was a dramatic shift in location of the homopolymeric tails present in all the PNPase mutant strains compared to the wild-type control (Figs. 3.3C, 3.4C, 3.8), particularly for transcripts directly associated with Rho-independent transcription terminators. These results were similar to what was observed for the

degradosome mutants and previously seen in *hfq-1* mutants (17). However, only a slight shift was seen for the *rpsJ* transcript (Fig. 3.8C), suggesting the shift was tied to the presence of a Rho-independent transcription terminator. These results suggest PNPase must be both present and functionally active for PAP I to polyadenylate mRNAs after Rho-independent transcription terminators and that when PNPase is absent, PAP I acts in a different manner to interact or act on its preferred mRNA substrates to post-transcriptionally add tails.

The shifts in location of tails raises the question of which interactions are key to PAP I's dependency on a functional degradosome, and if the effect of PNPase on PAP I polyadenylation is due to the direct interaction of PNPase with the degradosome. Further examination of the manner by which PNPase affects PAP I substrate affinity is necessary.

Processed ORF transcripts within a polycistronic transcript can have different polyadenylation profiles

Previous polyadenylation studies had not examined the polyadenylation of large polycistronic transcripts. Thus, the observation from macroarray analysis that many ORFs within a polycistronic transcript showed polyadenylation patterns that were directly related to the transcription terminator of the operon (11) suggested that the transcription terminator of a polycistronic transcript may be a polyadenylation signal for an entire operon. Our results demonstrate that this is not the case, but rather that individual processed ORF transcripts within a polycistronic transcript can have significantly different polyadenylation profiles. Of the three genes chosen here for

analysis, the majority of the tails associated in the wild-type control with the *rpsQ* and *rpsJ* ORF transcripts had been synthesized by PAP I, while the majority of the tails associated with *rplV* had been synthesized by PNPase (Table 3.3). This was also confirmed by the changes in the polyadenylation profiles of *rpsJ* and *rpsQ* degradosome scaffold mutant (*rne*Δ*374*), while *rplV* transcript profile remained unchanged compared to wild-type. These results suggest that the transcript terminator does not act as a polyadenylation signal for the entire polycistronic transcript.

Total PAP I polyadenylation levels are reduced in strains lacking either an intact degradosome or Hfq

When a poly(A) sizing assay on a degradosome scaffold mutant (*rne*Δ*374*) and *hfq-1* mutant was performed, a dramatic drop in the number and length of poly(A) tails was observed compared to the wild-type strain (Fig. 3.10), although the drop was not as dramatic as previously seen for a Δ*pcnB* deletion strain (17). These results were in agreement with previously published *hfq-1* poly(A) sizing assays (17).

This observed decrease in total polyadenylation levels would suggest that the shift for transcripts that are primarily polyadenylated by PAP I in wild-type strains to being primarily polyadenylated by PNPase in degradosome or *hfq-1* mutants (Fig. 3.3) was due to a decrease in overall PAP I polyadenylation as opposed to an increase in PNPase polyadenylation.

Proper PAP I polyadenylation of mRNAs is likely localized to the inner membrane

We hypothesize that the mechanism of polyadenylation of mRNAs is directly related to the interaction of the polyadenylation complex with the membrane-bound degradosome (40,41). This interaction is likely mediated through the action of the Hfq protein, which has been shown to interact with both the polyadenylation complex (17) and the degradosome scaffold region (25). The interaction of the two complexes brings PAP I in closer proximity to its mRNA substrates, which is important since PAP I is present in such low amounts in the cell (17). It may also explain why the polyadenylation of mRNAs requires Hfq, while the polyadenylation of tRNAs does not (13).

Conclusions

Taken together our results provide important insights into the role of an intact degradosome in PAP I polyadenylation in *E. coli*. Our data strongly suggest the presence of a more extensive polyadenylation complex and its need for interaction with an intact degradosome for normal PAP I polyadenylation. Our data also indicate that the polyadenylation complex interacts with the degradosome through some interaction, most likely with Hfq and possibly PNPase. Since previous studies have shown 90% of mRNA polyadenylation is done by PAP I under wild-type conditions (9,17), a degradosome-PAP I interaction could suggest a major role for the degradosome in proper mRNA polyadenylation in *E. coli*. The demonstration of a large polyadenylation complex is a novel concept in bacteria and will require further analysis to understand the precise role of PNPase and the degradosome in polyadenylation on PAP I polyadenylation.

Acknowledgements

Special thanks to Dr. A.J. Carpousis for his gift of AC-24 (*rne*Δ*10*), AC-26 (*rne*Δ*18*), and PNPase anti-rabbit antibodies. This work was supported by NIH grants GM57220 and GM81554 to S.R.K.

TABLES AND FIGURES

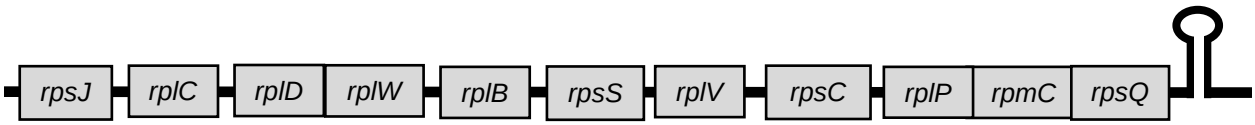

***rpsJ* operon**

Figure 3.1. Pictorial representation of the *rpsJ* operon, also known as the S10 operon. The operon contains 11 genes, all of which encode ribosomal proteins. The full-length transcript is approximately 5.2 kb in length and contains a Rho-independent transcription terminator.

Table 3.1. List of bacterial strains and plasmids used in this study.

Strains	Genotype	Reference or Source
AC-24	MC1061 *rne⊿10 (aa∆ 844-1045) zce-726::Tn10 Tc^R*	(31)
AC-26	MC1061 *rne⊿18 (aa∆ 728-845) zce-726::Tn10 Tc^R*	(31)
MG1693	*thyA715 rph-1*	*E. coli* Genetic Stock Center
SK2683	*rne⊿1018::bla thyA715 rph-1* pDHK3(Sp/Sm^R *rne∆374 single copy)*	This Study
SK4433	*rne⊿10(aa∆ 844-1045) zce-726::*Tn*10 thyA715 rph-1* Tc^R	This Study
SK4434	*rne⊿18(aa∆ 728-845) zce-726::*Tn*10 thyA715 rph-1* Tc^R	This Study
SK4436	*pnp⊿683::spc/str thyA715 rph-1* Sp/Sm^R pKMK12 (*rpsO*$^+$*pnp*$^+$, Ap^R low copy)	This Study
SK4437	*pnp⊿683::spc/str thyA715 rph-1* Sp/Sm^R pKMK13 (*rpsO*$^+$ *pnp*-R100D, Ap^R low copy)	This Study
SK4438	*pnp⊿683::spc/str thyA715 rph-1* Sp/Sm^R pKMK14 (*rpsO*$^+$ *pnp*-N435D, Ap^R low copy)	This Study
SK4439	*pnp⊿683::spc/str thyA715 rph-1* Sp/Sm^R pKMK15 (*rpsO*$^+$ *pnp*-D490N, Ap^R low copy)	This Study
SK4443	*pnp⊿683::spc/str thyA715 rph-1* Sp/Sm^R pWSK29 (empty vector, Ap^R low copy)	This Study
SK5704	*rne-1 pnp-7 rnb-500 thyA715 rph-1*	(38)
SK5726	*pnp-7 thyA715 rph-1* pDK39 *(*Cm^R *rnb-500)*	(38)
SK7988	*⊿pcnB::kan thyA715 rph-1* Km^R	(7)
SK9714	*rne⊿1018::bla thyA715 rph-1* pSBK1(*rne*+, Cm^R*)*	(32)
SK10019	*pnp⊿683::spc/str thyA715 rph-1* Sp/Sm^R	(20)
SK10023	*hfq-1::Ω thyA715 rph-1* Km^R	(17)

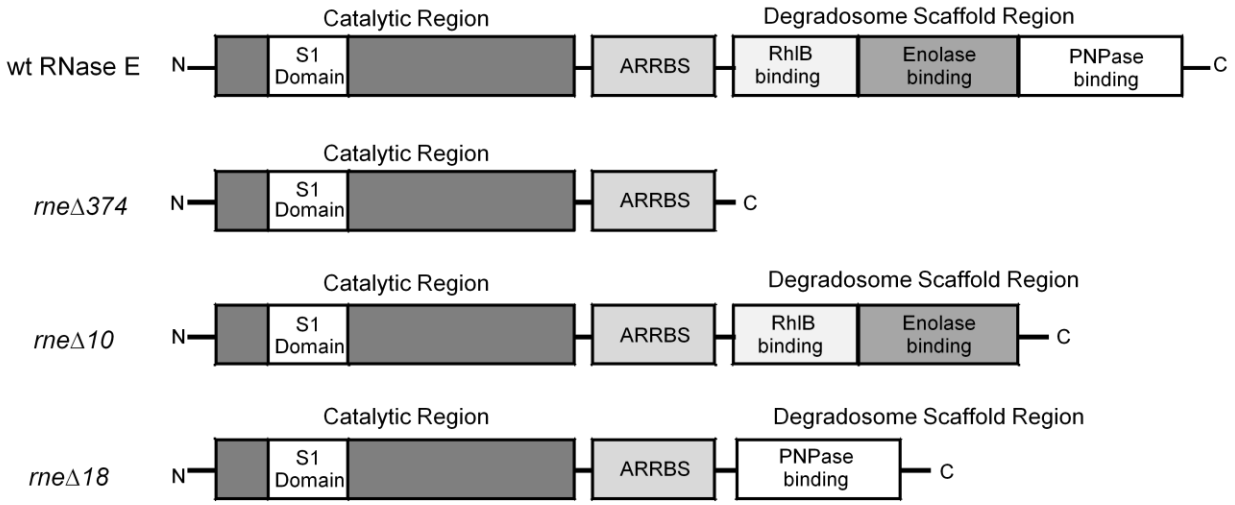

Figure 3.2. Description of the RNase E degradosome mutants used this study.

The label on the degradosome scaffold region indicates the associated binding site of the various proteins. The S1 domain is associated with RNA binding. The function of the arginine-rich RNA binding site (ARRBS) is not clear.

Table 3.2. Previously published activities of PNPase point mutants compared to a wild-type control (35).

PNPase Mutants	Exonuclease Activity	Biosynthetic Activity
R100D	0%	0%
N435D	26%	120%
D490N	70%	25%

Table 3.3. Comparison of the polyadenylation profiles of degradosome mutants. Poly(A) tails were compared with regards to percent of total tails in each tail type (homo-polymeric or heteropolymeric) and average length of each type of tail. Previously published polyadenylation profiles of *lpp* for wild-type and *hfq-1* (17) are included for comparison and are indicated by asterisks (*). N.D.= not determined.

	rpsJ					***rpsQ***					***lpp***					***rplV***	
	wt	*rneΔ374*	*rneΔ10*	*rneΔ18*	*hfq-1*	wt	*rneΔ374*	*rneΔ10*	*rneΔ18*	*hfq-1*	wt*	*rneΔ374*	*rneΔ10*	*rneΔ18*	*hfq-1**	wt	*rneΔ374*
n =	26	11	23	17	15	25	24	22	29	26	27*	25	22	21	46* (13)	25	24
% of homo-polymeric Tails (nt)	46	18	26	35	7	52	8	41	31	12	70*	24	32	43	28* (8)	20	25
Avg. homo-polymeric tail length (nt)	17	17	17	15	9	20	17	16	18	16	ND	15	15	16	ND* (11)	16	15
% of hetero-polymeric tails	54	82	74	65	93	48	92	59	69	88	30*	76	68	57	72* (92)	80	75
Avg. hetero-polymeric tail length (nt)	58	67	63	40	69	55	115	70	70	64	ND	42	44	53	ND* (70)	35	43

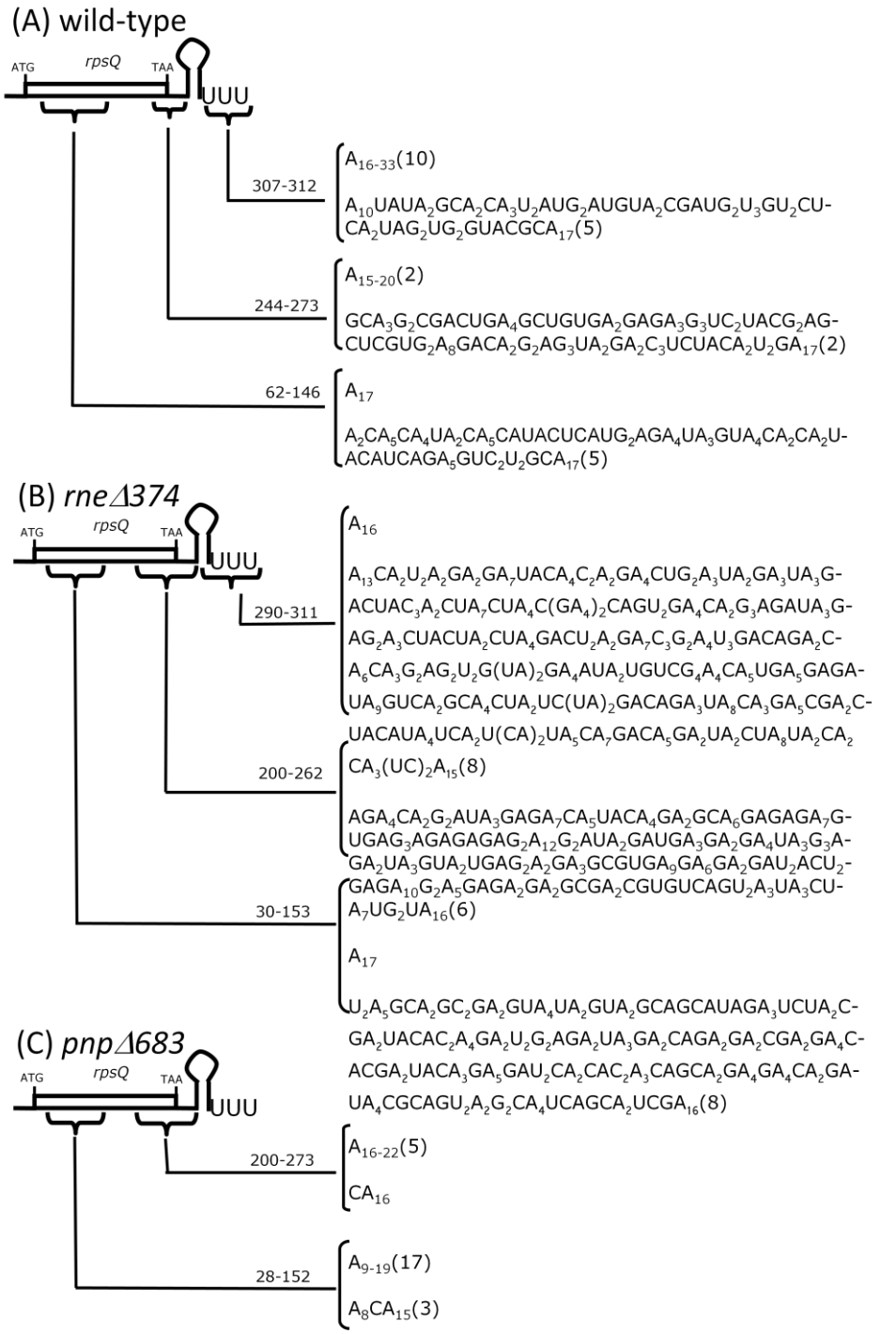

Figure 3.3. Pictorial representation of tails found on the *rpsQ* transcript. The number in parentheses following the tail is the number of that type of tail located in that region. Only the longest heteropolymeric tails are shown.

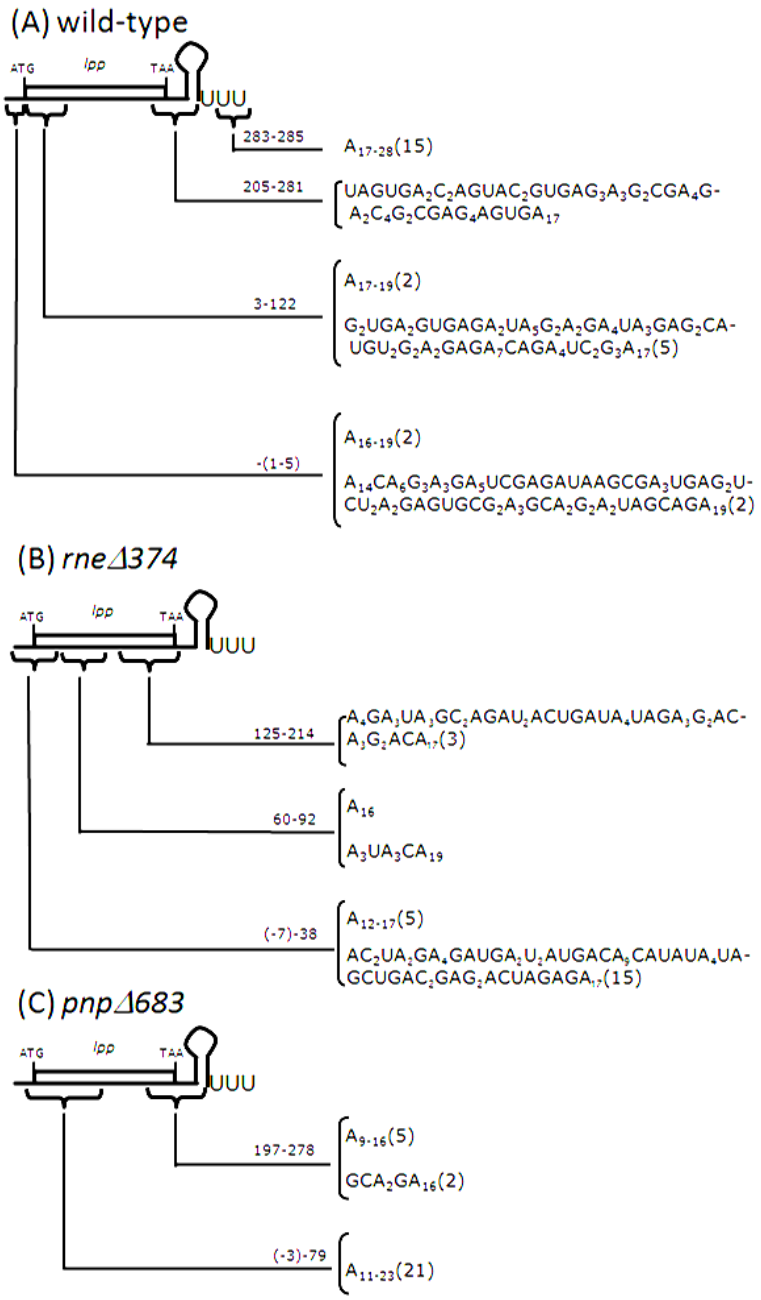

Figure 3.4. Pictorial representation of tails found on the *lpp* transcript. The number in parentheses following the tail is the number of that type of tail located in that region. Only the longest heteropolymeric tails are shown. The previously published polyadenylation profiles of *lpp* for wild-type (17) is included for comparison.

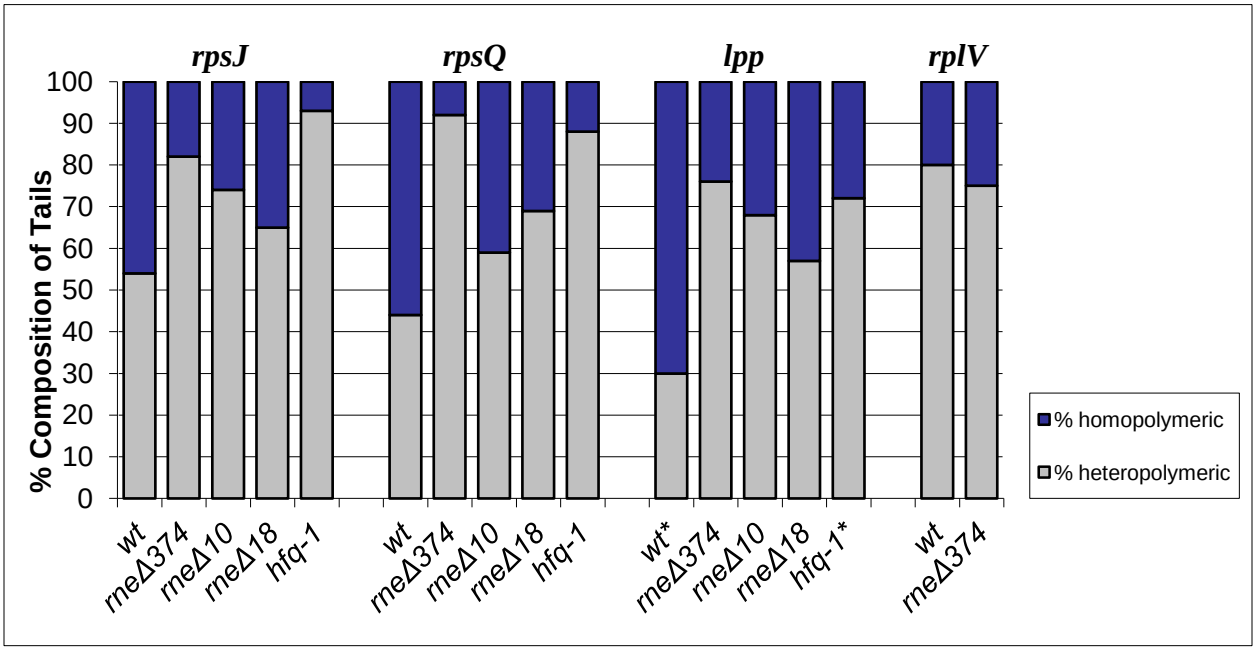

Figure 3.5. Percent composition of the post-transcriptionally added tails in various degradosome mutants. The complete data set is shown in Table 3.3. Previously published polyadenylation profiles of *lpp* for wild-type and *hfq-1* (17) are included for comparison and are indicated by asterisks (*).

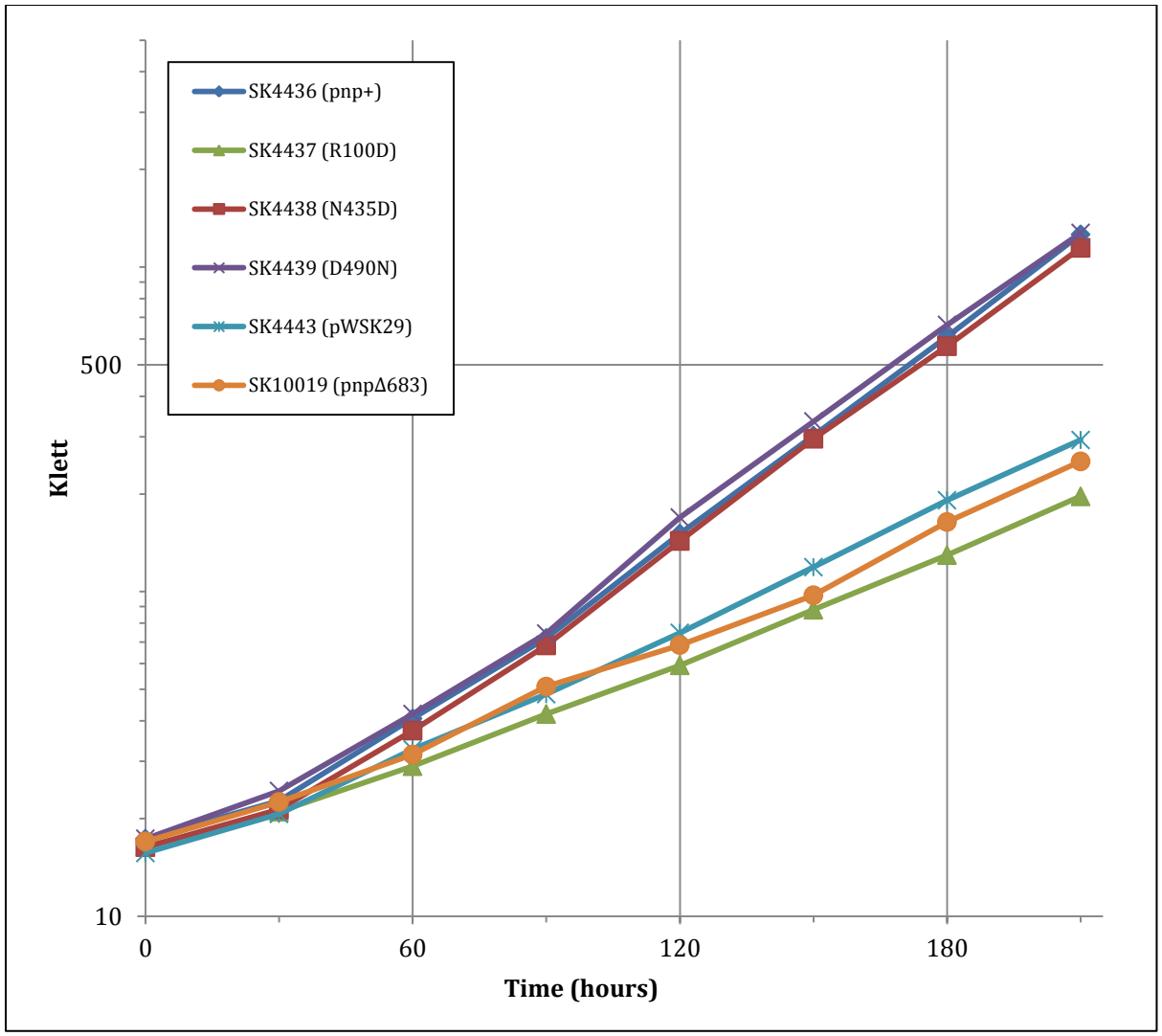

Figure 3.6. Growth curves for various PNPase mutants. Strains carrying the *pnp*$^{+}$, *pnp*-N435D, and *pnp*-D490N alleles grew with doubling times of 29.5 ± 2 minutes. The strains carrying the *pnp*-R100D allele and or an empty vector grew with doubling times of 52.5 ± 2 minutes and 45 ± 2 minutes, respectively.

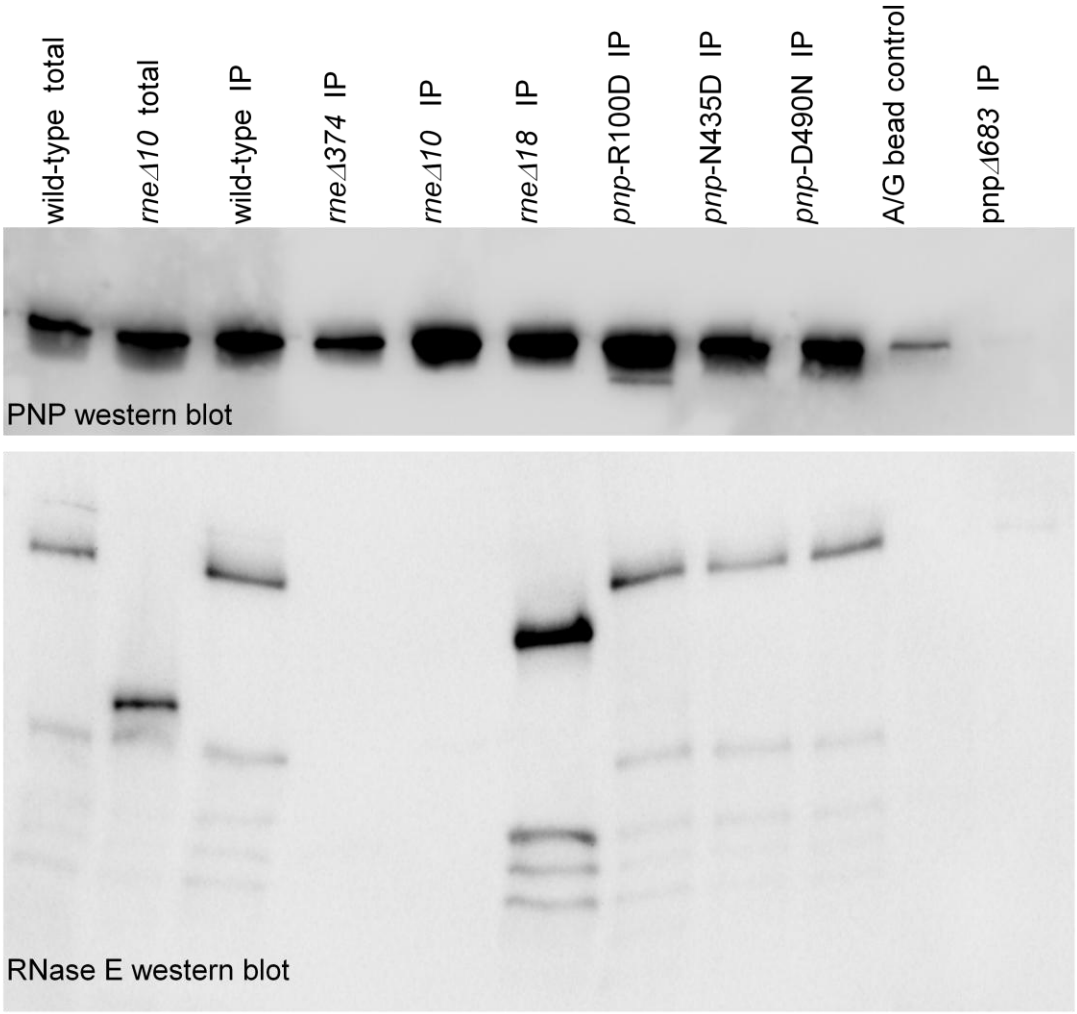

Figure 3.7. Immunoprecipitation of PNPase and scaffold mutants. Proteins were immunoprecipitated using PNP-tagged A/G beads. Subsequent pull-down elutions were run on SDS-PAGE and blotted to PVDF. Western blots were probed with either PNPase or RNase E.

Table 3.4. Comparison of the polyadenylation profiles of PNPase mutants.

Poly(A) tails were compared with regards to percent of total tails in each tail type (homopolymeric or heteropolymeric) and average length of each type of tail. Previously published polyadenylation profiles of *lpp* for wild-type (17) are included for comparison and are indicated by asterisks (*). N.D.= not determined.

	rpsJ					***rpsQ***					***lpp***				
	wt	*pnpΔ683*	*pnp*-R100D	*pnp*-N435D	*pnp*-D490N	wt	*pnpΔ683*	*pnp*-R100D	*pnp*-N435D	*pnp*-D490N	wt*	*pnpΔ683*	*pnp*-R100D	*pnp*-N435D	*pnp*-D490N
n =	26	22	20	18	25	25	26	27	23	21	27*	28	27	28	23
% of homo-polymeric Tails (nt)	46	91	85	33	12	52	85	96	43	29	70*	93	93	57	4
Avg. homo-polymeric tail length (nt)	17	17	16	16	16	20	16	17	20	17	ND	16	16	19	16
% of hetero-polymeric tails	54	9	15	67	88	48	15	4	57	71	30*	7	7	43	96
Avg. hetero-polymeric tail length (nt)	58	15	23	57	64	55	20	49	29	41	ND	18	16	51	48

Figure 3.8. Shift in location of homopolymeric tails on *rpsQ*, *lpp*, and *rpsJ* transcripts for wild-type versus PNPase mutants. The size of the dot is representative of the number of tails at particular location. Heteropolymeric tails are not shown. The *pnp*D490N mutants are not shown as there are not enough homopolymeric tails present. (See Table 3.4 for summary of heteropolymeric tail data).

(A) *rpsQ*

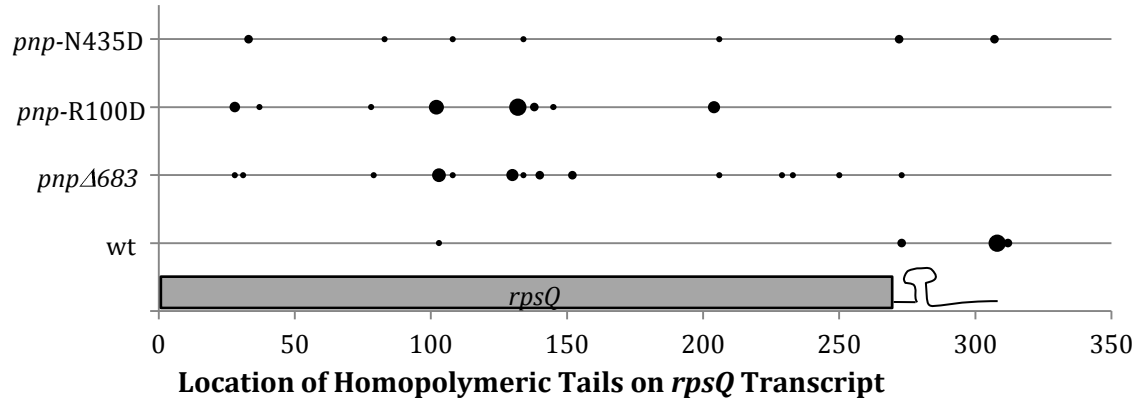

(B) *lpp*

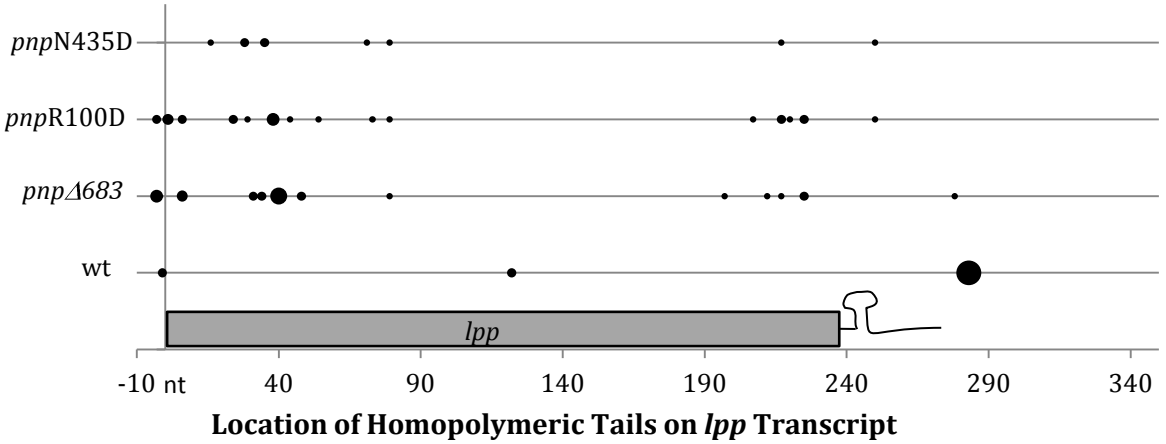

(C) *rpsJ*

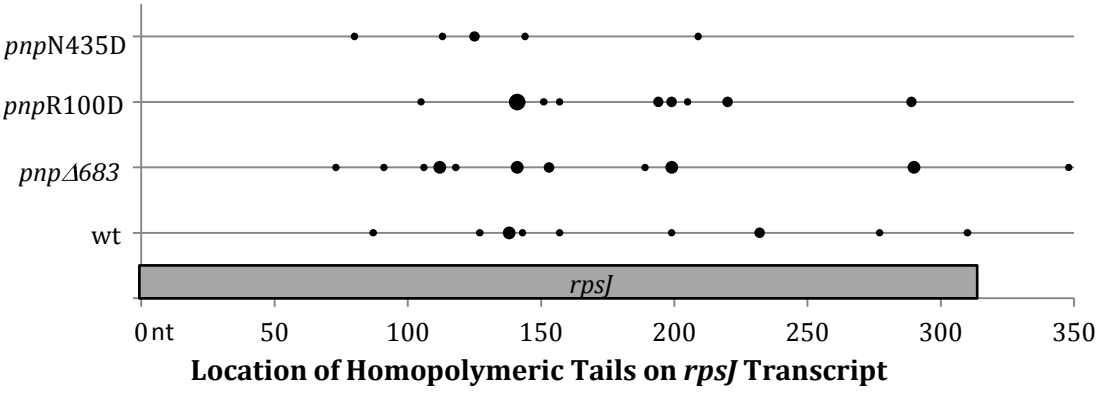

Table 3.5. Comparison of the polyadenylation profiles of strains carrying the *pnp-7* allele. Poly(A) tails were compared with regards to percent of total tails in each tail type (homopolymeric or heteropolymeric) and average length of each type of tail. Previously published polyadenylation profiles of *lpp* for wild-type (17) are included in this work for comparison and are indicated by asterisks (*). N.D.= not determined.

	rpsJ			***rpsQ***			***lpp***		
	wt	*rne-1 pnp-7 rnb-500*	*pnp-7 rnb-500*	wt	*rne-1 pnp-7 rnb-500*	*pnp-7 rnb-500*	wt*	*rne-1 pnp-7 rnb-500*	*pnp-7 rnb-500*
n =	26	13	22	25	23	24	27*	27	25
% of homo-polymeric Tails (nt)	46	85	95	52	96	96	70*	93	88
Avg. homo-polymeric tail length (nt)	17	16	16	20	17	16	ND	17	16
% of hetero-polymeric tails	54	15	5	48	4	4	30*	7	12
Avg. hetero-polymeric tail length (nt)	58	11	24	55	27	14	ND	20	19

Figure 3.9. Shift in location of homopolymeric tails on *rpsQ*, *lpp*, and *rpsJ* transcripts for wild-type versus other PNPase mutants. The size of the dot is representative of the number of tails at particular location. Heteropolymeric tails are not shown. (See Table 3.5 for summary of heteropolymeric tail data).

(A) *rpsQ*

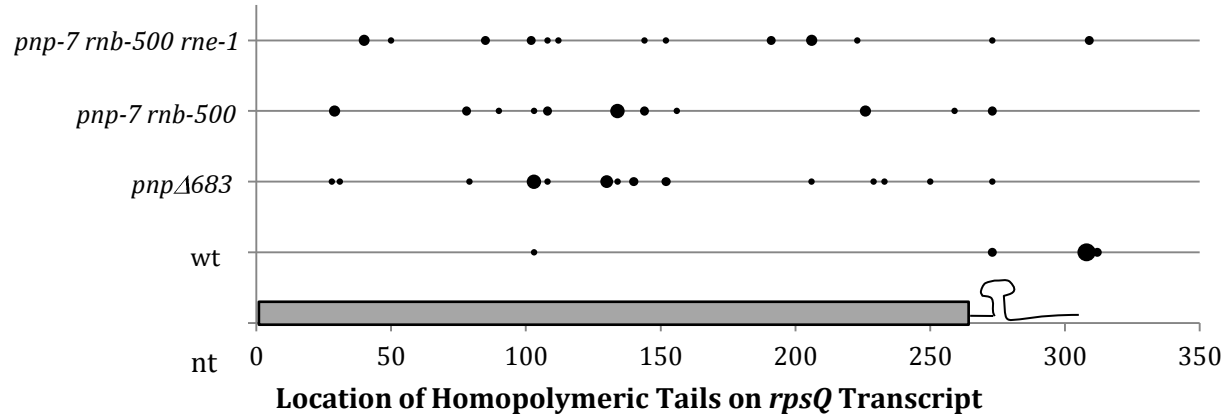

Location of Homopolymeric Tails on *rpsQ* Transcript

(B) *lpp*

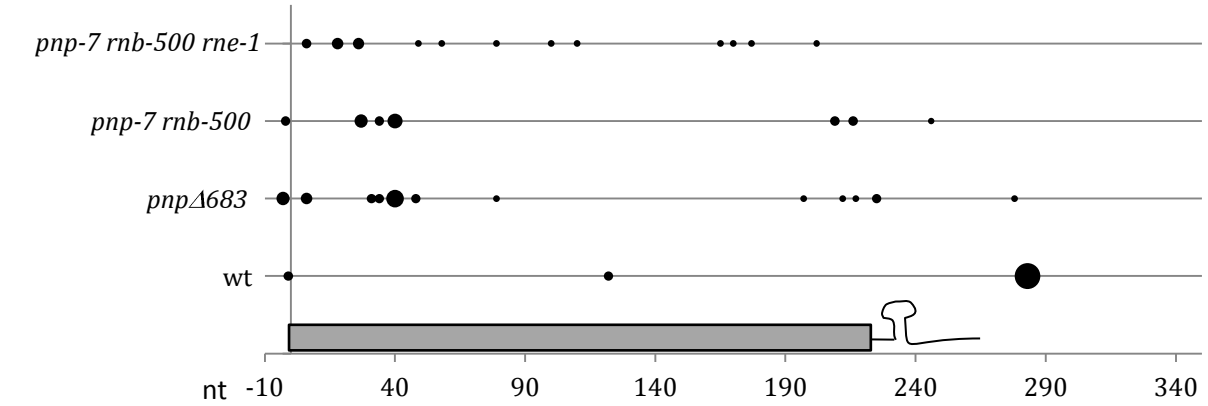

Location of Homopolymeric Tails on *lpp* Transcript

(C) *rpsJ*

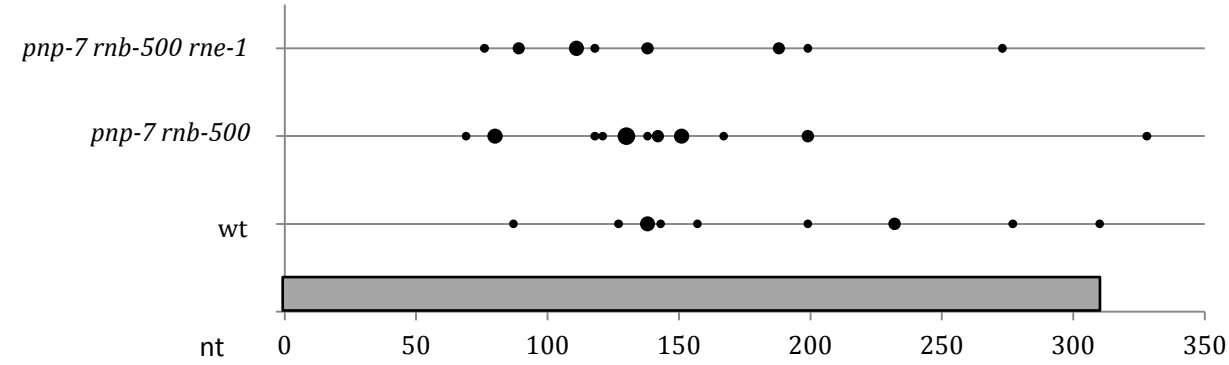

Location of Homopolymeric Tails on *rpsJ* Transcript

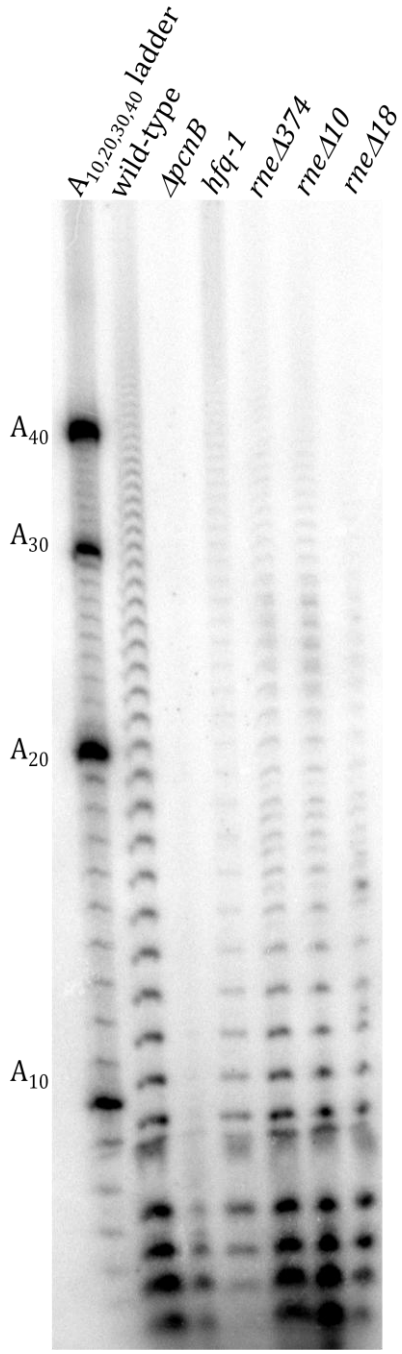

Figure 3.10. Poly(A) sizing assay for various mutants. Total RNA from MG1693, SK7988, SK10023, SK3564, SK4433, and SK4434 was 3'-end-labeled with [^{32}P]-pCp, digested, and then separated on a 20% polyacrylamide gel. A 5'-[^{32}P]-end-labeled oligo(dA) ladder is shown in lane 1.

REFERENCES

1. Ryan, K. and Bauer, D.L. (2008) Finishing touches: post-translational modification of protein factors involved in mammalian pre-mRNA 3' end formation. *Int. J Biochem. Cell Biol.*, **40**, 2384-2396.
2. Ross, J. (1996) Control of messenger RNA stability in higher eukaryotes. *Trends Genet.*, **12**, 171-175.
3. Caponigro, G. and Parker, R. (1996) Mechanism and control of mRNA turnover in *Saccharomyces cerevisiae*. *Microbiol. Rev.*, **60**, 233-249.
4. Li, Z., Pandit, S. and Deutscher, M.P. (1998) Polyadenylation of stable RNA precursors *in vivo*. *Proc. Natl. Acad. Sci. USA*, **95**, 12158-12162.
5. Coburn, G.A. and Mackie, G.A. (1996) Differential sensitivities of portions of the mRNA for ribosomal protein S20 to 3'-exonucleases is dependent on oligoadenylation and RNA secondary structure. *J. Biol. Chem.*, **271**, 15776-15781.
6. Hajnsdorf, E., Braun, F., Haugel-Nielsen, J. and Régnier, P. (1995) Polyadenylylation destabilizes the *rpsO* mRNA of *Escherichia coli*. *Proc. Natl. Acad. Sci. USA*, **92**, 3973-3977.
7. O'Hara, E.B., Chekanova, J.A., Ingle, C.A., Kushner, Z.R., Peters, E. and Kushner, S.R. (1995) Polyadenylylation helps regulate mRNA decay in *Escherichia coli*. *Proc. Natl. Acad. Sci. USA*, **92**, 1807-1811.
8. Xu, F. and Cohen, S.N. (1995) RNA degradation in *Escherichia coli* regulated by 3' adenylation and 5' phosphorylation. *Nature*, **374**, 180-183.

9. Mohanty, B.K. and Kushner, S.R. (1999) Analysis of the function of *Escherichia coli* poly(A) polymerase I in RNA metabolism. *Mol. Microbiol.*, **34**, 1094-1108.

10. Cao, G.J. and Sarkar, N. (1992) Poly(A) RNA in *Escherichia coli*: nucleotide sequence at the junction of the *lpp* transcript and the polyadenylate moiety. *Proc. Natl. Acad. Sci. USA*, **89**, 7546-7550.

11. Mohanty, B.K. and Kushner, S.R. (2006) The majority of *Escherichia coli* mRNAs undergo post-transcriptional modification in exponentially growing cells. *Nucleic Acids Res.*, **34**, 5695-5704.

12. Cao, G.-J. and Sarkar, N. (1992) Identification of the gene for an *Escherichia coli* poly(A) polymerase. *Proc. Natl. Acad. Sci. USA*, **89**, 10380-10384.

13. Mohanty, B.K., Maples, V.F. and Kushner, S.R. (2012) Polyadenylation helps regulate functional tRNA levels in *Escherichia coli*. *Nucleic Acids Res.*, **40**, 4589-4603.

14. Aiso, T., Yoshida, H., Wada, A. and Ohki, R. (2005) Modulation of mRNA stability participates in stationary-phase-specific expression of ribosome modulation factor. *J. Bacteriol.*, **187**, 1951-1958.

15. Mohanty, B.K. and Kushner, S.R. (2000) Polynucleotide phosphorylase, RNase II and RNase E play different roles in the *in vivo* modulation of polyadenylation in *Escherichia coli*. *Mol. Microbiol.*, **36**, 982-994.

16. Cao, G.J., Kalapos, M.P. and Sarkar, N. (1997) Polyadenylated mRNA in *Escherichia coli*: Modulation of poly(A) levels by polynucleotide phosphorylase and ribonuclease II. *Biochimie*, **79**, 211-220.

17. Mohanty, B.K., Maples, V.F. and Kushner, S.R. (2004) The Sm-like protein Hfq regulates polyadenylation dependent mRNA decay in *Escherichia coli*. *Mol. Microbiol.*, **54**, 905-920.

18. Mohanty, B.K. and Kushner, S.R. (2013) Deregulation of poly(A) polymerase I in *Escherichia coli* inhibits protein synthesis and leads to cell death. *Nucleic Acids Res.*, **41**, 1757-1766.

19. Grunberg-Manago, M. (1963) Polynucleotide phosphorylase. *P.N.A.R.*, **1**, 93-133.

20. Mohanty, B.K. and Kushner, S.R. (2000) Polynucleotide phosphorylase functions both as a 3' - 5' exonuclease and a poly(A) polymerase in *Escherichia coli*. *Proc. Natl. Acad. Sci. USA*, **97**, 11966-11971.

21. Carpousis, A.J., Van Houwe, G., Ehretsmann, C. and Krisch, H.M. (1994) Copurification of *E. coli* RNAase E and PNPase: evidence for a specific association between two enzymes important in RNA processing and degradation. *Cell*, **76**, 889-900.

22. Py, B., Causton, H., Mudd, E.A. and Higgins, C.F. (1994) A protein complex mediating mRNA degradation in *Escherichia coli*. *Mol. Microbiol.*, **14**, 717-729.

23. Py, B., Higgins, C.F., Krisch, H.M. and Carpousis, A.J. (1996) A DEAD-box RNA helicase in the *Escherichia coli* RNA degradosome. *Nature*, **381**, 169-172.

24. Vanzo, N.F., Li, Y.S., Py, B., Blum, E., Higgins, C.F., Raynal, L.C., Krisch, H.M. and Carpousis, A.J. (1998) Ribonuclease E organizes the protein interactions in the *Escherichia coli* RNA degradosome. *Genes Dev.*, **12**, 2770-2781.

25. Ikeda, Y., Yagi, M., Morita, T. and Aiba, H. (2011) Hfq binding at RhlB-recognition region of RNase E is crucial for the rapid degradation of target mRNAs mediated by sRNAs in *Escherichia coli*. *Mol. Microbiol.*, **79**, 419-432.

26. Liou, G.G., Jane, W.N., Cohen, S.N., Lin, N.S. and Lin-Chao, S. (2001) RNA degradosomes exist *in vivo* in *Escherichia coli* as multicomponent complexes associated with the cytoplasmic membrane via the N-terminal region of ribonuclease E. *Proc. Natl. Acad. Sci. USA*, **98**, 63-68.

27. Bralley, P., Gust, B., Chang, S.A., Chater, K.F. and Jones, G.H. (2006) RNA 3'-tail synthesis in *Streptomyces*: *in vitro* and *in vivo* activities of RNase PH, the SCO3896 gene product and polynucleotide phosphorylase. *Microbiol.-SGM*, **152**, 627-636.

28. Campos-Guillen, J., Bralley, P., Jones, G.H., Bechhofer, D.H. and Olmedo-Alvarez, G. (2005) Addition of poly(A) and heteropolymeric 3' ends in *B. subtilis* wild-type and polynucleotide phosphorylase deficient strains. *J. Bacteriol.*, **187**, 4698-4706.

29. Rott, R., Zipor, G., Portnoy, V., Liveanu, V. and Schuster, G. (2003) RNA polyadenylation and degradation in cyanobacteria are similar to the chloroplast but different from *Escherichia coli*. *J. Biol. Chem.*, **278**, 15771-15777.

30. Sohlberg, B., Huang, J. and Cohen, S.N. (2003) The *Streptomyces coelicolor* polynucleotide phosphorylase homologue, and not the putative poly(A) polymerase, can polyadenylate RNA. *J. Bacteriol.*, **185**, 7273-7278.

31. Leroy, A., Vanzo, N.F., Sousa, S., Dreyfus, M. and Carpousis, A.J. (2002) Function in *Escherichia coli* of the non-catalytic part of RNase E: role in the degradation of ribosome-free mRNA. *Mol. Microbiol.*, **45**, 1231-1243.

32. Ow, M.C., Liu, Q. and Kushner, S.R. (2000) Analysis of mRNA decay and rRNA processing in *Escherichia coli* in the absence of RNase E-based degradosome assembly. *Mol. Microbiol.*, **38**, 854-866.

33. Ow, M.C., Liu, Q., Mohanty, B.K., Andrew, M.E., Maples, V.F. and Kushner, S.R. (2002) RNase E levels in *Escherichia coli* are controlled by a complex regulatory system that involves transcription of the *rne* gene from three promoters. *Mol. Microbiol.*, **43**, 159-171.

34. Wang, R.F. and Kushner, S.R. (1991) Construction of versatile low-copy-number vectors for cloning, sequencing and gene expression in *Escherichia coli*. *Gene*, **100**, 195-199.

35. Jarrige, A.-C., Brechemier-Baey, D., Mathy, N., Duche, O. and Portier, C. (2002) Mutational analysis of polynucleotide phosphorylase from *Escherichia coli*. *J. Mol. Biol.*, **321**, 397-409.

36. Donovan, W.P. and Kushner, S.R. (1986) Polynucleotide phosphorylase and ribonuclease II are required for cell viability and mRNA turnover in *Escherichia coli* K-12. *Proc. Natl. Acad. Sci. USA*, **83**, 120-124.

37. Babitzke, P. and Kushner, S.R. (1991) The Ams (altered mRNA stability) protein and ribonuclease E are encoded by the same structural gene of *Escherichia coli*. *Proc. Natl. Acad. Sci. USA*, **88**, 1-5.

38. Arraiano, C.M., Yancey, S.D. and Kushner, S.R. (1988) Stabilization of discrete mRNA breakdown products in *ams pnp rnb* multiple mutants of *Escherichia coli* K-12. *J. Bacteriol.*, **170**, 4625-4633.

39. Mohanty, B.K., Giladi, H., Maples, V.F. and Kushner, S.R. (2008) Analysis of RNA decay, processing, and polyadenylation in *Escherichia coli* and other prokaryotes. *Methods Enzymol.*, **447**, 3-29.

40. Murashko, O.N., Kaberdin, V.R. and Lin-Chao, S. (2012) Membrane binding of *Escherichia coli* RNase E catalytic domain stabilizes protein structure and increases RNA substrate affinity. *Proc. Natl. Acad. Sci. USA*, **109**, 7019-7024.

41. Khemici, V., Poljak, L., Luisi, B.F. and Carpousis, A.J. (2008) The RNase E of *Escherichia coli* is a membrane-binding protein. *Mol. Microbiol.*, **70**, 799-813.

CHAPTER 4

CONCLUSIONS AND FUTURE DIRECTIONS

PROCESSING OF THE *RPSJ* OPERON

Understanding the mechanisms of RNA processing, degradation, and polyadenylation in *Escherichia coli* is key to understanding the basics of cellular metabolism and post-transcriptional regulation. In this work, we examined the processing and/or breakdown along with the polyadenylation profiles of the large polycistronic *rpsJ* mRNA transcript. Our data from Chapter 2 demonstrated that RNase E was the major ribonuclease involved in the initial processing of the *rpsJ* transcript and is responsible for the removal of the 3' Rho-independent transcription terminator, confirming experimentally the general assumption that large polycistronic transcripts are processed into smaller, more manageable pieces.

As shown in Chapter 2, the cellular ratios of the individual ORF transcripts of the polycistronic *rpsJ* operon remained relatively constant, despite changes in the processing of the full-length transcript in RNase E mutants. This result suggested that the flexibility and adaptation potential to control the amounts of ribosomal proteins at the transcript level was much greater than previously observed or envisioned.

POLYADENYLATION IN *E. COLI*

The Role of the RNase E based degradosome in Polyadenylation

Through the examination of the *rpsJ* operon transcript, our studies demonstrated the importance of the RNase E-based degradosome to maintain proper PAP I polyadenylation. In Chapter 3, we have shown that the presence of Hfq, a fully functional PNPase, and an intact degradosome are required for normal PAP I polyadenylation, particularly of transcripts containing a Rho-independent transcription terminator. When the scaffold region of the RNase E protein was deleted, the polyadenylation profiles of individual mRNAs encoded within the *rpsJ* operon (*rpsJ* and *rpsQ*) and a control transcript (*lpp*) changed dramatically both in the location of the post-transcriptionally added tails and in their nucleotide composition. The absence of PNPase or lack of functional PNPase resulted in similar observations. Our results provide important insight into the role of an intact degradosome in PAP I polyadenylation in *E. coli*, especially the need for interaction of the polyadenylation complex with an intact degradosome for normal PAP I activity.

The Polyadenylation Complex

As also shown in Chapter 3, our data suggested the existence of a much larger polyadenylation complex than previously proposed (1). We propose a complex composed of the RNase E-based degradosome, PNPase, PAP I, and Hfq. Our data also suggest a more direct link between mRNA degradation and polyadenylation than previously envisioned, with the polyadenylation complex interacting with the

degradosome via interactions with PNPase, Hfq, or both. The demonstration of a large polyadenylation complex is a novel concept in bacteria and requires further analysis to understand the precise role of PNPase and the degradosome on PAP I polyadenylation.

Further work needs to be done to examine the actual interaction of PNPase, Hfq, and the degradosome scaffold region. It is still unknown what key physical interactions, if any, are necessary. Additionally, as there is strong evidence that the majority of RNase E binds to the inner cytoplasmic membrane (2-5) and that PAP I is associated with or localized to the inner membrane during exponential growth (6,7), it needs to be determined if localization to the inner membrane is an important component of normal polyadenylation of mRNAs. Further examination is also necessary to understand if PAP I is localized to the inner membrane independently, or due to its interaction with the RNase E-based degradosome. These experiments are important because it does not appear that the PAP I polyadenylation of tRNAs requires Hfq.

PAP I Dependence on PNPase

While there is much known about the polyadenylation enzymes in *E. coli*, the exact mechanism by which PAP I and PNPase identify and select their RNA substrates is still not completely understood. The dependence of PAP I on PNPase needs to be examined more fully. Our work in Chapter 3 demonstrated that PNPase-mediated polyadenylation is independent of PAP I function and is not affected by the absence of an intact degradosome, but that PAP I polyadenylation is dependent on the function of PNPase, the presence of intact degradosome, and Hfq. It remains to be understood

why PAP I requires interaction with PNPase, Hfq, and the degradosome to function effectively as a poly(A) polymerase, while PNPase function is independent.

The Relationship of Polyadenylation and mRNA Processing and Decay

As the RNase E-based degradosome plays a major role in both processing and polyadenylation, the extent of the link between the polyadenylation and processing functions needs to be examined further. The link between the RNase E-based degradosome and normal PAP I polyadenylation suggests the possibility of a closer interaction between processing or breakdown/decay and polyadenylation than previously understood. It also remains to be seen if the poly(A) tails after a Rho-independent transcription terminator function differently compared to the tails added to processed transcripts. Furthermore, it is not known if such tails are recognized by different enzymes at different stages of the decay pathway.

Polyadenylation Signals

It remains unclear precisely what signals PAP I or PNPase to add a tail to a particular substrate, although our data in Chapter 2 has demonstrated that polyadenylation of polycistronic transcripts occurs even when separated from the transcription terminator. Additionally, since the processed ORFs of the *rpsJ* polycistronic transcript are not all polyadenylated in the same manner, there appears to be some distinct polyadenylation signaling that is unique to each ORF transcript fragment.

FINAL CONCLUSION

Overall, our work has provided insight into important aspects of processing and turnover/decay of mRNA transcripts that are essential for the cell's ability to rapidly adapt to changing environmental conditions. The understanding of these RNA processing, degradation, and polyadenylation activities in *Escherichia coli* is key to gaining a better understanding of the basics of cellular metabolism and regulation. Additionally, our work has strengthened the possibility of a closer tie between mRNA processing and turnover/decay than previously demonstrated, suggesting a larger control of these mechanisms by the involved enzymes.

REFERENCES

1. Mohanty, B.K., Maples, V.F. and Kushner, S.R. (2004) The Sm-like protein Hfq regulates polyadenylation dependent mRNA decay in *Escherichia coli*. *Mol. Microbiol.*, **54**, 905-920.
2. Khemici, V., Poljak, L., Luisi, B.F. and Carpousis, A.J. (2008) The RNase E of *Escherichia coli* is a membrane-binding protein. *Mol. Microbiol.*, **70**, 799-813.
3. Miczak, A., Srivastava, R.A. and Apirion, D. (1991) Location of the RNA-processing enzymes RNase III, RNase E and RNase P in the *Escherichia coli* cell. *Mol. Microbiol.*, **5**, 1801-1810.
4. Liou, G.G., Jane, W.N., Cohen, S.N., Lin, N.S. and Lin-Chao, S. (2001) RNA degradosomes exist *in vivo* in *Escherichia coli* as multicomponent complexes associated with the cytoplasmic membrane via the N-terminal region of ribonuclease E. *Proc. Natl. Acad. Sci. USA*, **98**, 63-68.
5. Taghbalout, A. and Rothfield, L. (2007) RNase E and the other constituents of the RNA degradosome are components of the bacterial cytoskeleton. *Proc. Natl. Acad. Sci. USA*, **104**, 1667-1672.
6. Jasiecki, J. and Wegrzyn, G. (2005) Localization of *Escherichia coli* poly(A) polymerase I in cellular membrane. *Biochem. Biophys. Res. Commun.*, **329**, 598-602.
7. Carabetta, V.J., Mohanty, B.K., Kushner, S.R. and Silhavy, T.J. (2009) The response regulator SprE (RssB) modulates polyadenylation and mRNA stability in *Escherichia coli*. *J. Bacteriol.*, **191**, 6812-6821.

APPENDIX A

DELETION MUTANTS OF TRANSFER RNA^{LEU2} ARE VIABLE AND EXHIBIT FLEXIBILITY IN CODON-ANTICODON RECOGNITION IN *ESCHERICHIA COLI*[1]

[1] Kristen B. Mildenhall, Bijoy K. Mohanty, and Sidney R. Kushner. To be submitted to Nucleic Acids Research.

ABSTRACT

The process of translation requires that the codons within an mRNA be accurately recognized by appropriately charged tRNAs. The *leuU* tRNA (encoding $tRNA^{Leu2}$) of *E. coli* is unique in several aspects. It is one of the few tRNAs encoded in a polycistronic operon that also contains an mRNA, being co-transcribed with *secG*, a membrane translocation protein. More importantly, of the eight leucine tRNAs in *E. coli*, $tRNA^{Leu2}$ is the only one that recognizes the CUC and CUU leucine codons in exponentially growing cells.

Here we report that *leuU* is not essential for cell viability in the MG1655, W3110, and C600 genetic backgrounds of *E. coli* K12. The Δ*secG leuU* strains are viable at 30^oC and 37^oC but not at 44^oC. Additionally, the cell morphology of the Δ*leuU* mutants was dramatically altered, with cells being significantly smaller in all dimensions compared to wild-type controls and the presence of elongated chains. Additionally, it was verified that the deletion of $tRNA^{Leu2}$ was the cause of decreased growth and viability, temperature sensitivity, and altered cellular morphology by using complementation plasmids carrying either $secG^+$ $leuU^+$ or just $leuU^+$.

We hypothesize that the cell is utilizing a more complex mechanism of alternative base-pairing to compensate for the inability to recognize the CUC and CUU codons, and that the CUC codon is also read by $tRNA^{Leu3}$ through a U:C wobble base pairing.

INTRODUCTION

The *leuU* tRNA (encoding $tRNA^{Leu2}$) of *E. coli* is unique in that it is one of the few tRNAs in a polycistronic operon that also contains an mRNA. It is co-transcribed with *secG*, a membrane translocation protein, which is directly involved in protein translocation across the membrane and is considered vital at low temperatures. A study done by Nishiyama *et al.* (1) demonstrated that considerable amounts of a SecG precursor accumulated at 20°C but not at 37°C, suggesting the importance of this protein at cold temperatures due to the cell's inability to survive in the absence of mature, functional protein.

More importantly, of the eight leucine tRNAs in *E. coli,* $tRNA^{Leu2}$ is the only one that recognizes the leucine CUU and CUC codons in exponentially growing cells. In fact, when Nishiyama and Tokuda (2) characterized the *secG leuU* transcript, they reported that a Δ*secG leuU* mutant was not viable. Since *secG* could be deleted without effecting cell viability, they concluded that *leuU* was essential. Subsequently, Sorensen *et al.* (3) also found that under starvation conditions, $tRNA^{Leu3}$ (encoded by *leuW*) uses wobble from a uridine-5-oxyacetic acid modification to also recognize the CUU codon.

However, when experiments in our laboratory demonstrated that the *leuU* tRNA was initially processed from the *secG leuU* transcript by an RNase P cleavage at the mature 5' terminus of *leuU* (4), the question arose as to whether the *leuU* tRNA was really essential for cell viability. Here we describe the construction and characterization of Δ*secG leuU* mutants in three different genetic backgrounds. In all cases, the presence of a functional *leuU* tRNA was not essential for cell viability at either 30°C or 37°C.

Even though Sorensen *et al.* (3) found that under starvation conditions $tRNA^{Leu3}$ (encoded by *leuW*) used wobble from a uridine-5-oxyacetic acid modification to also recognize the CUU codon, our results suggest a greater flexibility in codon-anticodon recognition, such that the cell can overcome the loss of this unique tRNA. We hypothesize that the cell is utilizing a more complex mechanism of alternative base-pairing to compensate for the inability to recognize the CUC and CUU codons, and that the CUC codon is also read by $tRNA^{Leu3}$ through a U:C wobble base pairing.

MATERIALS AND METHODS

Plasmids

Plasmids were isolated using the QIAprep Spin Miniprep Kit (Qiagen) or E.Z.N.A.® Plasmid Mini Kit (OMEGA Bio-Tek). pAG3 ($secG^+$ $leuU^+$ Ap^R) was obtained from KN470/pAG3 strain (2) and contained $secG^+$ $leuU^+$ under the control of an arabinose-inducible promoter.

pBMK48 ($leuU^+$ Cm^R) was constructed by using overlap PCR to create a DNA fragment containing the coding sequence and Rho-independent transcription terminator of *leuU* with a 5' *Bam*HI and a 3' *Hin*dIII restriction sites. The insert and vector pBMK11 DNA (5) were both digested with *Bam*HI and *Hin*dIII and ligated using Fast-Link™ DNA Ligase (Epicentre®). Plasmid DNA was sequenced to ensure successful cloning of the insert. pBMK48 has *leuU*+ under the control of an IPTG-inducible promoter and is a derivative of pAG702.

Bacterial Strains

Viable Δ*secG leuU* deletions were constructed in the MG1693, W3110, and C600 genetic backgrounds of *E. coli* K-12 using a P1 transducing lysate obtained from a strain carrying a Δ*secG leuU*::$Sm^{r/}Sp^{r}$ allele (K. Nishiyama laboratory). This mutation was a complete insertion/deletion of the dicistronic *secG leuU* operon. These three genetic backgrounds were selected, since C600 was used in the original work (2), while MG1693 (a MG1655 derivative) is the common strain used in our laboratory. W3110 was also included as its complete genome has also been sequenced. MG1693 (*thyA715 rph-1*) was provided by the *E. coli* Genetic Stock Center (Yale University).

Complementation plasmids were transformed into the desired strains by chemical transformation. Each parent wild-type strain and their four respective Δ*secG leuU* derivatives strains were transformed with either pAG3 ($secG^{+}$ $leuU^{+}$) or pBMK48 (leu^{+}). Following transformation, the resulting strains were analyzed for temperature sensitivity and growth phenotypes. When indicated, 1mM IPTG or 1 mM arabinose was added to induce pBMK48 ($leuU^{+}$) and pAG3 ($secG^{+}$ $leuU^{+}$), respectively.

PCR and Northern Analysis

The presence of the *leuU* deletion in transductants was confirmed by both PCR and northern blotting. Total RNA was isolated as described previously (6). Subsequent quantification and normalization of RNA samples and northern analysis were then carried out as described previously (7). Northern blots were probed with a *leuU* probe, stripped, and reprobed with a *glt* probe. The four *glt* tRNA genes are located between the 23S and 16S rRNA subunits in four of the seven *E. coli* ribosomal RNA operons.

Bacterial Growth and Viability

To obtain growth curves, bacterial strains were grown in Luria broth supplemented with thymine (50 µg/mL) and streptomycin (20 mg/mL), chloramphenicol (20 mg/mL) or ampicillin (200 mg/mL), where appropriate, at 30°C with shaking until they reached a cell density of approximately 50 Klett units above background. The Klett units were measured using a Klett-Summerson colorimeter with a green filter (No. 42). Subsequently, the cultures were shifted to 44°C for 2-3 hours, as indicated. Measurements were taken at 30 minute intervals throughout growth.

Cell viability was determined by plating dilutions of cultures immediately before shift to 44°C and at 30 minute time points following the shift. Luria agar plates supplemented with thymine and antibiotic, as needed, were then grown at 30^{o}C for 2-3 days and colonies were counted.

Microscopy

To examine cellular morphology, cultures were grown up with shaking, as described above, until they reached a cell density of 40-45 Klett units above background. Aliquots were removed and fixed with glutaraldehyde. The cultures were then shifted to 44°C. Aliquots were again taken at 150 min after shift and fixed with glutaraldehyde. Fixed cells were then placed in a solution of low-melting agarose, and imaged with a Leica DM6000B Light Microscope at 1000x.

RESULTS

Characterization, growth, and vialbility of Δ*secG leuU* mutant strains

After the Δ*secG leuU* deletions were confirmed by northern analysis (Fig. A.1), the growth properties for each Δ*secG leuU* deletion strain were compared to their respective wild-type controls. All of the deletion strains were temperature sensitive at 44°C (Table A.2), except in the MG1693 genetic background, where both temperature-sensitive and temperature resistant transductants were obtained. Additionally, all of the transductants were cold-sensitive (Table A.3), which was consistent with previously identified properties of *secG* mutants (1).

To examine the temperature sensitive growth of these mutant strains, growth was plotted before and after shift to the non-permissive temperature. Aliqouts were also taken at various points after temperature shift and plated at 30°C to examine the viability of the mutants. For the MG1693 derivatives, the temperature sensitive SK10457 (Δ*secG leuU)* mutant both grew more slowly at 30°C and then growth leveled off around 120 minutes after temperature shift (Fig. A.2A). The temperature resistant mutant, SK10456 (Δ*secG leuU)*, grew slower than the MG1693 wild-type, but its growth was not affected by the temperature shift. The viability of the SK10457 (Δ*secG leuU)* strain dropped at time points up to 90 minutes at which point it leveled off (Fig. A.2B).

For the W3110 derivative, the temperature sensitive SK10475 (Δ*secG leuU)* mutant grew more slowly at 30°C and then growth leveled off around 120 minutes after shift to 44°C (Fig. A.3A). Viability of the SK10474 (Δ*secG leuU)* mutant was lower than the wild-type control, but never decreased like what was observed with the MG1693-derivative mutant (Fig. A.3B).

For the C600 derivative, SK10473 (Δ*secG leuU)* mutant grew more slowly at 30°C. Growth leveled off around 90 minutes after temperature shift after which time cell density actually decreased (Fig. A.4A). The loss of cell viability in SK10473 (Δ*secG leuU)* was the most dramatic of the mutant strains, as it dropped immediately and never leveled off (Fig. A.4B).

Characterization of strain morphology in Δ*secG leuU* mutants

To examine the effect of the Δ*secG leuU* mutation on the morphology of the cell, both wild-type and mutants were examined using light microscopy. This showed that the cell morphology of the Δ*secG leuU* mutants was dramatically altered. The mutant cells were significantly smaller in all dimensions from the wild-type control and also contained elongated chains (Fig. A.5).

Complementation of Δ*secG leuU* mutant strains

Each parental wild-type strain and their respective Δ*secG leuU* derivatives strains were transformed with either pAG3 (*secG*$^+$ *leuU*$^+$) and pBMK48 (*leuU*$^+$) to verify by complementation that the *leuU* deletion was the cause of the growth defect at 44°C. The strains containing pBMK48 or pAG3 were tested for temperature sensitivity. Both the MG1693-derivative mutants and W3110 derivative mutants regained their growth (Figs. A.6, A.7) when complemented with either pAG3 (*secG*$^+$ *leuU*$^+$) or pBMK48 (*leuU*$^+$). Of particular interest was the fact that this complementation occurred even when the *leuU*$^+$ plasmid was not induced (Figs. A.6, A.7).

DISCUSSION

The *leuU* gene is not essential for cell viability at 30°C or 37°C but leads to sensitive growth at 44°C in all three genetic backgrounds

Here we show that the *leuU* gene is not essential for cell viability in the MG1655, W3110, or C600 *E. coli* K12 backgrounds. However, the Δ*secG leuU* deletion in each genetic background demonstrated slower growth at the permissive temperature. Temperature-sensitive growth was seen in all three genetic backgrounds (Tables A.2, A.3). The Δ*secG leuU* mutation exhibited the most dramatic effects in the C600 background, where we saw rapid loss in cell viability at 44^{o}C.

This loss of growth ability was demonstrated through complementation to be caused by the Δ*secG leuU* deletion, and was reversed by complementation of either a *secG*$^{+}$ *leuU*$^{+}$ or *leuU*$^{+}$ plasmid (Figs. A.6, A.7). Additionally, the complementation occurred even when the *leuU*$^{+}$ plasmid was present but not induced (Figs. A.6, A.7), suggesting that the minimal expression from the leakiness of the pBMK48 *lac* promoter was sufficient to restore the mutants to wild-type growth.

Another tRNA must be compensating for tRNA^{Leu2}

Since the *leuU* gene is not essential, but no tRNA is known to recognize the CUC codon, another tRNA must be compensating for the tRNA^{Leu2} through non-traditional wobble base pairing. Future peptide sequencing and subsequent analysis of specific tRNA charging levels in the cell will help determine which amino acid is being inserted opposite the CUC codon and compensating for the tRNA^{Leu2}. Regardless, this tRNA

compensation suggests a greater flexibility in codon-anticodon recognition, such that the cell can overcome the loss of this unique tRNA.

Acknowledgments

Special thanks to Dr. K. Nishiyama for his gift of pAG3. Additional thanks to undergraduate students Wyatt Ramey, for his work on the viability curves and construction of the complementation strains and Mayson Callaway, for his work on complementation growth curves. Also thanks to Dr. Richard Meagher and Dr. M.K. Kandasamy for use and help with the Leica DM6000B Light Microscope. This work was supported by NIH grants GM57220 and GM81554 to S.R.K.

TABLES AND FIGURES

Table A.1. List of bacterial strains and plasmids used in this study. The Δ*secG leuU*::*spc/str* is a complete deletion/insertion of the dicistronic *secG leuU* operon. Unless indicated otherwise, Δ*secG leuU* mutants are temperature sensitive at 44°C.

Strains	Genotype	Plasmid	Reference or Source
MG1693	*thyA715 rph-1*	n/a	*E. coli* Genetic Stock Center
SK10456	Δ*secG leuU*::*spc/str* (non-ts) *thyA715 rph-1*	n/a	This study
SK10457	Δ*secG leuU*::*spc/str thyA715 rph-1*	n/a	This study
SK5270	*thyA715 rph-1 leuU*$^+$	pBMK48 (*leuU*$^+$)	This study
SK5271	Δ*secG leuU*::*spc/str* (non-ts) *thyA715 rph-1 leuU*$^+$	pBMK48 (*leuU*$^+$)	This study
SK5273	Δ*secG leuU*::*spc/str thyA715 rph-1 leuU*$^+$	pBMK48 (*leuU*$^+$)	This study
SK5278	*thyA715 rph-1 secG leuU*$^+$	pAG3 (*secG*$^+$ *leuU*$^+$)	This study
SK5279	Δ*secG leuU*::*spc/str* (non-ts) *thyA715 rph-1secG*$^+$ *leuU*$^+$	pAG3 (*secG*$^+$ *leuU*$^+$)	This study
SK5280	Δ*secG leuU*::*spc/str thyA715 rph-1 secG*$^+$ *leuU*$^+$	pAG3 (*secG*$^+$ *leuU*$^+$)	This study
W3110	*rph-1*	n/a	*E. coli* Genetic Stock Center
SK10475	Δ*secG leuU*::*spc/str rph-1*	n/a	This study
SK5274	*leuU*$^+$	pBMK48 (*leuU*$^+$)	This study
SK5275	Δ*secG leuU*::*spc/str rph-1 leuU*$^+$	pBMK48 (*leuU*$^+$)	This study
SK5281	*secG leuU*$^+$	pAG3 (*secG*$^+$ *leuU*$^+$)	This study
SK5282	Δ*secG leuU*::*spc/str rph-1 secG leuU*$^+$	pAG3 (*secG*$^+$ *leuU*$^+$)	This study
C600	*leuB6 thr-1 thi-1 lacY1 glnV44 fhuA21 cyn-101 glpR200*	n/a	*E. coli* Genetic Stock Center
SK10473	*leuB6 thr-1 thi-1 lacY1 glnV44 fhuA21 cyn-101 glpR200*	n/a	This study
SK5276	Δ*secG leuU*::*spc/str leuB6 thr-1 thi-1 lacY1 glnV44 fhuA21 cyn-101 glpR200 leuU*$^+$	pBMK48 (*leuU*$^+$)	This study
SK5277	*leuB6 thr-1 thi-1 lacY1 glnV44 fhuA21 cyn-101 glpR200* Δ*secG leuU*::*spc/str leuU*$^+$	pBMK48 (*leuU*$^+$)	This study

SK5283	*leuB6 thr-1 thi-1 lacY1 glnV44 fhuA21 cyn-101 glpR200 secG leuU*$^+$	pAG3 (*secG*$^+$ *leuU*$^+$)	This study
SK5284	*leuB6 thr-1 thi-1 lacY1 glnV44 fhuA21 cyn-101 glpR200* Δ*secG leuU*::*spc/str secG leuU*$^+$	pAG3 (*secG*$^+$ *leuU*$^+$)	This study

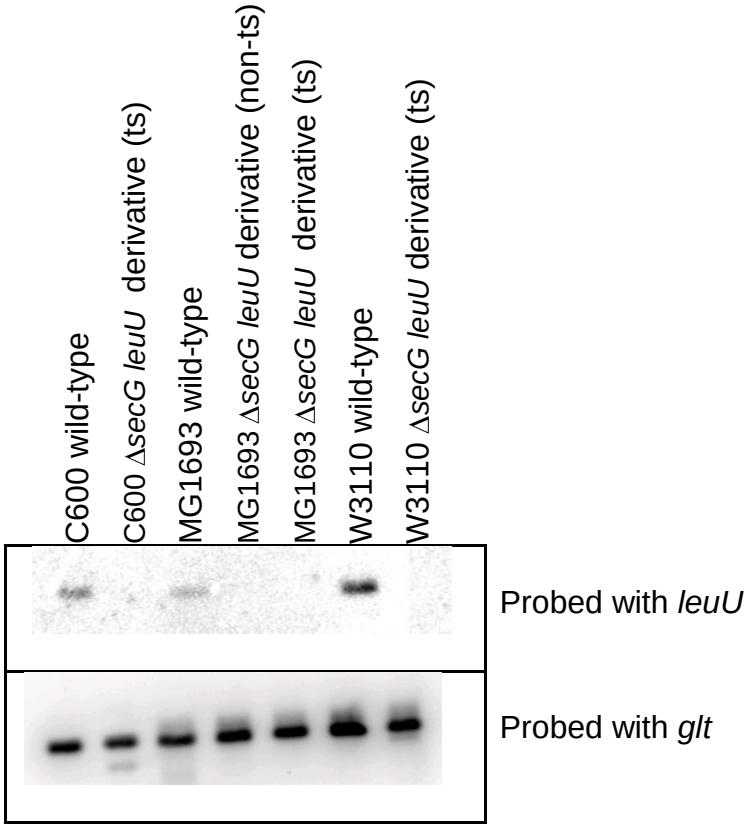

Figure A.1. The presence of the *leuU* deletion in transductants was confirmed by Northern blotting. Northern blots of all three wild-type strains and respective Δ*secG leuU* mutants probed with *leuU* and *glt* RNA probes. Cells were grown at 30°C. RNA was run on 1.2% polyacrylamide northern. Strains were as follows: C600, SK10473 (Δ*secG leuU)*, MG1693, SK10456(Δ*secG leuU)*, SK10457 (Δ*secG leuU)*, W3110, and SK10475 (Δ*secG leuU)* in Lanes 1-7, respectively.

Table A.2. Growth of strains on Luria broth plates after 48 hours. Strains were as follows: MG1693, SK10456(Δ*secG leuU)*, SK10457 (Δ*secG leuU)*, W3110, SK10475 (Δ*secG leuU)*, C600, and SK10473 (Δ*secG leuU)*.

	MG1693	SK10456	SK10457	W3110	SK10475	C600	SK10473
30°C	+	+	+	+	+	+	+
44°C	+	+	−	+	−	+	−

Table A.3. Cold sensitivity of SK10473

Viability of SK10473 at 4°C	
Original Cell Viability	**1.1 x 10^8 cfu**
Viability after 3 days at 4°C	**4.0 x 10^5 cfu**

A.

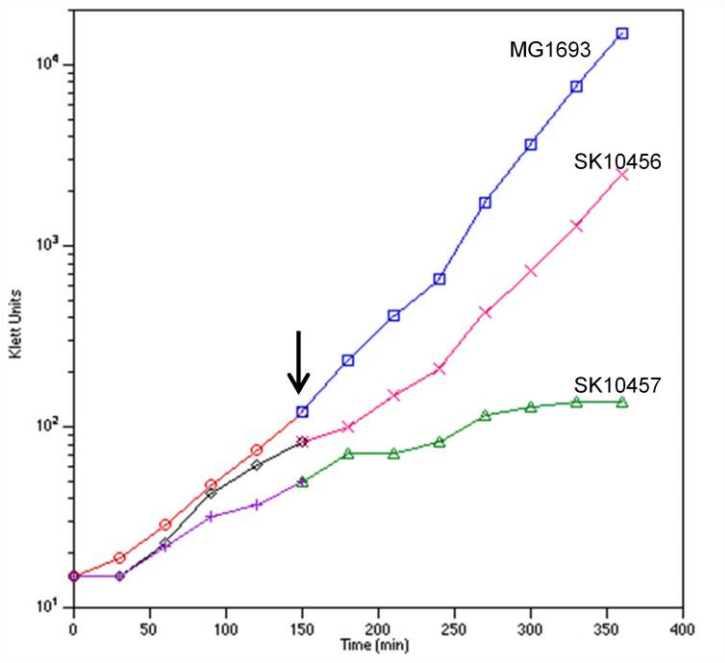

B.

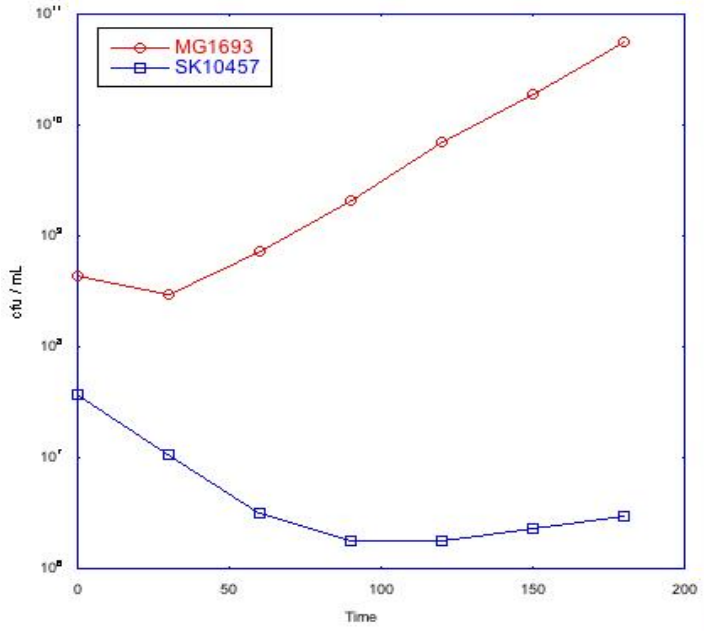

Figure A.2. Growth curve and viability curve of SK10456 and SK10457 Δ*secG leuU* mutants versus the MG1693 wild-type control. Growth is shown in panel A at 30°C and after shift (indicated by the arrow) to 44°C. Cell viability is shown in panel B and is taken at 30 minute time intervals after shift to 44°C. Viability data is not shown for temperature resistant derivative SK10456.

A.

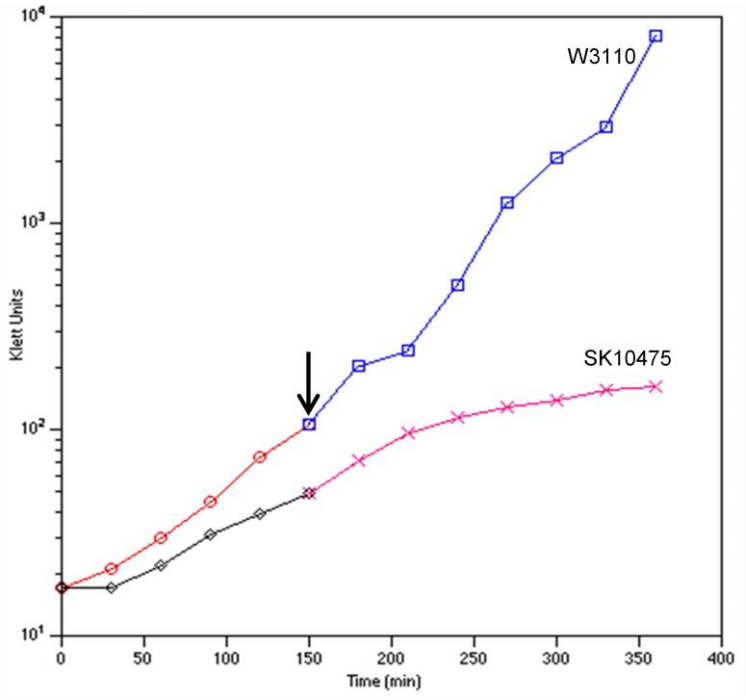

B.

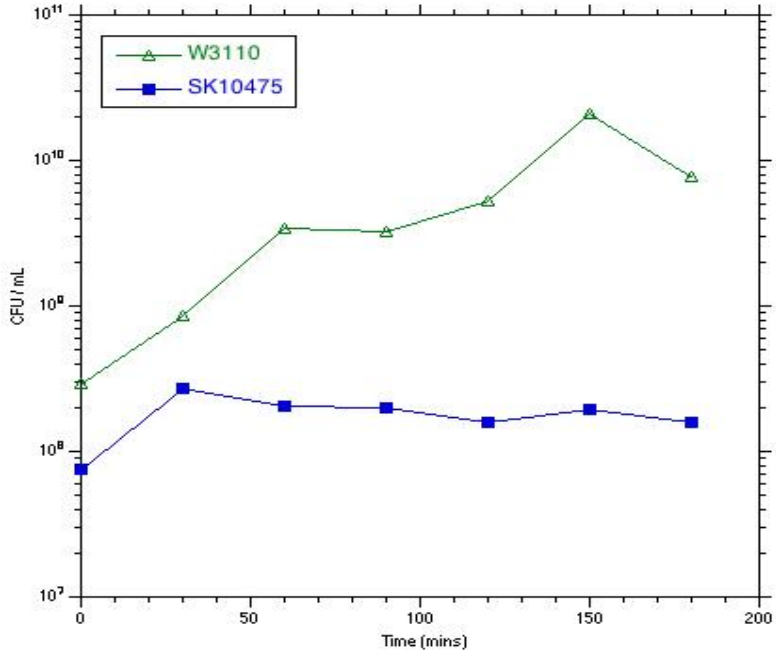

Figure A.3. Growth curve and viability curve of SK10475 Δ*secG leuU* mutant versus the W3110 wild-type control. Growth is shown in panel A at 30°C and after shift (indicated by the arrow) to 44°C. Cell viability is shown in panel B and is taken at 30 minute time intervals after shift to 44°C.

A.

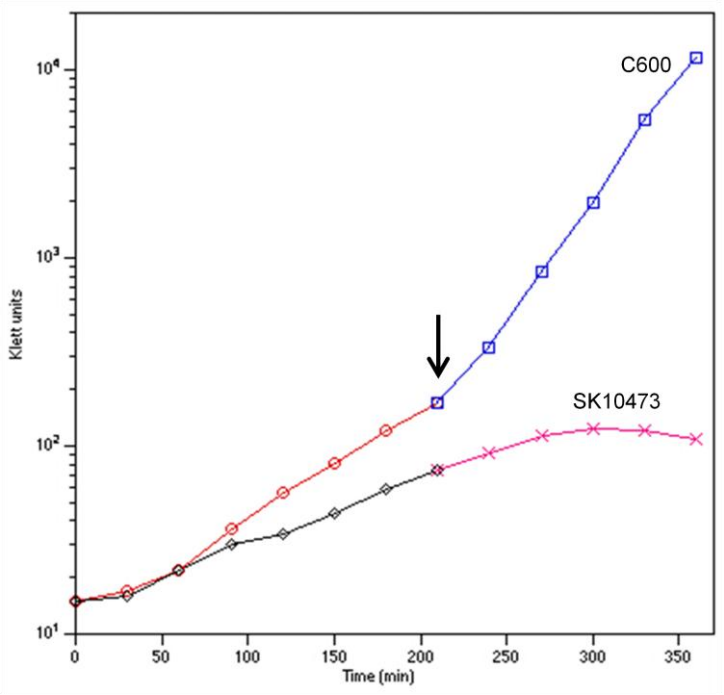

B.

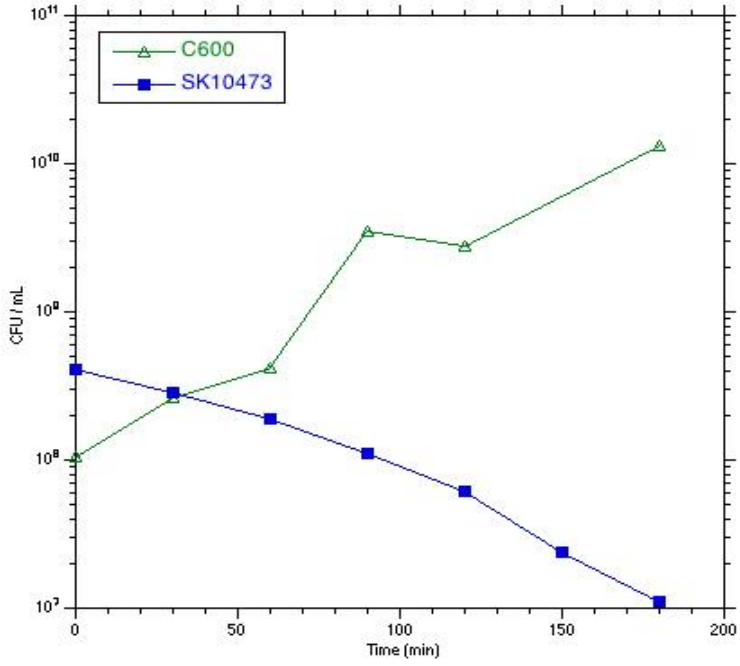

Figure A.4. Growth curve and viability curve of SK10473 Δ*secG leuU* mutant versus the C600 wild-type control. Growth is shown in panel A at 30°C and after shift (indicated by the arrow) to 44°C. Cell viability is shown in panel B and is taken at 30 minute time intervals after shift to 44°C.

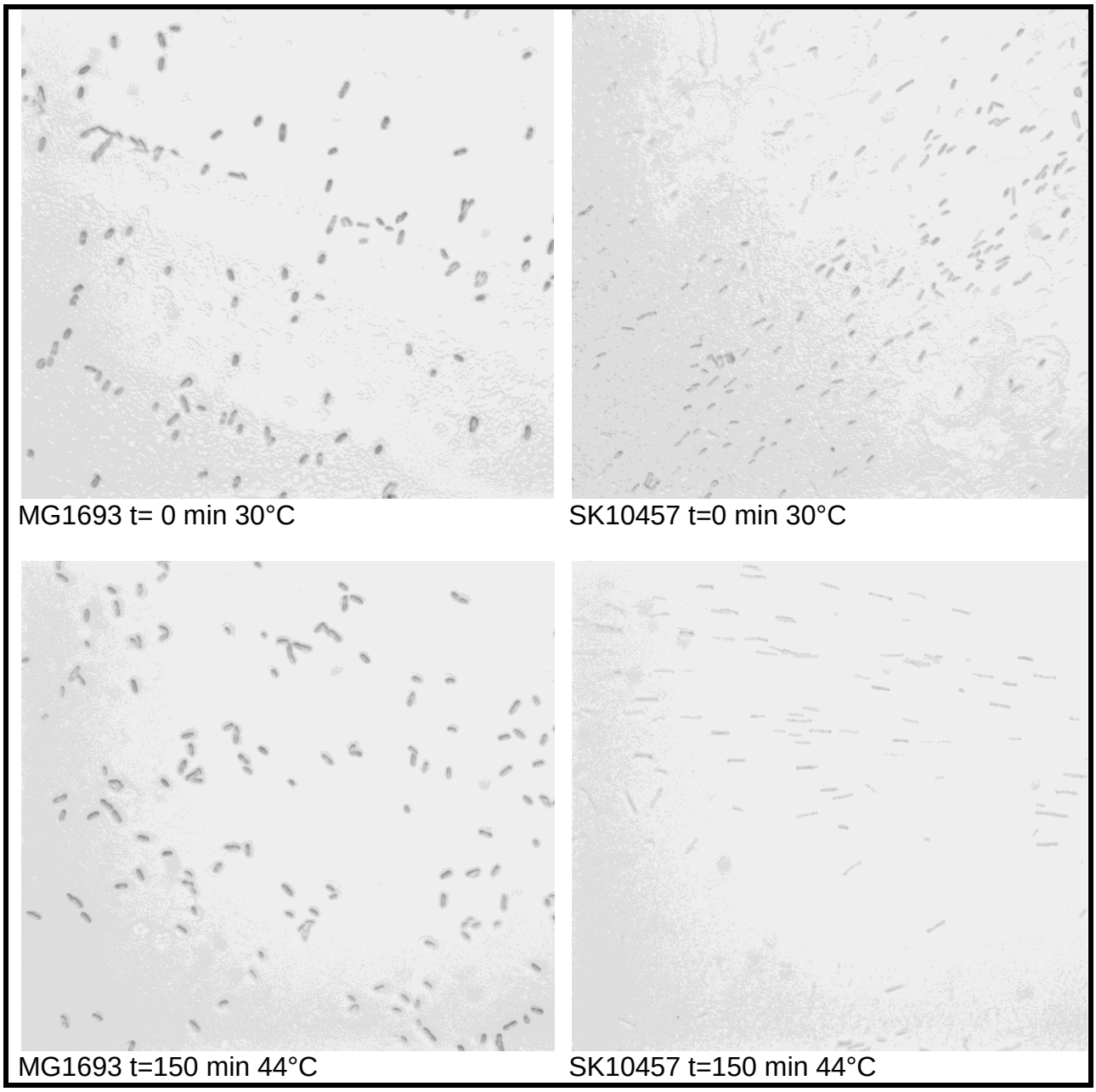

Figure A.5. Comparative morphology of wild-type versus Δ*secG leuU* deletion strain, as seen under bright field microscopy. The pictures of MG1693 and its Δ*secG leuU* derivative, SK10457 were taken prior to temperature shift, t= 0 (30°C) and again 150 minutes following the shift (44°C).

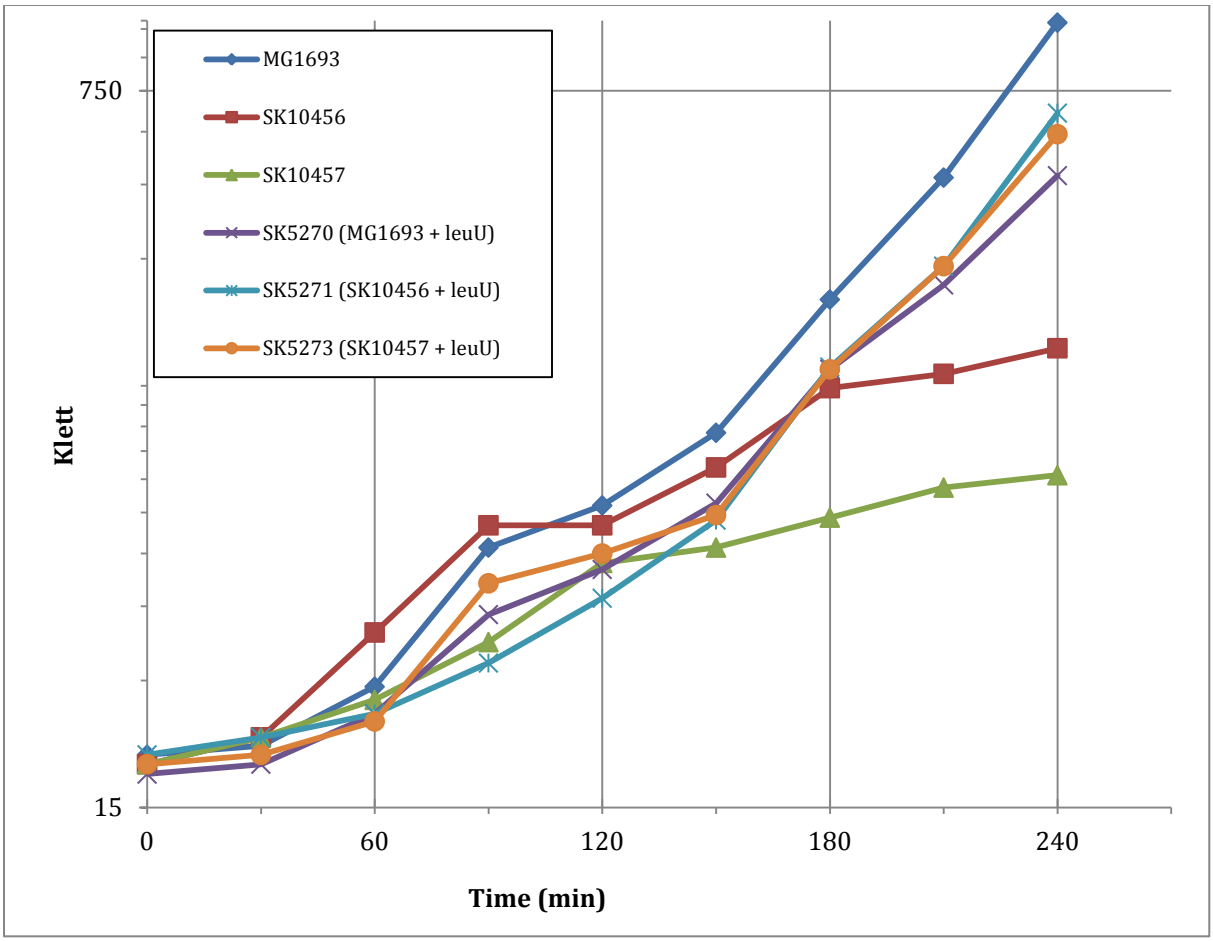

Figure A.6. MG1693 Δ*secG leuU* mutants with complementation in the absence of IPTG induction. Growth is shown at 30°C and after shift to 44°C at 210 minutes (panel A) and 120 minutes (panel B). Growth of SK5270, SK5271, SK5273 with pBMK48 (*leuU*$^{+}$) induction with 1mM IPTG (data not shown) was also plotted and does not show any differences from uninduced growth.

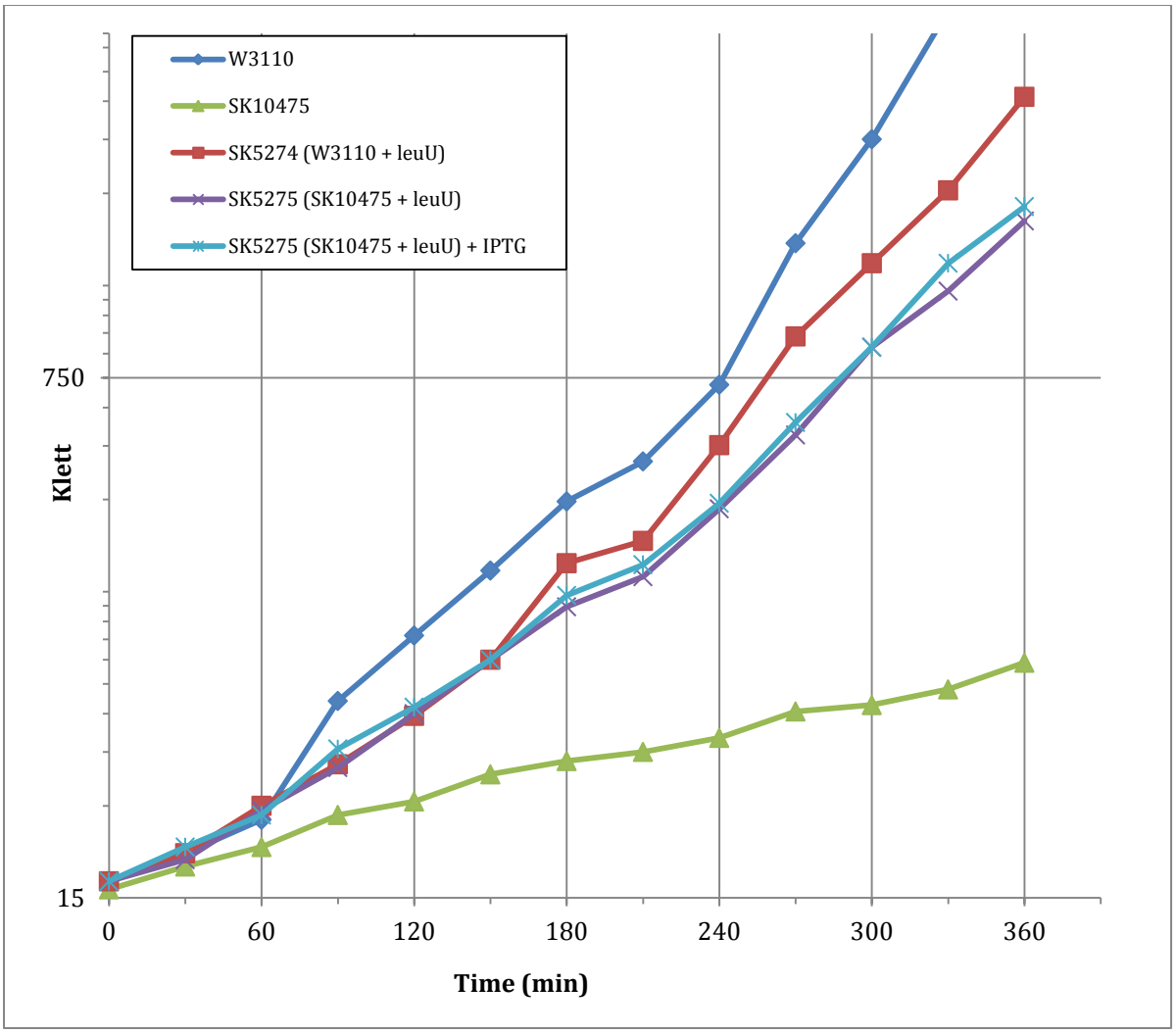

Figure A.7. W3110 Δ*secG leuU* mutant with complementation in the presence or absence of IPTG induction. Growth is shown in at 30°C and after shift to 44°C at 240 minutes. When indicated, 1mM IPTG was added to induce pBMK48 (*leuU*$^{+}$).

REFERENCES

1. Nishiyama, K., Hanada, M. and Tokuda, H. (1994) Disruption of the gene encoding p12 (SecG) reveals the direct involvement and important function of SecG in the protein translocation of *Escherichia coli* at low temperature. *EMBO J.*, **13**, 3272-3277.
2. Nishiyama, K. and Tokuda, H. (2005) Genes coding for SecG and Leu2-tRNA form an operon to give an unusual RNA comprising mRNA and a tRNA precursor. *Biochim. Biophys. Acta*, **1729**, 166-173.
3. Sorensen, M.A., Elf, J., Bouakaz, E., Tenson, T., Sanyal, S., Bjork, G.R. and Ehrenberg, M. (2005) Over expression of a tRNA(Leu) isoacceptor changes charging pattern of leucine tRNAs and reveals new codon reading. *J. Mol. Biol.*, **354**, 16-24.
4. Mohanty, B.K. and Kushner, S.R. (2008) Rho-independent transcription terminators inhibit RNase P processing of the *secG leuU* and *metT* tRNA polycistronic transcripts in *Escherichia coli*. *Nucleic Acids Res.*, **36**, 364-375.
5. Mohanty, B.K. and Kushner, S.R. (1999) Analysis of the function of *Escherichia coli* poly(A) polymerase I in RNA metabolism. *Mol. Microbiol.*, **34**, 1094-1108.
6. O'Hara, E.B., Chekanova, J.A., Ingle, C.A., Kushner, Z.R., Peters, E. and Kushner, S.R. (1995) Polyadenylylation helps regulate mRNA decay in *Escherichia coli*. *Proc. Natl. Acad. Sci. USA*, **92**, 1807-1811.
7. Mohanty, B.K. and Kushner, S.R. (2007) Ribonuclease P processes polycistronic tRNA transcripts in *Escherichia coli* independent of ribonuclease E. *Nucleic Acids Res.*, **35**, 7614-7625